UNITED NATIONS EDUCATIONAL, SCIENTIFIC AND CULTURAL ORGANIZATION
INTERNATIONAL ATOMIC ENERGY AGENCY
INTERNATIONAL CENTRE FOR THEORETICAL PHYSICS
I.C.T.P., P.O. BOX 586, 34100 TRIESTE, ITALY, CABLE: CENTRATOM TRIESTE

H4.SMR/994-2

SPRING COLLEGES IN COMPUTATIONAL PHYSICS

19 May - 27 June 1997

APPLICATIONS OF MONTE CARLO METHODS TO STATISTICAL PHYSICS

K. BINDER
Johannes Gutenberg-Universität
Institut für Physik
55099 Mainz
GERMANY

Applications of Monte Carlo methods to statistical physics

K. Binder

Institut für Physik, Johannes Gutenberg-Universität Mainz

Staudingerweg 7, D - 55099 Mainz, Germany

Abstract

Contents

Abstract

An introductory review of the Monte Carlo method for the statistical mechanics of condensed matter systems is given. Basic principles (random number generation, simple sampling versus importance sampling, Markov chains and master equations, etc.) are explained and some classical applications (self-avoiding walks, percolation, the Ising model) are sketched. The finite size scaling analysis of both second and first order phase transitions is described in detail, and also the study of surface and interfacial phenomena as well as the choice of appropriate boundary conditions is discussed. Only brief comments are given on topics such as applications to dynamic phenomena, quantum problems, and recent algorithmic developments (new sampling schemes based on reweighting techniques, nonlocal updating, parallelization, etc.). The techniques described are exemplified with many illustrative applications.

1. Introduction

Monte Carlo methods and Molecular Dynamics methods are the two main approaches of "computer simulation" in statistical physics. Such techniques are now recognized as an important tool in science, complementing both analytical theory and experiment. Since the problem of statistical thermodynamics, namely explaining the macroscopic properties of matter resulting from the interplay of a large number of atoms, is very complex, computer simulation plays a particularly important rôle there. Molecular dynamics amounts to numerically solving Newton's equations of the interacting many body system, and one can obtain static properties by taking averages along the resulting deterministic trajectory in phase space. Monte Carlo methods, on the other hand, aim at a probabilistic description from the outset, relying on the use of random numbers, and that is responsible for the name of the method. In practice, of course, these numbers are not truly random but rather are "pseudo-random numbers", i.e. a sequence of numbers produced on a computer with a suitable deterministic procedure from a suitable "seed" (see Sec. 2). In this way one can generate a stochastic trajectory through the phase space of the model considered and calculate thermal averages if one is interested in equilibrium statistical mechanics (Sec. 3). But Monte Carlo methods also find widespread applications to problems of statistical physics not related to thermodynamics but which are defined in terms of other probabilistic concepts. Examples are the generation of random walks to model diffusion processes, formation of random structures by various types of aggregation processes, or geometrical "phase transitions" like the percolation problem (the bonds of a lattice are randomly taken as conducting with probability p and as isolating with probability 1-p and one asks at which concentration p_c of conducting bonds the whole lattice may support an electric current, Sec. 4.1).

Why does one want to carry out such simulations, what does one learn that one does not learn otherwise? It turns out that most problems in statistical physics are too complicated to allow exact solutions and due to the necessity of uncontrolled approximations the accuracy of the results often is very uncertain. Therefore, in many cases also the comparison between theory and experiment is inconclusive: if discrepancies occur, one does not know whether to attribute them to inaccuracies of the mathematical treatment of a model, or to a choice of an inadequate model, or to both sources of error. Conversely, due to the presence of adjustable parameters it often happens that a wrong theory can be fitted to some (limited!) experimental data; of course then the adjusted parameters are not very meaningful since they are systematically in error.

As one example out of many, consider interdiffusion in random metallic alloys (Fig. 1) or polymer mixtures. The theoretical descriptions start from equations relating concentration currents to chemical potential gradients. Various rather arbitrary assumptions are then made about the phenomenological "Onsager coefficients" that enter (Brochard et al. 1983, Binder 1983, Kramer et al. 1984). Depending on the exact nature of the assumptions and approximations, rather contradictory results are obtained: according to the "slow mode theory" (Brochard et al. 1983) the slowly diffusing species controls interdiffusion, according to the "fast mode theory" (Kramer et al. 1984) the faster diffusing species dominates this process. Different researchers claimed evidence for either theory from some experiments (see e.g. Binder and Sillescu 1989 for a review). However, in this case fits or misfits between theory and experiment are not so meaningful - clearly the model of Fig. 1 is oversimplified in comparison with the materials available for the experiments. In contrast, the simulation (Kehr et al. 1989) can study precisely the same model (Fig. 1) on which the theories are based and can clearly bring out their strengths and/or weaknesses. All parameters used by the theory (e.g. the Onsager coefficients) can be independently estimated from the simulation, so there are no adjustable parameters in this comparison between theory and simulation whatsoever.

Nevertheless, the reader should be aware of the fact that simulations also have some problems, one must be aware of both "statistical errors" and "controllable systematic errors". In principle, statistical errors can be made as small as desired by increasing the computing time sufficiently. In practice, of course, this is not feasible for all problems that one would like to study (e.g. Quantum Monte Carlo methods, cf. Sec. 5.2, particularly those models that suffer from the "minus sign problem"). Another problem is that often it is difficult to estimate statistical errors reliably, in particular since they are "dynamically correlated" (Sec. 3.4). Many publications containing Monte Carlo results suffer either from the lack of error estimates or from severe underestimation of these statistical errors.

By "controllable systematic errors", we mean (apart from the lack of perfect randomness of the pseudo-random numbers, Sec. 2.1) limitations due to the finite size of the simulated system and the finite "observation time" during which a simulated system can evolve and is analyzed. Often one deals with a cubic box of size LxLxL containing typically between $N = 10^2$ and $N = 10^6$ degrees of freedom, depending on the complexity of the problem, and using periodic boundary conditions. The resulting systematic effects due to finite size (instead of the thermodynamic limit $L \rightarrow \infty$ and $N \rightarrow \infty$ which often is only of interest) need to be carefully considered (Sec. 4). This problem is obvious for critical points of second order phase transitions - a diverging correlation length of order parameter fluctuations does not fit into a finite simulation box. However, the "finite size scaling"-theory (Fisher 1971, Barber 1983, Privman 1990, Binder 1987a, 1992) developed for this problem has in fact become a powerful tool for the analysis of critical phenomena with simulations (Sec. 4). But there are many size effects unrelated to critical phenomena: e.g., path integral Monte Carlo studies of Argon crystals at low temperatures T do not yield the expected Debye law for the specific heat, $C \propto T^3$ but rather C vanishes according to an exponential law, $C \propto \exp(-\Delta/T)$ (Mueser et al. 1995): of course, no

acoustic phonons with wavelengths $\lambda > L$ are present and thus a small gap Δ in the phonon energy spectrum arises.

The notion of "observation time" alluded to above adopts the dynamic interpretation (Mueller-Krumbhaar and Binder 1973) of the Monte Carlo sampling as a numerical realization of the associate (markovian) master equation (see Secs. 3.4,5). This is the basis both for applications to study diffusion processes and relaxation phenomena (Sec. 5.1) and for understanding errors resulting from the finite length of this stochastic Monte Carlo "trajectory" through phase space along which averages are taken.

2. Random number generation and simple sampling of probability distributions

2.1 "Randomness" and "pseudo-random" number generators

The precise definition of "randomness" (see e.g. Compagner 1991) is outside of scope here. Truly random numbers are unpredictable in advance and must be produced by an appropriate physical process such as radioactive decay. Series of such numbers have been documented but would be very cumbersome to use for Monte Carlo simulations.

Here we are only concerned with pseudo-random numbers which are produced in the computer by one of several simple algorithms and thus are predictable as their sequence is exactly reproducible. This reproducibility, of course, is desirable as it allows detailed checks of the simulation programs. The pseudo-random numbers have statistical properties (nearly uniform distribution, nearly vanishing correlation coefficients, etc.) that are very similar to the statistical properties of truly random numbers, and thus a given sequence of pseudo-random

numbers appears "random" for many practical purposes. In the following, the prefix "pseudo" will be omitted.

What one needs are random numbers that are uniformly distributed in the interval [0,1] and that are uncorrelated. By "uncorrelated" we not only mean vanishing pair correlations for arbitrary distances along the random number sequence but also vanishing triplet and higher-order correlations. No algorithm exists that satisfies these needs fully, of course, and the extent to which the remaining correlations lead to erroneous results of simulations has been a longstanding concern (Knuth 1969, James 1990). Even random number generators that have passed all standard tests and have been used successfully for years may fail for a new application, in particular if it involves a new type of Monte Carlo algorithm (see e.g. Ferrenberg et al. 1992 for a recent example). The testing of such generators is a research subject in itself (see e.g. Marsaglia 1985, Compagner and Hoogland 1987, Compagner 1995).

A limitation due to the finite word length of computers is the finite period: every generator begins after a long but finite period to produce exactly the same sequence again. For example, simple generators for 32-bit computers have a maximum period of 2^{30} ($\approx 10^9$) numbers only. This is not enough for recent high-quality applications! Of course, one can get around this problem (Knuth 1969, James 1990) but at the same time one likes the code representing the random number generator to be "portable" (i.e. in a high-level programming language like FORTRAN or C++ be usable for computers from different manufacturers) and efficient (i.e. extremely fast so it does not unduly slow down the simulation program as a whole). Inventing new generators that are a better compromise between these partially conflicting requirements is still of interest (e.g. Marsaglia et al. 1990).

We now briefly describe a few frequently used generators. Best known is the linear multiplicative or congruential algorithm (Lehmer 1951) which produces integers X_i recursively using the formula

$$X_i = aX_{i-1} + c \text{ (modulo m)} \qquad (1)$$

which means that m is added when the result otherwise were negative. For 32-bit computers, $m = 2^{31}-1$ (the largest integer that can be used for that computer). The integer constants a,c need to be appropriately chosen (e.g. a = 16807, c = 0), and the starting value X_0 of the recursion (the "seed") must be odd. Obviously, the apparent randomness of the X_i results because after a few multiplications with a the result would exceed m and hence is truncated, and so the leading digits of X_i are more or less random. Carrying out a floating-point division with m numbers in the interval [0,1] are produced.

These generators are simple and popular but have significant triplet and higher order correlations. Using d-tuples of such numbers to represent points on d-dimensional lattices one finds that the points lie only on certain hyperplanes (Marsaglia 1968). Better random numbers are obtained, if one uses two different generators simultaneously, where one generator creates a table of random numbers from which the second one draws numbers at random.

Another popular algorithm is the shift register method (Tausworthe 1965, Kirkpatrick and Stoll 1981). A table of random numbers is first produced and a new random number is produced combining two different existing numbers according to

$$X_i = X_{i-p} \text{ .XOR. } X_{i-q} \quad , \qquad (2)$$

where .XOR. is the bitwise "exclusive or" operation, and p and q have to be properly chosen. E.g., the popular "R250" generator (Kirkpatrick and Stoll 1981) uses p = 250, q = 103, it needs 250 initializing random numbers. "Good" generators based on Eq. (2) have smaller correlations between the random numbers than those for Eq. (1) and a much longer period.

A third type of generators, the lagged Fibonacci generators, are also recommended in the literature (Knuth 1979, James 1990) but will not be further discussed here. But we add the general recommendation that no user of random numbers should rely on their quality blindly but rather perform his own tests in the context of his application.

2.2 Monte Carlo as a method of numerical integration

Many Monte Carlo computations may be viewed as attempts to estimate the value of a (multiple) integral. This is particularly true for the applications in equilibrium statistical thermodynamics, where one wishes to compute the thermal average $\langle A \rangle_T$ of an observable A ($\vec{X}$) {where $\vec{X}$ is a point in the phase space Ω} as an integral over phase space,

$$\langle A \rangle_T = \frac{1}{Z} \int_{\Omega} d\vec{X} A(\vec{X}) \exp\left[-\mathcal{H}(\vec{X}) / k_B T\right] \quad , \tag{3}$$

where Z is the partition function, k_B Boltzmann's constant, T temperature, and $\mathcal{H}(\vec{X})$ the Hamiltonian of the system. To give the flavor of the general idea, we first discuss the one-dimensional integral

$$I = \int_0^1 f(x)dx \tag{4}$$

which we first rewrite as

$$I = \int_0^1 \int_0^1 g(x,y)dxdy \tag{5}$$

with

$$g(x,y) = \begin{cases} 0 & \text{if } f(x)<y, \\ 1 & \text{if } f(x)\geq y. \end{cases} \tag{6}$$

We suppose for simplicity that also $0 \leq f(x) \leq 1$ for $0 \leq x \leq 1$. Then I is simply interpreted as the fraction of the unit square $0 \leq x,y \leq 1$ lying underneath the curve $y = f(x)$. Now a straightforward (though often not very efficient) Monte Carlo estimation of Eq. (4) is the "hit or miss" method. We take n points $(\gamma_{xi}, \gamma_{yi})$ uniformly distributed in the unit square, $0 \leq \gamma_{xi} \leq 1$, $0 \leq \gamma_{yi} \leq 1$. Then I is estimated by

$$\bar{g} = \frac{1}{n} \sum_{i=1}^{n} g(\gamma_{xi}, \gamma_{yi}) = n^*/n \quad , \tag{7}$$

n^* being the number of points for which $f(\gamma_{xi}) \geq \gamma_{yi}$. Thus, we count the fraction of points that lie underneath the curve $y = f(x)$.

Of course, such Monte Carlo methods for numerical integration are inferior to many other techniques of numerical integration, if the integration space is low-dimensional. But the situation is opposite for high-dimensional integration spaces: e.g., for any method using a

regular grid of points for which the integrand needs to be evaluated, the number of points sampled along each coordinate is $M^{1/d}$ in d dimensions which is small for any reasonable sample size M if d is very large.

In Eqs. (4-7) it was assumed that the integration space is limited to a bounded interval in space but this is not always true. E.g., the ϕ^4 model of field theory considers a field variable $\phi(\vec{x})$, where $\vec{x}$ is drawn from a d-dimensional space and $\phi(\vec{x})$ is a real variable with distribution

$$P(\phi) \propto \exp[-\alpha \left(-\frac{1}{2}\phi^2 + \frac{1}{4}\phi^4\right)], \alpha > 0, \ -\infty < \phi < +\infty . \qquad (8)$$

How can one then carry out multiple integrals over the space of the ϕ's ? This problem is solved observing that for any distribution $P(\phi)$ the normalized integrated distribution $P'(y)$ varies in the unit interval,

$$P'(y) = \int_{-\infty}^{y} P(\phi)d\phi \Big/ \int_{-\infty}^{+\infty} P(\phi)d\phi \quad , \qquad (9)$$

$0 \le P'(y) \le 1$. Hence, defining $Y = Y(P')$ as the inverse function of $P'(y)$, we can choose a random number ϑ uniformly distributed between zero and one to obtain $\phi = Y(\vartheta)$ distributed according to the chosen distribution $P(\phi)$. Of course, this method works not only for the example chosen in Eq. (8) but for any distribution of interest. This method applies for all cases where sampling from a non-uniform distribution is required. Suppose we wish to sample ϕ with $P(\phi) \propto \phi$ from the unit interval. Then $P'(y) = \int_0^y \phi d\phi \Big/ \int_0^1 \phi d\phi = y^2/2$, $Y(P') = \sqrt{2P'}$, and thus

$\phi = \sqrt{2\vartheta}$ will have the desired distribution if ϑ is uniformly distributed. Often (e.g. for the example of Eq. (8)) it will not be possible to obtain $Y(P')$ analytically but then one can compute numerically a table before the start of the sampling.

As a side remark that will be useful later, we spell out explicitly how a known probability distribution p_i that a (discrete) state i occurs with $1 \le i \le n$, with $\sum_{i=1}^{n} p_i = 1$, is numerically realized using random numbers uniformly distributed in the interval from zero to unity: defining the analogue of an integrated probability $P_i = \sum_{j=1}^{i} p_j$, we choose a state i if the random number ϑ satisfies $P_{i-1} \le \vartheta \le P_i$, with $P_0 = 0$. In the limit of a large number (M) of trials, the generated distribution approximates p_i, with errors of order $1/\sqrt{M}$.

Monte Carlo methods in equilibrium statistical mechanics can be viewed as an extension of this simple concept to the probability that a point $\vec{X}$ in phase space occurs,

$$P_{eq}(\vec{X}) = (1/Z) \exp[-\mathcal{H}(\vec{X})/k_B T] \ . \qquad (10)$$

Of course, the question arises: should one randomly select the points $\vec{X}$ from the phase space uniformly ("simple sampling") or must one resort to a non-uniform sampling? In fact, as will be discussed in Sec. 3, the distribution $P_{eq}(\vec{X})$ is extremely sharply peaked, and thus one needs "importance sampling" methods which generate points $\vec{X}$ preferably from the "important" region of space where this narrow peak occurs.

Before we treat this basic problem of statistical thermodynamics in more detail, we briefly mention the more straight-forward applications of "simple sampling" techniques in statistical physics. We simply list a few characteristic problems and indicate how random numbers enter the treatment. A particularly simple application is to generate configurations of randomly mixed crystals of a given lattice structure, e.g. a binary mixture of composition A_xB_{1-x} for which one assumes perfect random mixing. One just has to use random numbers ϑ_j uniformly distributed in [0,1] to choose the occupancy of lattice sites {j}: If $\vartheta_j < x$, the site is taken by an A atom, otherwise it is taken by a B atom. Such configurations can now be used as starting point for a numerical study of the dynamical matrix, if one is interested in the phonon spectrum of mixed crystals, for instance. Also these configurations can be used to study the site percolation problem (Stauffer 1985). We shall come back to the statistical properties of "percolation clusters" (defined in terms of groups of A-atoms such that each A-atom has at least one nearest neighbor of type A in the cluster) in Sec. 4.1.

If one is interested in the simulation of transport processes such as diffusion, a basic approach is the generation of simple random walks. Such random walks, resulting from addition of vectors whose orientation is random, can be generated both on lattices and in the continuum, and one can either choose a uniform step length of the walk, or choose the step length from a suitable distribution. Such simulations are desirable if one wishes to consider complicated geometries or boundary conditions of the medium where the diffusion takes place. Also, it is straightforward to include competing processes: e.g., in a reactor, diffusion of neutrons in the moderator competes with loss of neutrons due to nuclear reactions, radiation going to the outside, etc., or gain of neutrons due to fission events. Actually, this problem of reactor criticality (and related problems for nuclear weapons!) was the starting point for the first large-scale applications of Monte-Carlo methods by Fermi, von Neumann, Ulam and their coworkers (see Hammersley and Handscomb 1964 for a more detailed account on the history of Monte Carlo methods).

2.3 An application example: self-avoiding walks

Self-avoiding walks (SAWs) on lattices are widely studied as a simple model for the configurational statistics of polymer chains in good solvents (Kremer and Binder 1988, Sokal 1995). Suppose one considers a square or simple cubic lattice with coordination number z. Then, for a random walk (RW) with N steps, we would have $Z_{RW} = z^N$ configurations but many of these random walks intersect themselves and thus would not be self-avoiding. For SAWs, one only expects of the order of Z_{SAW} configurations, where

$$Z_{SAW} \propto N^{\gamma-1} z_{eff}^N \quad , \quad N \to \infty \quad . \tag{11}$$

Here $\gamma > 1$ is a characteristic exponent {which is believed to be $\gamma = 43/32$ in $d = 2$ dimensions (Nienhuis 1984), while in $d = 3$ dimensions it is only known approximately, $\gamma \approx 1.16$ (Sokal 1995)}, and z_{eff} ($\leq z-1$) is an "effective" coordination number (also not known exactly). But it is already obvious that an exact enumeration of all configurations would be possible for rather small N only, while most questions of interest refer to the behavior for large N, and though there do exist sophisticated techniques for the extrapolation of exact enumerations to large N (e.g. Guttmann 1989 and references therein), the use of these methods is fairly limited, and is not discussed here further. Here we are only concerned with Monte Carlo techniques to estimate quantities such as γ or z_{eff} or other quantities of interest, such as the end-to-end distance of the SAW,

$$\left\langle R^2 \right\rangle_{SAW} = \frac{1}{Z_{SAW}} \sum_{\vec{X}} \left[\vec{R}(\vec{X})\right]^2 \quad . \tag{12}$$

Here the sum is extended over all configurations of SAWs which we denote formally as points $\vec{X}$ in phase space. One expects that

$$\langle R^2 \rangle_{SAW} \propto N^{2\nu}, N \to \infty, \tag{13}$$

where ν is another characteristic exponent {$\nu = 3/4$ in $d = 2$ (Nienhuis 1985), while in $d = 3$ ν is only approximately known, $\nu \approx 0.588$ (Sokal 1995)}.

A Monte Carlo estimation of $\langle R^2 \rangle_{SAW}$ now is based on generating a sample of only $M << Z_{SAW}$ configurations $\vec{X}_i$, i.e.

$$\overline{R^2} = \frac{1}{M} \sum_{i=1}^{M} \left[\vec{R}(\vec{X}_i)\right]^2 \approx \langle R^2 \rangle_{SAW} \tag{14}$$

In the simple sampling generation of SAWs, the M configurations are statistically independent and hence standard error analysis applies. Thus we expect that the relative error behaves as

$$\frac{\overline{(\delta R^2)^2}}{\left(\overline{R^2}\right)^2} \approx \frac{1}{M-1} \left[\frac{\left\langle R^4 \right\rangle_{SAW}}{\langle R^2 \rangle_{SAW}^2} - 1 \right] \tag{15}$$

The law of large number then implies that $\overline{R^2}$ is gaussian distributed around $\langle R^2 \rangle_{SAW}$ with a variance determined by Eq. (15). One should note, however, that this variance does not decrease with increasing N. Statistical mechanics tells us that fluctuations decrease with increasing number N of degrees of freedom; i.e., one equilibrium configuration differs in its energy $E(\vec{X})$ from the average $\langle E \rangle$ only by an amount of order $1/\sqrt{N}$. This property is called "self-averaging". Obviously, such a property is not true for $\langle R^2 \rangle_{SAW}$. This "lack of self-averaging" (Milchev et al. 1986) is easy to show already for ordinary random walks (Binder and Heermann 1988).

The simple sampling technique can be generalized from these strictly athermal SAWs (alternatively we may think of the excluded volume interaction of an infinitely high repulsive potential if two different monomers occupy the same site) to thermal problems. Suppose an attractive energy $-\varepsilon$ ($\varepsilon > 0$) is won if two monomers occupy nearest neighbor sites on the lattice. It is then of interest to study the internal energy $\langle \mathcal{H} \rangle_T$ of the chain as well as the chain average linear dimensions (such as $\left\langle \vec{R}^2 \right\rangle_T$) as a function of the reduced temperature $k_B T/\varepsilon$. One expects that for $N \to \infty$ a special temperature $T = \theta$ occurs, the Theta point where the chain dimensions scale like ordinary random walks, $\left\langle R^2 \right\rangle_\theta \propto N$ (de Gennes 1979, Jannink and des Cloizeaux 1990), while for $T < \theta$ chains are collapsed ($\left\langle R^2 \right\rangle_{T<\theta} \propto N^{2/3}$).

Since a configuration with n nearest-neighbor contacts has a Boltzmann weight factor proportional to $\exp(n\varepsilon/k_B T)$, one needs to keep track of the (unnormalized) distributions that describe how often a quantity (such as $\vec{R}$) occurs together with having n nearest neighbor

contacts. Specifically, the Monte Carlo sampling attempts to sample $p_N(n,\vec{R}) = Z_N^{SAW}(n,\vec{R})/Z_N^{NRRW}$, where Z_N^{SAW} is the total number of SAW configurations of N steps with n nearest neighbor contacts and an end-to-end vector $\vec{R}$. The normalizing factor Z_N^{NRRW} is the total number of all simple random walks for which immediate reversals are forbidden ("non-reversal random walk"). Defining $p_N(n) = \int d\vec{R}\; p_N(n,\vec{R})$, the averages of interest are then obtained as

$$\left\langle R^2 \right\rangle_T = \sum_{n,\vec{R}} R^2 \exp(n\varepsilon / k_B T) p_N(n,\vec{R}) / \sum_n \exp(n\varepsilon / k_B T) p_N(n) \;, \tag{16}$$

$$\langle \mathcal{N} \rangle_T = -\varepsilon \sum_n n \exp(n\varepsilon / k_B T) p_N(n) / \sum_n \exp(n\varepsilon / k_B T) p_N(n) \;. \tag{17}$$

Obviously, if $p_N(n,\vec{R})$ has been sampled with sufficient accuracy, one can obtain thermal averages at any desired temperature T, one simulation yields the full range of temperatures. Also thermal derivatives such as those required for the computation of the specific heat per monomer

$$C/k_B = \frac{1}{N} \partial \langle \mathcal{N} \rangle_T / \partial (k_B T) = \frac{1}{N} \left(\left\langle \mathcal{N}^2 \right\rangle_T - \langle \mathcal{N} \rangle_T^2 \right) / (k_B T)^2 \tag{18}$$

can be carried out analytically. Of course, Eq. (18) is not restricted to this SAW example but holds generally.

Techniques of this type have indeed occasionally been used to study non-trivial scientific problems like the scaling properties near the Theta point (e.g. Kremer et al. 1982), or the

adsorption transition of chains at attractive walls (Eisenriegler et al. 1982). In the latter problem, one considers a SAW grafted with one end to an impenetrable planar wall. Whenever a monomer of the walk falls in this surface plane at z = 0, an energy-ε is gained. If we redefine n as the number of monomers in the plane z = 0, Eqs. (16)-(18) hold again. Now there occurs at $T = T_a$ an adsorption transition where the shape of the chain changes from a "mushroom" (for $T > T_a$) to a "pancake" (for $T < T_a$); i.e., for $T > T_a$ the perpendicular component of the mean square gyration radius $\left\langle R_{g\perp}^2 \right\rangle$ obeys the standard scaling while for $T < T_a$ it is finite,

$$\left\langle R_{g\perp}^2 \right\rangle_{T>T_a} \propto N^{2\nu} \quad , \qquad \left\langle R_{g\perp}^2 \right\rangle_{T<T_a} = \xi_\perp^2 \propto (1 - T/T_a)^{-y} \;, \tag{19}$$

where the exponent y characterizing the divergence of the thickness $\xi_\perp$ of the "pancake" is one quantity of interest. While such quantities are easily obtainable from various dynamic Monte Carlo algorithms, simple sampling still is useful for obtaining the exponents characterizing the number of configurations,

$$Z_{SAW}^{mushroom} \propto N^{\gamma_1 - 1} z_{eff}^N \;, T > T_a \;; \; Z_{SAW}^{mushroom} \propto N^{\gamma_1^{SB} - 1} z_{eff}^N \;, T = T_a \;. \tag{20}$$

Fig. 2 shows estimates that have been obtained from corresponding work (Eisenriegler et al. 1982). One analyses there the quantity $g(N) \equiv \ell n\, [Z(T,N)/Z(T,N+2)]$, since Eq. (20) implies that for large N $g(N) = 2\ell n\, z_{eff} + (1 - \gamma_1)(2/N) + \ldots$, and hence a plot of g(N) vs. 2/N should yield a straight line, the slope of which gives γ_1. Note that an increment of 2 from N to N + 2 helps here to avoid even-odd oscillations, that otherwise would occur at the tetrahedral lattice used here.

2.4 Biased sampling; advantages and limitations of simple sampling techniques

Apart from the problem of the lack of self-averaging mentioned above (the accuracy of the estimation of R^2 does not increase with the number of steps of the walk) it is also not easy to generate a large sample of configurations of SAWs for large N: whenever in the construction process of a SAW we attempt to choose a lattice site that is already taken, the attempted walk has to be terminated and the construction has to be started with the first step again. Now the fraction of walks that will continue successfully for N steps will only be of the order of $Z_{SAW} / (z\text{-}1)^N \propto [z_{eff} / (z\text{-}1)]^N N^{\gamma-1}$ which decreases to zero exponentially proportional to $\exp(-N\mu)$ with $\mu = \ln[(z\text{-}1)/ z_{eff}]$ for large N. This failure of success in generating long SAWs is called the "attrition problem".

The obvious recipe, to select at each step not blindly but only from among the lattice sites that do not violate the SAW restriction, does not give equal statistical weight for each configuration generated, of course, and so the average would not be the averaging that one needs in Eq. (12). One finds that this method would create a "bias" toward more compact configurations of the walk. But one can calculate the weights of configurations $w(\bar{X})$ that result in this so-called "inversely restricted sampling" (Rosenbluth and Rosenbluth 1955) and in this way correct for the bias and estimate the SAW averages as

$$\overline{R^2} = \left\{ \sum_{l=1}^{M} \left[w(\bar{X}_l) \right]^{-1} \right\}^{-1} \sum_{l=1}^{M} \left[w(\bar{X}_l) \right]^{-1} \left[\bar{R}(\bar{X}_l) \right]^2 \qquad (21)$$

However, error analysis of this biased sampling is rather delicate because the reweighted distribution is not symmetric around the most probable value and mean values may differ

appreciably from corresponding most probable values (Kremer and Binder 1988, Batoulis and Kremer 1989).

A popular alternative to overcome the above attrition problem is the "enrichment technique", founded on the principle "Hold fast to that which is good". Namely, whenever a walk attains a length that is a multiple of s steps without intersecting itself, n independent attempts to continue it (rather than a single attempt) are made. The numbers n,s are fixed and if we choose $n \approx \exp(\mu s)$, the numbers of walks of various lengths generated will be approximately equal. Enrichment has the advantage over inversely restricted sampling that all walks of a given length have equal weights, while the weights in Eq. (21) vary over many orders of magnitude for large N. But the disadvantage is, on the other hand, that the linear dimensions of the walks are highly correlated, since some of them have many steps in common! Nevertheless, these techniques still have useful applications : a variant of enrichment has been implemented to simulate configurations of star polymers with f arms (each arm grows by one step, $n \approx \exp(\mu f)$ is chosen (Ohno and Binder 1991)); and the Rosenbluth-Rosenbluth method is the starting point of the configurational bias Monte Carlo (CBMC) algorithm that is very successful in the generation of configurations for dense polymer systems (Frenkel 1993).

Due to the problems mentioned above, simple sampling and its extensions are useful only for a small fraction of problems in polymer science (Binder 1995) and now importance sampling (Sec. 3) is much more used. But we emphasize that related problems are encountered for the sampling of "random surfaces" (this problem arises in the field theory of quantum gravity), in path-integral Monte Carlo treatments of quantum problems and in several other contexts.

3. Importance sampling and the Metropolis method

3.1 Importance sampling in the canonical ensemble

In the canonical ensemble we wish to compute averages $\langle A\rangle_T$ of observables $A(\vec{X})$ as defined in Eq. (3), restricting attention to classical statistical mechanics for the moment. For this problem, the simple sampling technique as described in the previous section typically does not work: the probability distribution Eq. (10) has a very sharp peak in phase space in a region where all extensive variables $A(\vec{X})$ are close to their average values $\langle A\rangle$. E.g., we consider the distribution of the energy E per particle, p(E) which is obtained by integrating out all other variables in our system containing N particles

$$p(E) = \frac{1}{Z}\int d\vec{X}\delta\left[\mathcal{H}(\vec{X}) - NE\right]\exp\left[-\mathcal{H}(\vec{X})/k_B T\right] \quad . \tag{22}$$

Noting

$$\langle\mathcal{H}\rangle_T = N\int_{-\infty}^{+\infty} Ep(E)dE \quad , \qquad \left\langle\mathcal{H}^2\right\rangle_T = N^2\int_{-\infty}^{+\infty} E^2 p(E)dE \tag{23}$$

and invoking the general fluctuation relation for the specific heat C per particle, Eq. (18), we conclude that p(E) must have a peak of height proportional to $\sqrt{N}$ and width proportional to $1/\sqrt{N}$ near $E = \langle\mathcal{H}\rangle_T/N$. In fact, away from phase transitions p(E) is actually Gaussian (Landau and Lifshitz 1958)

$$p(E) \propto \exp\{-[E-\langle\mathcal{H}\rangle_T/N]^2\, N/(2Ck_B T^2)\} \tag{24}$$

Now it is clear that with a simple sampling procedure only very rarely can we expect to generate a phase space point $\vec{X}$ with energy E in the region of this sharp peak. This problem is very serious because it applies simultaneously to several variables. Consider for instance an Ising model of a ferromagnet,

$$\mathcal{H}_{Ising} = -J\sum_{(ij)} S_i S_j - H\sum_i S_i \, , \quad S_i = \pm 1 \quad , \tag{25}$$

where Ising spins sit on sites i of a regular lattice, <ij> is a summation over nearest neighbor pairs, J the exchange constant, H the magnetic field, and the phase space for this problem $\vec{X}$ is the set of all possible spin orientations $\{S_1 = \pm 1, S_2 = \pm 1, \ldots, S_N = \pm 1\}$. A quantity of interest $A(\vec{X})$ then is the magnetization per spin,

$$m = (1/N)\sum_i S_i \tag{26}$$

Again we conclude that the distribution p(m) will be very sharply peaked around the average value $\langle m\rangle_T$ (for temperatures T less than the critical temperature T_c there occur in fact two peaks at $\pm m_{sp}$, according to the two possible signs of the spontaneous magnetization m_{sp}). Fig. 3 illustrates that indeed very sharply peaked distributions are obtained for rather small systems.

Suppose now we would do simple sampling for the Ising model, i.e. we choose the spin orientations completely at random: the resulting distribution of m is a gaussian centered at zero of width $1/\sqrt{N}$, $P^{SS}(m) \propto \exp^2(-m^2N/2)$ {SS stands for "simple sampling"}. Obviously, this distribution would have hardly any overlap with the actual distribution P(m) at thermal equilibrium, cf. Fig. 3. The same is true for P(E) {note that for Eq. (25) P^{SS} (E) also is a

gaussian centered at zero}. Thus, by simple sampling most of the computational effort would be wasted for exploring a completely uninteresting part of the phase space.

Therefore, a method is needed that leads us automatically in the important region of phase space, sampling points preferentially from the region which yields the peak of distributions such as P(m), P(E), etc. Such a method actually exists, the importance sampling scheme of Metropolis et al. [3] chooses the states $\vec{X}_\nu$ with a probability $P(X_\nu)$ that is proportional to the Boltzmann factor, $P_{eq}(\vec{X}_\nu)$, Eq. (10). Thus the average over the sample of M phase space points $\{\vec{X}_\nu\}$

$$\overline{A(\vec{X})} = \frac{\sum_{t=1}^{M} \exp\left[-\mathcal{H}(\vec{X}_t)/k_B T\right] A(\vec{X}_t)/P(\vec{X}_t)}{\sum_{t=1}^{M} \exp\left[-\mathcal{H}(\vec{X}_t)/k_B T\right]/P(\vec{X}_t)} \qquad (27)$$

reduces to a simple arithmetic average,

$$\overline{A(\vec{X})} = \frac{1}{M}\sum_{t=1}^{M} A(\vec{X}_t) \quad . \qquad (28)$$

Unlike simple sampling {$P(\vec{X}_t)$ = const in Eq. (27)} all members of the considered sample contribute with equal weight to the average which clearly is desirable. The problem is, of course, to find a procedure which practically realizes this so-called "importance sampling" (where one chooses the phase space points not at all completely at random but samples them preferentially from this region of phase space which is most important for the average, with the given choice of external parameters that define the chosen statistical ensemble, such as T and H for the canonical ensemble of an Ising magnet). This problem was solved by Metropolis et al. (1953) who proposed to generate a sequence of states $\vec{X}_\nu \rightarrow \vec{X}_{\nu+1} \rightarrow \vec{X}_{\nu+2} \rightarrow \ldots$ recursively one from the other, with a carefully designed transition probability $W(\vec{X}_\nu \rightarrow \vec{X}_{\nu+1})$. From the theory of Markov processes, one can show that the Markov chain of states $\vec{X}_\nu$ for $M \rightarrow \infty$ generates a sample $\{\vec{X}_\nu\}$ that is distributed according to the canonical distribution, Eq. (10).

The "move" $\vec{X} \rightarrow \vec{X}'$ may be chosen as is convenient for the considered model: for the Ising magnet, this may be a single spin flip, an exchange of two neighboring spins, or the overturning of a large cluster of spins (Swendsen et al. 1992); for a fluid, the move may be a random displacement of a particle from its old position $(\vec{r}_i)$ to a new position $(\vec{r}_i')$ in its environment (Metropolis et al. 1953, Wood 1968, Allen and Tildesley 1987); for a self-avoiding walk, the move may be a "kink-jump" or "crankshaft" rotation of a group of two or three neighboring bonds (Verdier and Stockmayer 1962, Kremer and Binder 1988), a "slithering-snake"-displacement of a bond from one chain end to the other in a randomly chosen direction (Wall and Mandel 1975), or a "pivot move" where one rotates one part of the chain at a randomly chosen bead against the rest of the chain in a randomly chosen direction (Madras and Sokal 1988, Sokal 1995). These moves are illustrated in Fig. 4.

It must be emphasized, however, that in some cases it is very difficult to find acceptable moves. E.g., for polymers due to the connectivity of the chains many algorithms suffer from a lack of ergodicity. E.g., for SAWs there may occur certain configurations that may neither be relaxed nor be reached by a particular algorithm (Sokal 1995). In fact, both algorithms of Fig. 4a,b suffer somewhat from this problem, although it is believed that this problem is not so serious in practice (Kremer and Binder 1988). Another problem may be a very low acceptance

probability of a move. E.g., in a dense system containing many polymeric chains the "pivot moves" (Fig. 4c) almost always will violate the exclude volume constraint that no lattice site can be occupied by more than one bead, and hence the moves are disallowed. For off-lattice problems, it often is a non-trivial matter to carry out moves such that in the absence of the Boltzmann weight phase space is uniformly sampled {as it should be, cf. Eq. (3)}. Thus, designing more efficient "moves" still is an active area of research (Binder 1992b, 1995), particularly for SAWs (Sokal 1995).

Now convergence of this Markov process towards thermal equilibrium is ensured by imposing the condition of detailed balance,

$$P_{eq}(\bar{X})\, W(\bar{X} \to \bar{X}') = P_{eq}(\bar{X}')\, W(\bar{X}' \to \bar{X}) . \tag{29}$$

A convenient choice (Metropolis et al. 1953) that satisfies Eq. (29) is expressed in terms of the energy change $\delta\mathcal{H} \equiv \mathcal{H}(\bar{X}') - \mathcal{H}(\bar{X})$ caused by the move

$$W(\bar{X} \to \bar{X}') = \begin{cases} \tau_0^{-1} , & \delta\mathcal{H} < 0 , \\ \tau_0^{-1} \exp(-\delta\mathcal{H}/k_B T) , & \delta\mathcal{H} > 0 . \end{cases} \tag{30}$$

Here arbitrarily a time constant τ_0 was introduced setting a time scale, so that W acquires the meaning of a transition probability per unit time (which is useful in the context of the dynamic interpretation of Monte Carlo averaging, to be discussed in Subsec. 3.4). One chooses one Monte Carlo step (MCS) per particle as the unit of this Monte Carlo "time". Obviously, Eq. (29) is satisfied by the choice Eq. (30) irrespective of τ_0.

Here we shall not give a general proof that Eq. (29) suffices that states $\bar{X}_\nu$ are asymptotically (i.e., for large M) chosen with the correct Boltzmann weight (see e.g. Wood 1968, Kalos and Whitlock 1986) but we simply follow Metropolis et al. (1953) in quoting a plausibility argument to show this. Let us consider a large number of Markov chains in parallel. We assume that at a given step of the process there are N_r systems in state r, N_s systems in state s, etc.; and that $\mathcal{H}(\bar{X}_r) < \mathcal{H}(\bar{X}_s)$. Using random numbers, one may construct moves $\bar{X}_r \to \bar{X}_s$, as will be discussed below. Disregarding the energy change $\delta\mathcal{H}$, the transition probability for these moves should be symmetric, i.e. $W_{\delta\mathcal{H}=0}(\bar{X}_r \to \bar{X}_s) = W_{\delta\mathcal{H}=0}(\bar{X}_s \to \bar{X}_r)$. With these "a priori transition probabilities" (also called "proposition probabilities") $W_{\delta\mathcal{H}=0}$, it is easy to construct transition probabilities which are in accord with Eqs. (29), (30), namely

$$W(\bar{X}_r \to \bar{X}_s) = W_{\delta\mathcal{H}=0}(\bar{X}_r \to \bar{X}_s) \exp\{-[\mathcal{H}(\bar{X}_s) - \mathcal{H}(\bar{X}_r)]/k_B T\}, \tag{31a}$$

$$W(\bar{X}_s \to \bar{X}_r) = W_{\delta\mathcal{H}=0}(\bar{X}_s \to \bar{X}_r) = W_{\delta\mathcal{H}=0}(\bar{X}_R \to \bar{X}_s) . \tag{31b}$$

The total number $N_{r\to s}$ of transitions from $\bar{X}_R$ to $\bar{X}_s$ at this step of the Markov chains is

$$N_{r\to s} = N_r W(\bar{X}_r \to \bar{X}_s) = N_r\, W_{\delta\mathcal{H}=0}(\bar{X}_r \to \bar{X}_s) \exp\{-[\mathcal{H}(\bar{X}_s) - \mathcal{H}(\bar{X}_r)]/k_B T\}, \tag{32}$$

while the total number of inverse transitions is

$$N_{s\to r} = N_s W(\bar{X}_s \to \bar{X}_r) = N_s\, W_{\delta\mathcal{H}=0}(\bar{X}_r \to \bar{X}_s) \tag{33}$$

Now the net number of transitions $\Delta N_{r\to s}$ becomes

$$\Delta N_{r\to s} = N_{r\to s} - N_{s\to r} = N_r\, W_{\delta\mathcal{H}=0}(\vec{X}_r \to \vec{X}_s)\left(\frac{\exp\left[-\mathcal{H}(\vec{X}_s)/k_BT\right]}{\exp\left[-\mathcal{H}(\vec{X}_r)/k_BT\right]} - \frac{N_s}{N_r}\right) \qquad (34)$$

Eq. (34) is the key result of this argument which shows that the Markov process has the desired property that states occur with probability proportional to the canonic probability $P_{eq}(\vec{X})$ as given in Eq. (10). As long as N_s/N_r is smaller than the ratio of the canonic probabilities we have $\Delta N_{r\to s} > 0$, i.e. the ratio N_s/N_r increases towards the ratio of canonic probabilities; conversely, if N_s/N_r is larger than the "canonic ratio", $\Delta N_{r\to s} < 0$ and hence again N_s/N_r decreases towards the correct canonic ratio. Thus asymptotically for $t \to \infty$ a steady-state distribution is reached, where N_s/N_r has precisely the value required by the canonic distribution. Instead of considering many Markov chains in parallel, we may equivalently cut one very long Markov chain into equally long pieces and apply the same argument to the subsequent pieces of the chain.

3.2 Some comments on models and algorithms

We return to the question what is meant in practice by the transition from $\vec{X}$ to $\vec{X}'$. It has already been emphasized above that there is a considerable freedom in the choice of this move but one has to be careful to ensure large enough acceptance rates. Since Eq. (29) implies that $W(\vec{X} \to \vec{X}')/W(\vec{X}' \to \vec{X}) = \exp(-\delta\mathcal{H}/k_BT)$, $\delta\mathcal{H}$ being the energy change caused by the move from $\vec{X} \to \vec{X}'$, typically it is necessary to consider small changes of the $\vec{X}$ only. Otherwise the absolute value of the energy change $|\delta\mathcal{H}|$ would be rather large, and then either $W(\vec{X} \to \vec{X}')$ or $W(\vec{X}' \to \vec{X})$ would be very small. Then it would be almost always forbidden to carry

out that move and the procedure would be poorly convergent. Of course, there are exceptions to this rule, like the cluster algorithms for Ising models and other spin models at the critical point (Swendsen et al. 1992), or the semi-grand canonical algorithm for binary (AB) symmetrical polymer mixtures (Sariban and Binder 1987) where one takes out a whole polymer chain containing N monomers of one type, and replaces it by a polymer chain in the same configuration but of different type. All such exceptions are rather special and require special reasons to work: e.g., in this polymer example the temperatures of interest are very large, of order $k_BT \propto \varepsilon N$, where ε is the interaction energy between a pair of monomers, and although $|\delta\mathcal{H}|$ is of order N $|\delta\mathcal{H}/k_BT|$ is still of order unity!

We now consider a few examples of models that can be studied easily with Monte Carlo methods, and of the corresponding moves that are used, so the reader can get a flavor of how one proceeds in practice. In the lattice gas model at constant particle number, a transition $\vec{X} \to \vec{X}'$ may consist of moving one particle to a randomly chosen neighboring site. In the lattice gas at constant chemical potential, one removes (or adds) just one particle at a time which is isomorphic to single flips in the Ising model of anisotropic magnets. Fig. 5 now illustrates some of the moves commonly used for a variety of models under study in statistical mechanics. For the Ising model the most commonly used algorithms are the single spin-flip algorithm and the spin-exchange algorithm (Fig. 5a,b). The single spin-flip algorithm obviously does not leave the total magnetization of the system invariant, while the spin-exchange algorithm does. Thus, these algorithms correspond to realizations of different thermo-dynamic ensembles: (a) realizes a "grand-canonical" ensemble, temperature T and field H being the independently given thermodynamic variables, conjugate thermodynamic quantities (the magnetization $\langle m\rangle_T$ is conjugate to H) need to be calculated. Fig. 5b realizes a "canonical" ensemble, T and m being

the independently given variables, now the field $\langle H \rangle_T$ is the conjugate variable we may wish to calculate from the simulation.

In calling the (T,H) ensemble "grand-canonical" and the (T,m) ensemble "canonical", we apply a language appropriate to the lattice gas interpretation of the Ising model where the spin S_i is reinterpreted as a local density $\rho_i = (1-S_i)/2$ (= (0,1)). Then $\langle m \rangle_T$ is related to the average density $\langle \rho_i \rangle_T$ as $\langle m \rangle_T = 1 - 2 \langle \rho_i \rangle_T$, and H is related to the chemical potential of the particles which may occupy the lattice sites.

In the thermodynamic limit $N \to \infty$, different ensembles in statistical mechanics yield equivalent results. Thus, the choice of the ensemble and hence the associate algorithm may seem a matter of convenience. However, finite-size effects are quite different in the various ensembles, and also "rates" at which equilibrium is approached in a simulation will differ. Thus, the choice of the appropriate ensemble is a delicate matter. Using the word "rate", we have in mind the dynamic interpretation (Müller-Krumbhaar and Binder 1973) of the Monte Carlo process: then case a) realizes the Glauber (1963) kinetic Ising model which is a purely relaxational model without any conservation laws, while Fig. 5b realizes the Kawasaki (1972) kinetic Ising model which conserves magnetization.

For models with continuous degrees of freedom, such as XY or Heisenberg magnets

$$\mathcal{H}_{XY} = -J \sum_{\langle i,j \rangle} \left(S_i^x S_j^x + S_i^y S_j^y \right) - H_x \sum_i S_i^x , \quad \left(S_i^x\right)^2 + \left(S_i^y\right)^2 = 1 \quad , \tag{35}$$

$$\mathcal{H}_{Hei} = -J \sum_{\langle i,j \rangle} \left(\vec{S}_i \cdot \vec{S}_j \right) - H_z \sum_i S_i^z , \quad \vec{S}_i \cdot \vec{S}_i = \left(S_i^x\right)^2 + \left(S_i^y\right)^2 + \left(S_i^z\right)^2 = 1 \quad , \tag{36}$$

but also for models of fluids (Fig. 5 c,d), it often is advisable to choose the new degree(s) of freedom of a particle not completely at random but rather in an interval around their previous values. This interval can then be adjusted such that the average acceptance rate for the trial moves considered in Fig. 5 does not get too small.

It may also be inconvenient (or even impossible) to sample the full phase space for a single degree of freedom uniformly. For example, we cannot sample ϕ_i in Fig. 5(e) uniformly from the interval $[-\infty, +\infty]$. Such a problem arises for the so-called ϕ^4 model,

$$\mathcal{H}_{\phi 4} = \sum_r \left(\frac{1}{2} A \phi_i^{\,2} + \frac{1}{4} B \phi_i^{\,4} \right) + \sum_{\langle i,j \rangle} \frac{1}{2} C \left(\phi_i - \phi_j \right)^2 \quad , -\infty < \phi_i < +\infty \quad , \tag{37}$$

A,B,C being constants (for $A < 0, B > 0$ the single site potential $V(\phi_i) = \frac{1}{2} A \phi_i^{\,2} + \frac{1}{4} B \phi_i^{\,4}$ has the double-minimum shape of Fig. 5(e)). There it is advisable to choose the ϕ_i's already from an importance sampling scheme, i.e. one constructs an algorithm which generates the ϕ_i proportional to the distribution $p(\phi_i) \propto \exp[-V(\phi_i)/k_B T]$, as discussed in Eqs. (8),(9).

Another arbitrariness concerns the order in which the particles are selected for considering a move. Often one chooses to select them in the order of their labels (in the simulation of a fluid or lattice gas at constant particle number) or go through the lattice in a regular typewriter-type fashion (in the case of spin models, for instance). For lattice systems, it may be convenient to use sublattices. E.g. in the "checkerboard algorithm" the white and black sublattices are updated alternatively, for the sake of an efficient "vectorization" of the program (see e.g. Landau 1992). An alternative is to choose the lattice sites (or particle numbers) randomly; this is more time-consuming but is preferable if one is interested in dynamical properties (we again

anticipate here that the Monte Carlo process can be interpreted as a dynamical evolution of a model described by a master equation, see Sec. 3.4).

It is also helpful to realize that often the transition probability $W(\vec{X} \to \vec{X}')$ can be written as a product of an "attempt frequency" times an "acceptance frequency". By clever choice of the attempt frequency, it is sometimes possible to attempt large moves and still have a high acceptance and thus make the computations more efficient.

We also emphasize that the detailed balance principle {Eq. (29)} does not fix the choice of the transition probability $W(\vec{X} \to \vec{X}')$ uniquely. An alternative to Eq. (30) is the "heat bath method". There one assigns the new value α_i' of the i'th local degree of freedom in the move from $\vec{X}$ to $\vec{X}'$ irrespective of what the old value α_i was. One therefore considers the local energy $\mathcal{H}_i$ (α_i') and chooses the state α_i' with probability $\exp[-\mathcal{H}_i(\alpha_i')/k_BT]/\sum_{\{\alpha_i''\}} \exp\left[-\mathcal{H}_i\left(\alpha_i''\right)/k_BT\right]$. We now outline the realization of the sequence of states $\vec{X}$ with chosen transition probability W. At each step of the procedure, one performs a trial move $\alpha_i \to \alpha_i'$, computes $W(\vec{X} \to \vec{X}')$ for this trial move, and compares it with a random number η, uniformly distributed in the interval $0 < \eta < 1$. If $W < \eta$, the trial move is rejected, and the old state (with α_i) is counted once more in the average, Eq. (28). Then another trial is made. If $W > \eta$, on the other hand, the trial move is accepted, and the new configuration thus generated is taken into account in the average. This new state then also serves as a starting point for the next step.

Since subsequent states $\vec{X}_\nu$ in this Markov chain differ by the coordinate α_i of one particle only (if they differ at all), they are highly correlated. Therefore, it is not straightforward to estimate the error of the average, Eq. (28). Let us assume for the moment that, after n steps, these correlations have died out. Then we may estimate the statistical error δA of the estimate $\overline{A}$ from the standard formula,

$$\overline{(\delta A)^2} = \frac{1}{k(k-1)} \sum_{\mu=\mu_0}^{k+\mu_0-1} \left[A\left(\vec{X}_\mu\right) - \overline{A}\right]^2 \quad , \quad k >> 1 \tag{38}$$

where the integers μ_0, μ, k are defined by $k = (M-M_0)/n$, μ_0 labels the state $\nu = M_0 + 1$, $\mu = \mu_0 + 1$ the state $\nu = M_0 + n + 1$, etc. Then for consistency $\overline{A}$ should be calculated as

$$\overline{A} = \frac{1}{k} \sum_{\mu=\mu_0}^{k+\mu_0-1} A\left(\vec{X}_\mu\right) \quad . \tag{39}$$

In Eqs. (38),(39) we have anticipated that one has to omit the first M_0 states that are not yet characteristic for thermal equilibrium, from the average. If the computational effort of carrying out the "measurement" of $A\left(\vec{X}_\mu\right)$ in the simulation is rather small, it is advantageous to keep taking measurements every Monte Carlo step per degree of freedom but to construct block averages over n succesive measurements, varying n until uncorrelated block averages are obtained.

3.3 An application example: The Ising model

Suppose we wish to simulate the nearest neighbor Ising ferromagnet on a LxLxL simple cubic lattice measuring lengths in units of the lattice spacing so $N = L^3$, and using periodic boundary conditions and the single spin flip algorithm. We first specify an initial spin configuration, e.g. all spins are initially pointing up. Now one repeats again and again the following steps:

1. Select one lattice site i at which the S_i is considered for flipping ($S_i \rightarrow - S_i$).
2. Compute the energy change $\delta\mathcal{H}$ associated with that flip.
3. Calculate the transition probability $\tau_0 W$ for that flip.
4. Draw a random number η uniformly distributed between zero and unity.
5. If $\eta < \tau_0 W$ flip the spin, otherwise do not flip it. In any case, the configuration of the spins obtained in this way at the end of step (5) is counted as a "new configuration".
6. Analyze the resulting configuration as desired, store its properties to calculate the necessary averages. For example, if we are just interested in the (unnormalized) magnetization M_{tot} and its distribution $P(M_{tot})$, we may update M_{tot} by replacing M_{tot} by $M_{tot} + 2S_i$, and then replacing $P(M_{tot})$ by $P(M_{tot}) + 1$ (appropriate initial values before the process starts are set to $M_{tot} = L^3$, P(M') = 0, P(M') being an array where M' can take integer values from $- L^3$ to $+ L^3$).

It should be clear from the above list that it is fairly straightforward to generalize this kind of algorithm {see e.g. Binder and Heermann (1988) for an explicit listing of a corresponding FORTRAN program} to systems other than Ising models, such as considered in Fig. 5. The words "spin" and "flip (ping)" simply have to be replaced by the appropriate words for that system. We also note that one can save computer time by storing at the beginning of the calculation the small number of different values $\{W_k\}$ that the transition probability W for spin

flips may have, rather than evaluating the exponential function again and again. This "table method" works for all problems with discrete degrees of freedom, not only for the Ising model.

At very low temperatures in the Ising model, nearly every attempt to flip a spin is bound to fail. One can construct a more complicated but quicker algorithm by keeping track of the number of spins with a given transition probability W_k at each instant of the simulation. Choosing now a spin from the k'th class with a probability proportional to W_k, one can make every attempted spin flip successful (Bortz et al. 1975). An extension of this algorithm to the spin-exchange model has also been given (Sadiq 1984). A systematic generalization of such techniques due to Novotny (1995) yields huge speed-ups in the study of metastable states and their decay at low temperatures.

When we now use a simulation program for the Ising model that records the distribution function of the total magnetization $P(M_{tot})$ or the related distribution $P_L(s)$ of a normalized quantity $s = M_{tot}/L^d$ (d being the dimensionality of the system) we will find that it is a non-trivial matter to judge where (in the absence of symmetry-breaking magnetic fields) the expected transition from a paramagnetic state (with $\langle s \rangle \equiv 0$) to a ferromagnetic state takes place (where a spontaneous magnetization $\pm m_{spont}$ exists). In fact, one finds that $P_L(s)$ changes very gradually from a symmetric single peak distribution above T_c to a symmetric double peak distribution below T_c, and the symmetry $P_L(s) = P_L(-s)$ implies that $\langle s \rangle \equiv 0$ at all temperatures (Fig. 6). For $T > T_c$ and linear dimensions L exceeding the correlation length ξ of order parameter fluctuations ($\xi \propto |T-T_c|^{-\nu}$), this distribution resembles a gaussian,

$$P_L(s) = L^{d/2} (2\pi k_B T \chi^{(L)})^{1/2} \exp[-s^2 L^d/(2k_B T \chi^{(L)})], \; T > T_c, \; H = 0. \qquad (40)$$

The "susceptibility" $\chi^{(L)}$ defined in Eq. (40) from the half-width of the distribution should smoothly tend towards the susceptibility χ of the infinite system as $L \to \infty$ (remember $\chi \propto |T-T_c|^{-\gamma}$). For $T < T_c$ but again $L >> \xi$, the distribution is peaked at values $\pm s_{max}^{(L)}$ near $\pm m_{sp}$; near those peaks again a description in terms of Gaussians applies approximately,

$$P_L(s) = \frac{L^{d/2}}{\left(2\pi k_B T \chi^{(L)}\right)^{1/2}} \left\{ \frac{1}{2} \exp\left[- \frac{\left(s - s_{max}^{(L)}\right)^2 L^d}{2 k_B T \chi^{(L)}} \right] + \frac{1}{2} \exp\left[- \frac{\left(s + s_{max}^{(L)}\right)^2 L^d}{2 k_B T \chi^{(L)}} \right] \right\} \quad , \quad (41)$$

for $T < T_c$, $H = 0$.

We thus can obtain an estimate for the order parameter when we restrict attention to only the positive part of the distribution,

$$\langle s \rangle_L' = \int_0^\infty s P_L(s) ds \Big/ \int_0^\infty P_L(s) ds = \langle |s| \rangle_L \quad . \quad (42)$$

But from Eqs. (40),(42) it is clear that for finite L $\langle |s| \rangle_L$ is non-zero also in the disordered phase and thus the smooth non-singular temperature variation of $\langle |s| \rangle_L$ results that is shown qualitatively in Fig. 6. Other estimates for m_{spont} can be extracted from the position of the maximum $s_{max}^{(L)}$ or the root mean square magnetization $\left\langle s^2 \right\rangle_L^{1/2}$, but Fig. 7 clearly shows that all these estimates do depend on the length scale L, and thus an extrapolation to the thermodynamic limit, $L \to \infty$, clearly is required:

$$m_{spont} = \lim_{L \to \infty} s_{max}^{(L)} = \lim_{L \to \infty} \langle |s| \rangle_L = \lim_{L \to \infty} \left\langle s^2 \right\rangle_L^{1/2} \quad . \quad (43)$$

All these extrapolations are more convenient to use than the double limiting procedure that is often used in analytical work where a symmetry-breaking field is taken to zero after the thermodynamic limit has been taken,

$$m_{spont} = \lim_{H \to 0} \lim_{L \to \infty} \langle s \rangle_{L,T,H} \quad . \quad (44)$$

Fig. 7 illustrates the fact that one can avoid the cumbersome study of many different sizes of (small) systems by rather analyzing subsystems of one large system. As we will see below, doing this with the single-spin-flip-algorithm described above is not really convenient because of "critical slowing down" but this problem can be eased by using cluster algorithms instead (Sec. 7). In any case, near T_c the size effects are clearly very pronounced and thus the naive extrapolation as shown in Fig. 7 is not very accurate. This problem is even more severe for the susceptibility χ, which could be extracted from the following extrapolations (Δs is the half-width of a gaussian peak)

$$k_B T \chi = \lim_{L \to \infty} \left(\left\langle s^2 \right\rangle_L L^d \right) = \lim_{L \to \infty} P_L^{-2}(0) L^d / (2\pi) = \lim_{L \to \infty} (\Delta s)^2 L^d / (8 \ln 2) \quad , \quad T > T_c \quad (45)$$

or

$$k_B T \chi = \lim_{L \to \infty} \left(\left\langle s^2 \right\rangle_L - \langle |s| \rangle_L^2 \right) L^d = \lim_{L \to \infty} P_L^{-2}\left(s_{max}^{(L)} \right) L^d / (8\pi) = \lim_{L \to \infty} (\Delta s)^2 L^d / (8 \ln 2) \quad , T < T_c \quad (46)$$

A more efficient way of carrying out this extrapolation to the thermodynamic limit will be provided by the finite size scaling theory (Sec. 4).

3.4 The dynamic interpretation of Monte Carlo sampling; statistical errors; time-displaced correlation functions

Configurations generated sequentially one from the other in the Markov chain are highly correlated with each other. Clearly, these correlations strongly affect the accuracy that can be obtained with a given number of total steps by the Monte Carlo program. These correlations can be understood by a dynamic interpretation of the Monte Carlo process in terms of a master equation describing a well defined dynamic model with stochastic kinetics (Müller-Krumbhaar and Binder 1973). At the same time, this forms the basis for the application of Monte Carlo methods to the simulation of dynamic processes (Binder and Kalos 1979, Kehr and Binder 1984, Binder and Young 1986, Herrmann 1986, Baumgärtner 1985, Binder 1995). These dynamic applications include such diverse fields as the Brownian motion of macromolecules (Baumgärtner 1985, Binder 1995), relaxation phenomena in spin glasses (Binder and Young 1986), nucleation and spinodal decomposition (Binder and Kalos 1979, Gunton et al. 1983), diffusion-limited aggregation (DLA) and related growth phenomena (Herrmann 1986), diffusion in alloys (Kehr and Binder 1984) and at surfaces (Sadiq and Binder 1983), etc. Note that the references just quoted actually constitute only a small sample of all existing work!

In this dynamic interpretation, we just associate a "time" t with the scale ν of the subsequent configurations, normalizing the time scale such that $N\tau_0^{-1}$ single-particle transitions are attempted in unit time. This "time" unit is called 1 MCS (Monte Carlo step per particle). We consider the probability $P(\vec{X},t) = P(\vec{X},\nu)$ that at time t a configuration $\vec{X}$ occurs in the Monte Carlo process. This probability satisfies a Markovian master equation

$$\frac{dP(\vec{X},t)}{dt} = -\sum_{\vec{X}'} W(\vec{X}\to\vec{X}')P(\vec{X},t) + \sum_{\vec{X}'} W(\vec{X}'\to\vec{X})P(\vec{X}',t) \qquad (47)$$

Eq. (47) describes the balance that was considered already above {Eqs. (31)-(34)} by a rate equation, the first sum on the right-hand side representing all processes where one moves away from the considered state $\vec{X}$ (and hence its probability decreases) while the second sum contains all reverse processes (which hence lead to an increase of the probability of finding $\vec{X}$). In thermal equilibrium the detailed balance principle {Eq. (29)} ensures that these two sums always cancel and hence for $P(\vec{X},t) = P_{eq}(\vec{X})$ we have $dP(\vec{X},t)/dt = 0$, as is required. In fact, $P_{eq}(\vec{X})$ is the steady-state solution of the above master equation.

If the potential energy $\mathcal{H}(\vec{X})$ is finite for all configurations $\{\vec{X}\}$ of the system, it follows from the finiteness of the system that it is ergodic. However, as soon as infinite potentials occur (such as the excluded-volume interaction for self-avoiding walks), this is no longer true. Even in finite systems certain configurations $\vec{X}$ may be in disjunct "pockets" of phase space that are mutually inaccessible. There is no general rule under which conditions this happens, it depends on the detailed rules for the considered moves. E.g. for the algorithms of Fig. 4a,b one may construct configurations of SAWs that can neither be reached nor left (Sokal 1995), and so the algorithms of Figs. 4a,b are manifestly non-ergodic - although this does not seem to affect the accuracy in practice much (Sariban and Binder 1988).

A practically more important apparent "breaking of ergodicity" occurs for systems which are ergodic if the "time" over which one averages is not long enough, i.e. less than the so-called "ergodic time" τ_e (Palmer 1982, Binder and Young 1986). This ergodicity-breaking is intimately related to spontaneous symmetry-breaking associated with phase transitions in the

system. In a strict sense, these phase transitions can occur only in the thermodynamic limit N $\rightarrow \infty$, and also τ_e diverges only for N $\rightarrow \infty$ but can nevertheless be very large already for finite N. E.g. for the Ising ferromagnet studied in Sec. 3.3 we have for $T < T_c$ $\tau_e \propto P_L(s_{max})/P_L(s = 0) \propto \exp[2f_{int} L^{d-1}/k_BT]$, where f_{int} is the interfacial tension between coexisting phases of opposite magnetization, as shall be discussed below. Thus $\ln \tau_e \propto N^{1-1/d}$, i.e. τ_e increases rapidly with N for $T < T_c$. Nevertheless, we assume in the following that $\lim_{t\to\infty} P(\bar{X},t) = P_{eq}(\bar{X})$, i.e. the ergodicity property can be realized in practice.

In Eq. (47) we have written $dP(\bar{X},t)/dt$ rather than $\Delta P(\bar{X},t)/\Delta t$, although there is a discrete time increment $\Delta t = \tau_0/N$. This step is justified since one can consider Δt as a continuous variable stochastically fluctuating with distribution $(N/\tau_0) \exp[-\Delta t N/\tau_0]$ which has a mean value $\overline{\Delta t} = \tau_0/N$. Since the time scale on which dynamic correlations decay is at least of the order of τ_0, these fluctuations of the "time" variable proceeding in regular steps $\Delta t = \tau_0/N$ are not important for the calculation of time-displaced correlation functions. The inhomogeneous updating of "time", however, is crucial when one uses the "n-fold way" (Bortz et al. 1975) or related algorithms, where particles are chosen for a move proportional to their transition probability W_k.

Thus we reinterpret Eq. (39) as a time average along the stochastic trajectory in phase space, controlled by the master equation for the system, Eq. (47):

$$\overline{A} = \left(t_M - t_{M_0}\right)^{-1} \int_{t_{M_0}}^{t_M} A(t)dt \qquad (48)$$

where t_M $\left(t_{M_0}\right)$ is the time elapsed after $M(M_0)$ configurations have been generated ($t_M = M\tau_0/N$, $t_{M_0} = M_0\tau_0/N$. The time t is related to the label ν of the configurations as $t = \nu\tau_0/N$. Comparing the time average, Eq. (48), with the ensemble average, Eq. (3) which was the starting point of our considerations, it is obvious that ergodicity may be a problem for importance sampling Monte Carlo, as anticipated above.

Time-displaced correlations $\langle A(t)B(0)\rangle_T$ or $\overline{A(t)B(0)}$ are then defined as

$$\overline{A(t)B(0)} = \left(t_M - t - t_{M_0}\right)^{-1} \int_{t_{M_0}}^{t_M - t} A(t+t')B(t')dt' \quad , \qquad t_M - t > t_{M_0} \qquad (50)$$

Of course, one wants that t_{M_0} can be chosen large enough so the system has already relaxed towards equilibrium during the time t_{M_0}, and then the states $\bar{X}(t)$ included in the sampling from t_{M_0} to t_M are already distributed according to the equilibrium distribution, $P(\bar{X},t) = P_{eq}(\bar{X})$, independent of time. But it is also interesting to study the initial non-equilibrium relaxation process by which equilibrium is approached. Then $A(t) - \overline{A}$ depends systematically on the observation time t, and an ensemble average $\langle A(t)\rangle_T - \langle A(\infty)\rangle_T$ is non-zero {remember that $\lim_{t\to\infty} \overline{A} = \langle A\rangle_T = \langle A(\infty)\rangle_T$ if the system is ergodic}. We have defined $\langle A(t)\rangle_T$ as

$$\langle A(t)\rangle_T = \sum_{\bar{X}} P(\bar{X},t)A(\bar{X}) = \sum_{\bar{X}} P(\bar{X},0)A(\bar{X}(t)) \quad . \qquad (51)$$

Here we have reinterpreted the ensemble average involved as an average weighted with $P(\bar{X},0)$ over an ensemble of initial states $\bar{X}(t=0)$ which then evolves as described by the

master equation, Eq. (47). In practice, Eq. (51) is realized by averaging over $n_{run} >> 1$ statistically independent runs,

$$[A(t)]_{av} = n_{run}^{-1} \sum_{l=1}^{n_{run}} A(t,l) \quad , \tag{52}$$

A(t,l) being the observable A recorded at time t in the l-th run of this non-equilibrium Monte Carlo averaging. E.g., these runs may differ in their random number sequence and/or their initial condition $\bar{X}(t = 0)$, etc.

A discussion of the question to which type of problems such master equation descriptions {Eq.s (47)-(52)} are applicable will be deferred to Sec. 5. Here we are rather interested in applying this formalism to a discussion of statistical errors. Suppose n successive observations A_μ, $\mu = 1,..., n$, of a quantity A have been recorded (n>> 1). We consider the expectation value of the square of the statistical error

$$\langle(\delta A)^2\rangle = \left\langle \left[\frac{1}{n} \sum_{\mu=1}^{n} \left(A_\mu - \langle A \rangle \right) \right]^2 \right\rangle = \frac{1}{n^2} \sum_{\mu=1}^{n} \left\langle \left(A_\mu - \langle A \rangle \right)^2 \right\rangle$$

$$+ \frac{2}{n^2} \sum_{\mu_1=1}^{n} \sum_{\mu_2=\mu_1+1}^{n} \left(\langle A_{\mu_1} A_{\mu_2} \rangle - \langle A \rangle^2 \right) \tag{53}$$

Changing the summation index μ_2 to $\mu_2 + \mu$ yields

$$\langle(\delta A)^2\rangle = \frac{1}{n} \left[\langle A^2 \rangle - \langle A \rangle^2 + 2 \sum_{\mu=1}^{n} \left(1 - \frac{\mu}{n} \right) \left(\langle A_0 A_\mu \rangle - \langle A \rangle^2 \right) \right] . \tag{54}$$

Now we transform to the time variable $t = \delta t\mu$, δt being the time interval between two successive observations A_μ, $A_{\mu+1}$ {often it is more efficient to take $\delta t = \tau_0$ or even $10\ \tau_0$ rather than $\delta t = \Delta t = \tau_0/N$, so one need not take observations at every microstep of the procedure}. Transforming the sum to an integral yields ($t_n = n\ \delta t$)

$$\langle(\delta A)^2\rangle = \frac{1}{n} \left\{ \left\langle A^2 \right\rangle - \langle A \rangle^2 + \frac{2}{\delta t} \int_0^{t_n} \left(1 - \frac{t}{t_n} \right) \left[\langle A(0)A(0) \rangle - \langle A \rangle^2 \right] dt = \right.$$

$$= \frac{1}{n} \left(\left\langle A^2 \right\rangle - \langle A \rangle^2 \right) \left\{ 1 + \frac{2}{\delta t} \int_0^{t_n} \left(1 - \frac{t}{t_n} \right) \phi_A(t) dt \right\} \quad . \tag{55}$$

In the last step we have introduced the normalized relaxation function

$$\phi_A(t) = [\langle A(0)A(t) \rangle - \langle A \rangle^2] / [\langle A^2 \rangle - \langle A \rangle^2], \tag{56}$$

with $\phi_A(0) = 1$ and $\phi_A(t \to \infty) = 0$. We define a relaxation time from the integral

$$\tau_A = \int_0^\infty \phi_A(t) dt \tag{57}$$

For $t_n >> \tau_A$ Eq. (55) reduces to

$$\langle(\delta A)^2\rangle = \frac{1}{n} [\langle A^2 \rangle - \langle A \rangle^2] \left(1 + 2\tau_A/\delta t \right) \tag{58}$$

If $\delta t >> \tau_A$, then the second parenthesis in Eq. (58) is unity to a very good approximation, the statistical error then is the same as for simple sampling of uncorrelated data. In the inverse case where $\delta t << \tau_A$ we have

$$\langle(\delta A)^2\rangle \approx \frac{2\tau_A}{n\delta t}[\langle A^2\rangle - \langle A\rangle^2] = \frac{2\tau_A}{t_n}[\langle A^2\rangle - \langle A\rangle^2], \qquad (59)$$

which shows that the statistical error then is independent of the choice of the time interval δt: although for a given averaging time t_n a smaller δt increases the number of observations, it does not decrease the statistical error: only the ratio between the relaxation time τ_A and the observation time t_n matters.

Since τ_A becomes very large near second order phase transitions ("critical slowing down", Hohenberg and Halperin 1977), choice of algorithms that reduce τ_A becomes very important, see Sec. 5.3. On the other hand, careful "measurements" of both $\langle(\delta A)^2\rangle$ and $\langle A^2\rangle - \langle A\rangle^2$ allow via Eq. (58) a straightforward estimation of τ_A (Kikuchi and Ito 1993).

We conclude this subsection by defining a non-linear relaxation function

$$\phi^{(nl)}(t) = [\langle A(t)\rangle_T - \langle A(\infty)\rangle_T]/[\langle A(0)\rangle_T - \langle A(\infty)\rangle_T] \qquad (60)$$

and the corresponding non-linear relaxation time

$$\tau_A^{(nl)} = \int_0^\infty \phi_A^{(nl)}(t)dt \quad . \qquad (61)$$

The condition that the system is well equilibrated then simply becomes

$$t_{M_0} >> \tau_A^{(nl)} \quad . \qquad (62)$$

Eq. (62) must hold for all quantities A, and hence one must focus on the slowest relaxing quantity (for which $\tau_A^{(nl)}$ is largest) to estimate t_{M_0} reliably. Near second-order phase transitions, the slowest relaxing quantity usually is the order parameter of the transition and not the internal energy. Hence the "rule" published in some Monte Carlo work that the equilibration of the system is established by monitoring the time evolution of the internal energy is a procedure that is clearly not valid in general.

3.5 Other ensembles of statistical physics

So far the discussion has been mostly restricted to the canonical ensemble: i.e., for an Ising magnet, the number of lattice sites (spins) N, the temperature T and the external magnetic field H are the given (independent) thermodynamic variables. Of course, it is possible to also carry out simulations in other ensembles, e.g. one may choose an ensemble where the variable thermodynamically conjugate to H, namely the magnetization m, is given (and fixed). In fact, the spin-exchange algorithm of Fig. 5b realizes that ensemble.

In such a simulation using the (NmT) ensemble the magnetic field H then is a nontrivial quantity which one may wish to calculate. This is not so straightforward as the calculation of m in the (NHT) ensemble {Eq. (26)}, because unlike the latter variable H (or other intensive

thermodynamic variables, for other ensembles) cannot be directly expressed as function of the microscopic degrees of freedom.

For systems with discrete degrees of freedom, such as the Ising model, this problem can be handled by the concept of "local states" (Alexandrowicz 1975, 1976, Meirovitch and Alexandrowicz 1977). We use here the "lattice gas model" language of the Ising problem, i.e. lattice sites i are occupied {local density $\rho_i = (1 - S_i) / 2 = 1$, i.e. $S_i = -1$} or empty {$\rho_i = 0$, $S_i = +1$}; constant magnetization corresponds then to constant density (or particle number $\mathfrak{N}$, respectively) in the lattice gas, and H translates into the chemical potential μ of the particles (note that the NmT ensemble of the Ising magnet corresponds to the canonical $\mathfrak{N}$ VT ensemble of the lattice gas, while the NHT ensemble of the magnet corresponds to the grand-canonical μ VT ensemble). Assuming a nearest neighbor energy $-\varepsilon$ is won if two neighboring sites of a square lattice are occupied, the interaction energy of an atom can take the five values $E_\alpha = 0$, $-\varepsilon$, -2ε, -3ε and -4ε, respectively. We define a set of five conjugate states α' by removing the central atom of each state α, with $E_{\alpha'} = 0$. If the frequencies of occurrence of the local states α and α' are denoted as ν_α and $\nu_{\alpha'}$, the condition of detailed balance {Eq. (29)} requires that

$$\nu_\alpha / \nu_{\alpha'} = \exp[(- E_\alpha + \mu)/k_B T], \quad \frac{\mu}{k_B T} = \ell n \, (\nu_\alpha / \nu_{\alpha'}) + E_\alpha / k_B T \quad . \tag{63}$$

To smooth out fluctuations it is advisable to average μ over all (five) local states. This technique has been used to study problems such as the excess chemical potential in a system where a droplet coexists with surrounding vapor (Furukawa and Binder 1982), for instance.

For off-lattice systems the standard method to sample the chemical potential is the "test particle insertion method" (Widom 1963): one tries to insert a particle at a randomly chosen position, calculates the change in energy ΔE_t due to this test particle, and estimates μ from

$$(\mu - \mu_0)/k_B T = - \ell n \left\langle \exp(-\Delta E_t) / k_B T \right\rangle_{\mathfrak{N}VT} \tag{64}$$

Here μ_0 is the chemical potential of an ideal gas of $\mathfrak{N}$ particles at temperature T in the same volume V. Applications of Eq. (64) are ubiquitous (Allen and Tildesley 1987, 1993, Allen 1996). Particular problems arise, of course, when either the system is very dense or the particle to be inserted is a complex object (e.g. a macromolecule): then ΔE_t is very large and the sampling of $\exp(- \Delta E_t / k_B T)$ will not work out in practice. E.g., for the bond fluctuation model (Carmesin and Kremer 1988) of flexible polymers a chain is represented by effective monomers connected by effective bonds on a lattice, assuming that each "monomer" blocks all 8 sites of an elementary cube for further occupation. For this excluded volume interaction, $\Delta E_t = \infty$ as soon as a monomer of the test chain overlaps with just one occupied site only. Therefore, the probability that one can insert a long chain into a dense system without overlap is extremely small - e.g., Müller and Paul (1994) estimate that for chain length N = 80 and volume fraction $\phi = 0.5$ of occupied sites this insertion probability is as small as 10^{-76}! Various specialized techniques have been devised to overcome this problem: stepwise growth of macromolecules (Kumar 1994), configurational bias Monte Carlo (Frenkel 1993), thermodynamic integration (Müller and Paul 1994), "multicanonical" sampling (Wilding and Müller 1994), and sampling in an ensemble with fluctuating chain lengths (Escobedo and de Pablo 1995).

For simulations of fluids in the ηVT ensemble there is another intensive variable of interest, namely the pressure p. In systems with additive pairwise potentials $\varphi(\vec{r})$ it is usually calculated from the Virial theorem (Hill 1956, Wood 1968)

$$pV/\eta k_B T = 1 - 1/(6k_B T) \int_0^\infty g(r)\,[d\varphi(r)/dr]\,4\pi r^2 dr \quad , \tag{65}$$

where g(r) is the radial density pair distribution function.

Eqs. (64),(65) are very useful since combining them with thermodynamic relations for the entropy S such as

$$TS = pV + E - \eta\mu \tag{66}$$

one can obtain all thermodynamic potentials of interest. Alternative methods for obtaining free energy F = E - TS or entropy S rely on "umbrella sampling" (Valleau and Torrie 1977) or thermodynamic integration methods, e.g. the relation for the specific heat C_V

$$(\partial S/\partial T)_{V,\eta} = C_V/T \tag{67}$$

is integrated as

$$F = E - T \int_0^T [C_V(T')/T']dT' \quad . \tag{68}$$

We emphasize that this thermodynamic integration technique is very general, it applies to both lattice and continuum models, and is particularly convenient in conjunction with histogram reweighting techniques (Swendsen et al. 1992). Of course, any other derivatives of thermodynamical potentials can also be exploited: e.g. for Ising magnets the relation for the magnetization m {Eq. (26)}

$$m = -(\partial F/\partial H)_T \quad , \quad F(T,H_2) = F(T,H_1) - \int_{H_1}^{H_2} m\,dH \tag{69}$$

is particularly convenient (Binder 1981b). The key point of all these techniques {Eqs. (68),(69)} is that thermodynamic potentials such as F are completely specified by the independent thermodynamic variables describing the considered state, but do not depend on the particular path on which one may think the system was brought from a "reference state" (for which F and S are known) to the desired state. Consequently, one can choose the most convenient path for the problem under consideration.

For off-lattice fluids, of course, it is very natural to consider simulations not only in the canonical ensemble (ηVT) considered above, or in the grand-canonical ensemble (μVT), where moves need to be considered where particles are added or removed from the system, {see e.g. Levesque et al. 1984 for a discussion} but also in the constant pressure ensemble (ηpT) where the volume V is a dynamical variable to be included in the state variable $\vec{X}$ in the average, Eq. (28). This is recognized from noting that (Wood 1968)

$$\langle A\rangle_{\eta pT} = \frac{\int_0^\infty dV \exp[-pV/k_BT] Z_\eta(V,T) A}{\int_0^\infty dV \exp[-pV/k_BT] Z_N(V,T)} = \frac{\int_0^\infty dV \int d\hat{\vec{X}} \exp\left\{-\left[pV + \varkappa_N\left(\hat{\vec{X}}\right)\right]/k_BT\right\} A}{\int_0^\infty dV \int d\hat{\vec{X}} \exp\left\{-\left[pV + \varkappa_N\left(\hat{\vec{X}}\right)/k_BT\right]\right\}} \tag{70}$$

where $\hat{\bar{X}}$ is the state vector in the phase space of the canonic ensemble. Since Eq. (70) is formally analogous to the canonical average, Eq. (3), it is clear that one can straightforwardly generalize the Monte Carlo sampling, taking $\bar{X}=\left(V,\hat{\bar{X}}\right)$ and modifying Eqs. (29),(30) as follows

$$\frac{W\left(\bar{X}\rightarrow\bar{X}'\right)}{W\left(\bar{X}'\rightarrow\bar{X}\right)} = \exp\{ - [p\delta V + \delta\mathcal{H}]/k_BT\} \qquad (71)$$

One must take into account, of course, that the different ensembles of statistical mechanics yield equivalent results in the thermodynamic limit only, while finite size effects are different (Hill 1956).

For simulations of solids, the anisotropy of the crystal structure may require to consider boxes with different linear dimensions L_x, L_y, L_z in different coordinate axis directions. Then it is also natural not to consider only uniform volume changes δV, but rather separate changes δL_x, δL_y and δL_z , and remember that p as used above really is nothing but the trace of the pressure tensor $\Pi_{\alpha\beta}$. In this context, we note that the virial relation, Eq. (65) generalizes as follows $\left[\vec{r}_{ij} = \vec{r}_i - \vec{r}_j\right]$

$$\Pi_{\alpha\beta}\, V/\mathcal{N}k_BT = \delta_{\alpha\beta} - \frac{1}{6\mathcal{N}k_BT}\left\langle \sum_{i\neq j}\left(\vec{r}_{ij}\right)_\alpha \frac{\partial\varphi\left(\vec{r}_{ij}\right)}{\partial\left(\vec{r}_{ij}\right)_\beta}\right\rangle \quad , \qquad (72)$$

where $\varphi\left(\vec{r}_{ij}\right)$ is the total potential acting between particles at points $\vec{r}_i$, $\vec{r}_j$. Following corresponding molecular dynamics methods (Parrinello and Rahman 1980) where both size and shape of the box are dynamical variables also analogous Monte Carlo methods have been

developed (Najafabadi and Yip 1983, Ray 1993). For more details on Monte Carlo methods for off-lattice systems in various ensembles see also Frenkel and Smit (1996).

While for fluids the microcanonical ($\mathcal{N}$VE) ensemble is realized, of course, if one applies standard Molecular Dynamics techniques (Ciccotti and Hoover 1986, Sprik 1996), the realization and application of the microcanonical ensemble for lattice systems such as Ising or Potts models (Potts 1952, Wu 1982) has given rise to a longstanding discussion (Creutz 1983, Bhanot et al. 1984, Harris 1985, Desai et al. 1988, Litz et al. 1991, Hüller 1992, 1994, Gerling and Hüller 1993, Ray 1991, Hammrich 1993, Promberger and Hüller 1995, Lee 1995, Gross et al. 1996). Some researchers maintain that this ensemble has practical advantages particularly for the study of first order phase transitions (Hüller 1992, 1994, Gross et al. 1996), even in comparison with the popular "multicanonical" method (Berg and Neuhaus 1992, Berg 1992), see Sec. 5.3.

At this point we mention that it is sometimes convenient to define artificial "ensembles" that are not found in the standard text books of statistical mechanics, but can also be translated into an importance sampling Monte Carlo method: the "gaussian ensemble" of Challa and Hetherington (1988) in a sense "interpolates" between the canonical and microcanonical ensemble; and particularly important is the "Gibbs ensemble"(Panagiotopoulos 1987, 1992, 1994, Smit 1993, Allen 1996) for the study of gas-liquid coexistence. There one considers two systems at the same temperature with particle numbers $\mathcal{N}_1$, $\mathcal{N}_2$, and volumes V_1 , V_2 such that $V_1 + V_2 = V_{tot}$ = const, $\mathcal{N}_1 + \mathcal{N}_2$ = const, but allows exchange of both particles and volume between the two boxes. E.g. by a choice of initial condition, one can ensure (at temperatures sufficiently below the critical point) that one system equilibrates at the density of the gas and the other at the liquid density. The chemical potential adjusts itself to its value at the

coexistence curve μ_{coex} automatically (in the limit $V_{tot} \to \infty$). This method outside of the critical region works rather well already for rather small sizes of the total volume V_{tot}, and hence has found widespread practical application (Allen 1996, Frenkel and Smit 1996). However, once more we add the warning that finite size effects differ in different ensembles and need careful consideration, see e.g. Mon and Binder (1992), Recht and Panagiotopoulos (1993), and Bruce (1996).

4. Finite size effects

Simulations deal with a much smaller number of degrees of freedom (typically the particle number $\mathcal{N}$ is in the range $10^2 \le \mathcal{N} \le 10^6$) than typical experiments ($\mathcal{N} \approx 10^{22}$). Finite size effects thus can be a serious limitation, particularly near phase transitions where such effects are large. On the other hand, unlike experiment one can easily vary the system linear dimension over a wide range as a control parameter (avoiding unwanted surface effects by periodic boundary conditions), and apply the corresponding finite size scaling theory (Fisher 1971, Barber 1983, Binder 1987a, 1992a, Privman 1990, Dünweg 1996) as a powerful tool of analysis for the simulation data. In this spirit, this section will provide a brief introduction to the main ideas of the subject.

4.1 The percolation transition and the geometrical interpretation of finite size scaling

Consider an infinite lattice (d-dimensional cubic lattice of volume L^d, lattice spacing being unity, for $L \to \infty$) where each site is randomly occupied (with probability p) or empty (probability 1 - p), and define "clusters" of neighboring occupied sites (Stauffer and Aharony 1992). There exists a critical value p_c such that for $p < p_c$ there exist only clusters of finite "size" ℓ (= number of sites belonging to the cluster, $\ell = 1,2,3,...$) on the lattice, while for $p \ge p_c$ an infinite cluster has formed that spans from one boundary of the lattice to the opposite one. The probability that an occupied site is part of the percolating cluster is called the percolation probability $P_\infty(p)$, while a percolation susceptibility $\chi(p)$ is defined in terms of the concentrations $n_\ell(p)$ of clusters containing ℓ occupied sites,

$$\chi(p) = \sum_{\ell=1}^{\infty}{}' \ \ell^2 n_\ell(p)/p \tag{73}$$

Here the prime means that the largest cluster (for $p > p_c$ this is the percolating infinite cluster) is omitted from the summation. Both $\chi(p)$ and the percolation order parameter $P_\infty(p)$ exhibit critical singularities as $|p - p_c| \to 0$, with critical exponents β_p, γ_p and amplitudes $\hat{B}_p$, $\hat{\Gamma}_p^{\pm}$,

$$P_\infty(p) = \hat{B}_p \left(p / p_c - 1\right)^{\beta_p} \quad , p > p_c \ , \tag{74}$$

while per definition $P_\infty(p) = 0$ for $p < p_c$, and

$$\chi(p) = \begin{cases} \hat{\Gamma}_p^{+}(1-p/p_c)^{-\gamma_p} & , \ p<p_c \ , \\ \hat{\Gamma}_p^{-}(p/p_c-1)^{-\gamma_p} & , \ p>p_c . \end{cases} \tag{75}$$

In a finite lattice, $\chi(p)$ cannot diverge but reaches a maximum of finite height only: Eq. (73) then is a finite sum over clusters of finite "mass" ℓ, infinitely large clusters would not fit on a finite lattice. Similarly, the percolation probability $P_\infty(p)$ does not vanish at any $p > 0$, but must attain small non-zero values as soon as $p > 0$: percolation only requires a string of L occupied sites running through the system, which occurs with probability $p^L = \exp(L\ell np) \to 0$ as $p \to 0$.

Thus in a finite lattice the singularities described by Eqs. (74),(75) are smoothed out: this rounding of the transition is qualitatively obvious geometrically.

For a quantitative description of this finite size rounding, we need the detailed properties of the percolation clusters near p_c (Stauffer 1979). Calling ℓ the "mass" of a cluster, the mass distribution $n_\ell(p)$ satisfies a scaling property for $L \to \infty$,

$$n_\ell(p) = \ell^{-\tau}\, \tilde{n}\,\{\ell^{\sigma}(1 - p/p_c)\} \quad , p \to p_c, \ell \to \infty \tag{76}$$

$\tilde{n}\,(y)$ being a scaling function, and the exponents τ,σ are related to β_p , γ_p ,

$$\tau = 2 + \beta_p/(\gamma_p + \beta_p) \quad , \ \sigma = 1/(\gamma_p + \beta_p) \quad . \tag{77}$$

The large clusters near p_c actually are "fractals" (Mandelbrot 1982, Feder 1988), i.e. their mass ℓ and radius r_ℓ are not related via space dimensionality d but via a smaller "fractal dimensionality" d_f ,

$$r_\ell = \hat{r}\ell^{\,1/d_f} \quad , \quad \ell \to \infty \quad , \quad p = p_c \, . \tag{78}$$

Noting that in a finite subsystem of linear dimension L_s a percolating cluster has $r_\ell = L_s$, we find a relation between d_f and τ, since the probability $P_s^{(L_s)}(p_c)$ that such a cluster occurs that spans the subsystem is of order unity,

$$P_s^{(L_s)}(p_c) \approx L_s^d \int_{r_\ell = L_s}^{\infty} n_\ell(p_c)\, d\ell \approx L_s^d \tilde{n}(0) \int_{(L_s/\hat{r})^{d_f}}^{\infty} \ell^{-\tau}\, d\ell \propto 1 \tag{79}$$

In a finite subsystem, percolation can occur via any cluster of linear dimension $r_\ell = L_s$ or larger, but these possibilities are mutually exclusive in this subsystem, and thus their probabilities simply add up. For large ℓ, $\sum_\ell$ can be replaced by $\int d\ell$, and using Eq. (76) we arrive at Eq. (79), which yields further

$$L_s^{d+d_f(1-\tau)} \propto 1 \ , \ d_f = d/(\tau - 1) = d - \beta_p/\nu_p \quad . \tag{80}$$

Since the first equation of Eq. (80) must hold for any L_s, the second equation follows, using also Eq. (77) and the "hyperscaling relation" (Fisher 1974)

$$d\nu_p = \gamma_p + 2\beta_p \quad . \tag{81}$$

In Eqs. (80),(81), ν_p is the critical exponent of the correlation length ξ_p which describes the decay of the pair connectedness function,

$$\xi_p \propto |p - p_c|^{-\nu_p} \quad . \tag{82}$$

The number of sites ℓ in a cluster that spans the distance L_s is simply {Eqs. (78),(80)}

$$\ell_{L_s} = (L_s/\hat{r})^{d_f} \propto L_s^{\,d-\beta_p/\nu_p} \tag{83}$$

Since the subsystem contains L_s^d sites, the fraction of its sites belonging to such a spanning cluster are of the order of

$$P_\infty^{(L)}(p_c) = L^{-d}\ell_L \propto L^{-\beta_p/\nu_p} \tag{84}$$

In Eq. (84), we have omitted the index s (for "subsystem") from L_s, since the result applies to a finite system with periodic boundary conditions as well. Relations such as Eq. (78) hold in finite systems essentially also, as long as $r_\ell < L$: the finite size yields a cutoff to the distribution $n_\ell(p)$ at the value $\ell_L \propto L^{d_f}$ corresponding to $r_\ell = L$.

This argument also yields the rounding of the divergence of the percolation susceptibility, Eq. (75) since the sum in Eq. (73) must be cut off at ℓ_L, see Binder (1972),

$$\chi^{(L)}(p) \approx (1/p)\sum_{\ell=1}^{\ell_L} \ell^2 n_\ell(p) \ , \tag{85}$$

and using Eq. (76) for $p = p_c$ yields, with the help of Eqs. (83),(77)

$$\chi^{(L)}(p_c) \propto \int_0^{\ell_L} \ell^{2-\tau} d\ell \propto \ell_L^{3-\tau} \propto L^{\gamma_p/\nu_p} \ . \tag{86}$$

Note that the selfconsistency of this scaling description of percolation critical phenomena and the scaling of the mass distribution can also be checked defining ξ_p from the average cluster radius,

$$\xi_p^2 \equiv \sum_{\ell=1}^{\infty}{}' r_\ell^2 \ell^2 n_\ell(p) / \sum_{\ell=1}^{\infty}{}' \ell^2 n_\ell(p) \ . \tag{87}$$

Using Eqs. (76),(78) and transforming sums to integrals one readily finds Eq. (82), if Eq. (81) holds.

To obtain the finite size behavior of $\chi^{(L)}(p)$ for $p \neq p_c$ but near p_c, we use again Eqs. (76),(85)

$$\begin{aligned} \chi^{(L)}(p) &\approx (1/p)\int_0^{(L/\tilde{r})^{d_f}} \ell^{2-\tau}\tilde{n}\left(\ell^\sigma(1-p/p_c)\right)d\ell \\ &\propto (1-p/p_c)^{-\gamma_p}\int_0^{\left[(L/\tilde{r})(1-p/p_c)^{\nu_p}\right]^{d_f}} x^{2-\tau}\tilde{n}\left(x^\sigma\right)dx \ , \end{aligned} \tag{88}$$

where integration variables where transformed from ℓ to $x = \ell(1-p/p_c)^{1/\sigma}$. From Eq. (88) we see that $\chi^{(L)}(p)$ depends on L only in the scaled combination $L(1-p/p_c)^{\nu_p} \propto L/\xi_p$: this is the principle of finite size scaling that one must compare lengths, "L scales with ξ_p". Thus Eq. (88) can be rewritten as

$$\chi^{(L)}(p) = (1-p/p_c)^{-\gamma_p}\tilde{F}\left\{L(1-p/p_c)^{\nu_p}\right\} = L^{\gamma_p/\nu_p}\tilde{\chi}(L/\xi_p) \ , \tag{89}$$

where the scaling function $\tilde{F}(\gamma) = \gamma^{\gamma_p/\nu_p}\tilde{\chi}$ (γ const), the constant being a (nonuniversal) metric factor. The scaling functions $\tilde{F},\tilde{\chi}$ obviously describe a smooth interpolation between the power laws Eqs. (75),(86). Of course, the explicit expression resulting from Eq. (88) for $\tilde{F}(\gamma)$

is approximate only, since the sharp cutoff of the integral at $r_\ell = L$ is an approximation. Thus the treatment given here is only a justification for the general structure of Eq. (89). A similar result holds for the percolation probability and for the spanning probability

$$P_\infty^{(L)}(p) = L^{-\beta_p/\nu_p}\,\tilde{P}\left(L/\xi_p\right) \quad , \; L \to \infty, \; p \to p_c \quad , \tag{90}$$

$$P_S^{(L)}(p) = \tilde{P}_S\left(L/\xi_p\right) \quad , \; L \to \infty, \; p \to p_c \quad , \tag{91}$$

By writing the appropriate limits we have emphasized here that finite size scaling holds only asymptotically for p close to p_c and large L, while for p not so close to p_c (and L not so large) corrections to scaling come into play (their origin is best understood in terms of renormalization group arguments, see e.g. Domb and Green (1976)). In the finite size scaling limit, we see that $P_S^{(L)}$ ($p = p_c$) should take a L-independent universal value, $\tilde{P}_S(0)$. This property is useful for locating p_c from simulation data - a plot of $\tilde{P}_S^{(L)}(p)$ vs. p for different L should yield a family of curves that intersect in a unique point, the abscissa of this point is p_c. This intersection method indeed works well in practice (Kirkpatrick 1979), and also the finite size scaling relations Eqs. (89)-(91) have readily been verified for the percolation problem (Heermann and Stauffer 1980).

4.2 Broken symmetry and finite size effects at critical points

We now discuss thermally driven phase transitions where the state of the system changes from the disordered phase at high temperatures to a spontaneously ordered state at a temperature T below the critical temperature T_c of a second-order transition, using the Ising ferromagnet as a

prototype example. The low temperature phase is a state with nonzero spontaneous magnetization $\pm m_{spont}$ for zero applied field H = 0 (cf. Figs. 6,7).

As described already in Sec. 3.2, there is always a nonzero probability in a finite system to "move" from the state near $+m_{spont}$ to the state with $-m_{spont}$ or vice versa, and thus $\langle m \rangle \equiv 0$ for H = 0. The standard recipe {also useful for vector order parameters, as they occur for XY or Heisenberg models, Eqs. (35),(36)} is to record the root mean square order parameter (Binder 1972)

$$m_{rms}(T) = \sqrt{\left\langle m^2 \right\rangle_T} = \left\langle \left(\sum_{i=1}^{N} S_i / N \right)^2 \right\rangle_T^{1/2} = \frac{1}{N} \left(\sum_{i,j=1}^{N} \langle S_i S_j \rangle_T \right)^{1/2} \tag{92}$$

Now the correlation function ($\vec{r} = \vec{r}_i - \vec{r}_j$ is the distance between sites i,j)

$$G(r,T) \equiv \langle S_i S_j \rangle_T \tag{93}$$

satisfies a power law decay for $T = T_c$ (Fisher 1974)

$$G(r,T_c) = \hat{G}\, r^{-(d-2+\eta)} \quad , \; r \to \infty \tag{94}$$

with η the corresponding exponent and $\hat{G}$ the critical amplitude. We can approximately evaluate Eq. (92) for $T = T_c$, using Eqs. (93),(94) and replacing the sum Σ by an integral over distances from 0 to L/2 ($N = L^d$), to obtain

$$\sum_{i=1}^{N}\langle S_i S_j\rangle_{T_c} \propto \int_0^{L/2} r^{d-1}\,dr\, G(r,T_c) \propto L^{2-\eta} \qquad (95)$$

and hence (Müller-Krumbhaar and Binder 1972)

$$m_{rms}^{(L)}(T_c) \propto \left(L^{2-d-\eta}\right)^{1/2} \propto L^{-\beta/\nu} \quad , \qquad (96)$$

using scaling relations (Fisher 1974) $2 - \eta = \gamma/\nu$, $d = (2\beta + \gamma)/\nu$. Also the fluctuation relation for the susceptibility {cf. Eq. (45)} yields (remember H = 0)

$$k_B T\,\chi(T) = \frac{1}{N}\sum_{i,j}\langle S_i S_j\rangle_T \underset{T=T_c}{\propto} L^{2-\eta} = L^{\gamma/\nu} \quad , \qquad (97)$$

using again Eq. (95). Eqs. (96),(97) are exactly analogous to the results Eqs. (84),(86) for the percolation problem.

Of course, the analogy between the finite size results for the Ising model and for random percolation is no surprise at all: the mapping proved by Fortuin and Kasteleyn (1972) between bond percolation and the limit $q \to 1$ of the q-state Potts model (Potts 1953, Wu 1982) provides a description of the thermal order-disorder transition of the Ising model (and related spin models) as a percolation of "physical clusters" (Coniglio and Klein 1980, Hu 1984, Swendsen and Wang 1987). Any state of the Ising lattice can be described in terms of "geometrical clusters" of, say, "down spins" in a surrounding background of "up spins" (Fisher 1967, Binder 1976). However, throughout the paramagnetic phase we encounter a percolation transition of these "geometrical clusters" when we vary the magnetic field H from strongly

positive to negative values. Rather one has to distinguish between "active" and "inactive" bonds in a geometrical cluster. The probability p for a bond to be active is

$$p = 1 - \exp(-2J/k_B T) \quad , \qquad (98)$$

and only spins connected by "active bonds" form a "physical cluster" (Coniglio and Klein 1980). This rule can be proven (Fortuin and Kasteleyn 1972) by deriving a percolation representation of the Potts model partition function Z_{Potts}, J_p being the interaction constant of the Potts Hamiltonian (note that $\mathcal{H}_{Potts}$ reduces to $\mathcal{H}_{Ising}$ for q = 2, choosing $J_p = 2J$)

$$\mathcal{H}_{Potts} = -J_p \sum_{(i,j)} \delta_{\sigma_i \sigma_j} \quad , \qquad \sigma_i = 1,2,\ldots q, \qquad (99)$$

$$Z_{Potts} = \operatorname*{Tr}_{\{\sigma_i\}} \exp\left(-\mathcal{H}_{Potts}/k_B T\right) = \sum p^{N_b}(1-p)^{N_m} q^{N_c} \quad , \qquad (100)$$

where N_b is the number of bonds, N_m is the number of missing bonds, and N_c is the number of clusters in a given bond configuration. The sum in Eq. (100) is over all bond configurations.

For expressing the variables of interest, we now need two "cluster coordinates" (Binder 1976), the cluster magnetization $m_{cl} = \pm \ell$ (the sign gives the orientation of the spins inside the cluster, which we label as cl), and the number of active bonds in the cluster, which we denote as u_{cl} p. Denoting the number of clusters per lattice sites with these properties as $p(m_{cl}, u_{cl})$, magnetization and energy per spin at H = 0 are written, for a lattice of coordination number z,

$$m = \sum_{m_{cl}} m_{cl} P(m_{cl}) \quad , \qquad P(m_{cl}) \equiv \sum_{u_{cl}} p(m_{cl}, u_{cl}) \qquad (101)$$

$$E = \langle \mathcal{H}_{Ising} \rangle / N = -\frac{z}{2} J \left(\sum_{m_{cl}} \sum_{u_{cl}} u_{cl} p(m_{cl}, u_{cl}) - 1 \right) = -\frac{z}{2} J \left(p\langle N_b \rangle / N - 1 \right) , \qquad (102)$$

remembering that N_b is the total number of (active) bonds in a configuration. Also the thermal averages of fluctuations can be expressed in terms of suitable properties of the clusters; e.g., the specific heat per lattice site becomes

$$C = \partial E / \partial T = [1/(N k_B T^2)] \left(\left\langle \mathcal{H}^2_{Ising} \right\rangle - \left\langle \mathcal{H}_{Ising} \right\rangle^2 \right) =$$

$$= \frac{1}{4} z^2 J^2 / (N k_B T^2 p^2) \left\{ \left\langle N_b^2 \right\rangle - \langle N_b \rangle^2 - (1-p)\langle N_b \rangle \right\} \qquad (103)$$

Splitting off from $P(m_{cl})$ the contribution of the largest cluster in the system, which we denote as m_{cl}^{∞},

$$P(m_{cl}) \equiv p'(m_{cl}) + \frac{1}{N} \delta_{m_{cl}, m_{cl}^{\infty}} , \qquad (104)$$

the absolute value of the magnetization is (D'Onorio De Meo et al. 1990)

$$\langle |m| \rangle = \left\langle \left| \frac{m_{cl}^{\infty}}{N} + \sum_{m_{cl}} m_{cl} p'(m_{cl}) \right| \right\rangle \qquad (105)$$

While the susceptibility for $T > T_c$ is just the analog of the percolation susceptibility, Eq. (73),

$$k_B T \chi = k_B T \, (\partial \langle m \rangle / \partial H)_{T, H=0} = \sum_{m_{cl}} m_{cl}^2 P(m_{cl}) = \sum_{\ell}{}' \ell^2 n_\ell \qquad , \qquad (106)$$

since $P(m_{cl}) + P(-m_{cl}) = n_\ell$, for $T < T_c$ one must single out the contribution from the largest cluster (that becomes the percolating cluster for $N \to \infty$) to obtain (D'Onorio De Meo et al. 1990)

$$k_B T \chi' = N(\langle m^2 \rangle - \langle |m| \rangle^2) = \sum_{\ell}{}' \ell^2 n_\ell + N\left(\left\langle P_\infty^2 \right\rangle - \langle |m| \rangle^2 \right) \approx$$

$$\approx \sum_{\ell}{}' \ell^2 n_\ell + N\left(\left\langle P_\infty^2 \right\rangle - \langle P_\infty \rangle^2 \right) \qquad (107)$$

The simple physical interpretation of Eq. (107) is, of course, that below T_c the response function picks up contributions both from all finite clusters (the term $\sum_{\ell}{}' \ell^2 n_\ell$, only considered in the percolation problem) and from the fluctuations in size of the largest (percolating) cluster. It turns out that estimating χ, χ' from these relations in terms of clusters is advantageous in comparison with the fluctuaton relations expressing them by magnetization fluctuations, since Eqs. (106),(107) exploit the fact that there are no correlations between different clusters: thus the statistical noise is less, the right hand side of Eqs. (106),(107) are "improved estimators". Similar "improved estimators" can be introduced for other quantities as well, e.g. the pair correlation function (Wolff 1989a, Janke 1994), wavevector-dependent susceptibility, and fourth-order cumulant (Baker and Kawashima 1995, 1996). Since Monte Carlo "cluster algorithms" (Swendsen and Wang 1987, Swendsen et al. 1992, Wolff 1988a,b, 1989a-c, 1992, Edwards and Sokal 1989, Hu and Mak 1989, Wang et al. 1989, Kandel et al. 1990, Hasenbusch and Meyer 1991) are attractive because they reduce "critical slowing down" (Li and Sokal 1989, 1991, Wang 1991, Heermann and Burkitt 1990, Tamayo et al. 1990, Wolff 1992), one can apply Eqs. (101)-(107) at no extra computational cost. Fig. 8 shows an example for the d = 2 Ising square lattice. It is clearly seen that for finite systems the

percolation probability $P_\infty = \left\langle \left| m_{cl}^{\infty} \right| \right\rangle / N$ is always smaller than $\langle |m| \rangle$, as expected from Eq. (105), although in the limit $N \to \infty$ both quantities converge to the spontaneous magnetization. Note that even for $N \to \infty$ the term $N\left(\left\langle P_\infty^2 \right\rangle - \langle P_\infty \rangle^2\right)$ must not be neglected in $k_B T\chi'$ in comparison to $\sum_{\ell}{}' \ell^2 n_\ell$ for $T < T_c$, although it is negligible for $T > T_c$ {one can show that $N\left(\left\langle P_\infty^2 \right\rangle - \langle P_\infty \rangle^2\right) \propto L^{-d} \log^2 L$ for $L \to \infty$ and $T > T_c$, see Margolina and Heermann 1984}.

While in the percolation problem one hence can use the same expression, Eq. (73), to obtain the percolation susceptibility for $p < p_c$ and for $p > p_c$, this is not true for the phase transition of the Ising model, Eqs. (106) and (107) differ from each other significantly.

This difference, of course, is intimately linked to the occurrence of spontaneous symmetry breaking in the Ising model, already alluded to in Fig. 6 and Eqs. (45), (46). As illustrated in Fig. 9, the fluctuation relation for the susceptibility $k_B T\chi = L^d (\langle m^2 \rangle - \langle m \rangle^2) = L^d \langle m^2 \rangle$ (for zero field $H = 0$) smoothly converges to the correct answer for $T > T_c$, but for $T < T_c$ it converges to $k_B T\chi \approx L^d \langle |m| \rangle^2$ as $L \to \infty$, measuring the fluctuations between the two phases with opposite magnetization, rather than the fluctuations in a pure phase. On the other hand, $k_B T\chi'$ as defined by Eq. (107) for $T > T_c$ does not converge to the right answer either: as one can easily work out from a gaussian distribution (Binder and Heermann 1988), $\chi' = \chi(1 - 2/\pi)$ for $L \to \infty$. Thus χ' diverges with the same critical exponent as χ does, but the prefactor (the critical amplitude) is reduced by a factor $1 - 2/\pi$.

The fact that the spontaneous symmetry breaking in phase transitions requires the use of different fluctuation formulas on both sides of the transition is sometimes ignored in the literature, which hence leads to confusion: for a finite system in zero field, $\langle m \rangle^2$ and hence $L^d(\langle m^2 \rangle - \langle m \rangle^2)$ is not a useful quantity, if a single spin flip algorithm is used. For $T << T_c$, the observation time t_{obs} of the simulation will be much smaller than the "ergodic time" τ_e needed to move from one peak of $P_L(m)$ in the lower part of Fig. 6 to the other one, and hence $\langle m \rangle^2 \approx \langle |m| \rangle^2$, and then $L^d(\langle m^2 \rangle - \langle m \rangle^2)$ will coincide with $k_B T\chi$! For $T \geq T_c$, t_{obs} will exceed τ_e by orders of magnitude, and then $\langle m \rangle^2 \approx 0$, i.e. one obtains $k_B T\chi$ (Fig. 9). However, in the region where t_{obs} and τ_e are of the same order of magnitude, the magnetization will jump between the two peaks of $P_L(m)$ only very few times, and then one obtains rather erratic results of $L^d(\langle m^2 \rangle - \langle m \rangle^2)$, since $\langle m \rangle$ is not well-defined here.

From the percolation interpretation of the transition, it is clear that finite size scaling expressions analogous to Eqs. (89)-(91) hold for $\langle |m| \rangle, \chi, \chi'$ and a further useful quantity, the normalized fourth-order cumulant U_L (Binder 1981a) of the distribution $P_L(m)$,

$$U_L = 1 - \langle m^4 \rangle / (3\langle m^2 \rangle^2) \quad . \tag{108}$$

In terms of $\varepsilon = T/T_c - 1$ we have, with $\tilde{M}, \tilde{\tilde{M}}, \tilde{\chi}, \tilde{\tilde{\chi}}, \tilde{\chi}', \tilde{\tilde{\chi}}', \tilde{U}, \tilde{\tilde{U}}$ being suitable scaling functions

$$\langle |m| \rangle = L^{-\beta/\nu} \tilde{M}(L/\xi) = L^{-\beta/\nu} \tilde{\tilde{M}}(\varepsilon L^{1/\nu}) \quad , \tag{109}$$

$$k_B T\chi = L^{\gamma/\nu} \tilde{\chi}(L/\xi) = L^{\gamma/\nu} \tilde{\tilde{\chi}}(\varepsilon L^{1/\nu}) \quad , \tag{110}$$

$$k_B T\chi' = L^{\gamma/\nu} \tilde{\chi}'(L/\xi) = L^{\gamma/\nu} \tilde{\tilde{\chi}}'(\varepsilon L^{1/\nu}) \quad , \tag{111}$$

$$U_L = \tilde{U}(L/\xi) = \tilde{\tilde{U}}(\varepsilon L^{1/\nu}) \quad . \tag{112}$$

Fig. 10 shows an example where the scaling of $k_B T\chi'$ {Eq. (111)} is tested. It must be emphasized that all these scaling relations are only supposed to hold in the limits $L \to \infty$, $\varepsilon \to 0$ (keeping $\varepsilon L^{1/\nu}$ or L/ξ fixed). While it is gratifying to note that in the example shown in Fig. 10 rather small L (such as L = 20 in d = 2) already satisfy this finite size scaling hypothesis, one cannot imply that this "data collapsing" on the scaling function will work for rather small L in general {in fact, when one has crossover from one universality class to another, e.g. from the Ising class to mean field behavior (Mon and Binder 1993, Deutsch and Binder 1993a, Binder et al. 1996, Luijten et al. 1996) finite size scaling only works for $L >> \xi_{cross}$, with ξ_{cross} a length characterizing this crossover (Binder and Deutsch 1992)}. For small L one thus must expect corrections to finite size scaling. Thus methods where one ignores such corrections and tries to estimate both T_c and the exponents $1/\nu$, γ/ν (and/or β/ν) from a simultaneous fit to a scaling function {"data collapsing", see e.g. Binder (1974), Landau (1976 a,b) and Binder and Landau (1980) for some well-known examples}, may suffer from systematic errors. This criticism also applies to recent claims (Kim 1993, Brown and Cittan 1996) that high precision can be gained by extrapolation from small lattices, as pointed out by Patrasciou and Seiler (1994) and Holm and Janke (1996).

In an attempt to estimate T_c unbiased from estimates of critical exponents, Binder (1981a) suggested to plot U_L vs. T for various choices of L, since in the limit where finite size scaling holds these curves should intersect in a common intersection point $\tilde{U}(0)$ at T_c, and moreover $\tilde{U}(0)$ is universal (though dependent on the type of boundary conditions). In fact, other dimensionless moments of the order parameter distribution may be used in the same way, e.g. $\langle m^2 \rangle / \langle |m| \rangle^2$ (Deutsch and Binder 1992). Fig. 11 presents a typical example of the accuracy that is reached by such techniques, namely about 0.3% even for rather complicated models such as polymer mixtures. Of course, a close inspection of Fig. 11 shows that the three curves

do not intersect precisely in a point, buth there rather is a small temperature interval over which these intersections are spread out. To some extent this spread is due to statistical errors, to some extent to corrections to scaling.

If T_c is known the exponent β/ν can be estimated from a log-log plot of $\langle |m| \rangle$ vs. L at T_c, using Eq. (109). The exponent γ/ν can be estimated both from log-log plots of $k_B T\chi$ or $k_B T\chi'$ vs. L at T_c, or alternatively from a log-log plot of the maximum value $k_B T \chi_{max}$ vs. L (this has the advantage that a possible inaccuracy of T_c does not matter). From Eq. (111) we realize that the location of this maximum can be used to estimate the exponent $1/\nu$, since the maximum occurs at some fixed value $x_m = \varepsilon_m L^{1/\nu}$ of the scaling function {$\varepsilon_m \equiv T_m/T_c - 1$, $T_m(L)$ being the temperature of the maximum}

$$T_m(L)/T_c - 1 = x_m L^{-1/\nu} \quad , L \to \infty \, . \tag{113}$$

Alternatively, one can use the slope of $U_L - \tilde{\tilde{U}}(0) \propto \varepsilon L^{1/\nu}$ for small $\varepsilon L^{1/\nu}$ {Eq. (112)}. In addition, one can use the position of the maximum of the slope of U_L vs. T, the specific heat maximum, the maximum of the temperature derivative of $\langle |m| \rangle$ or $\langle m^2 \rangle$ etc. (Ferrenberg and Landau 1991). One can also use such quantities to try to obtain both $1/\nu$ and T_c from a simultaneous fit.

In principle, for obtaining very precise estimates the effect of correction terms must be considered. E.g., at T_c we expect instead of Eq. (97)

$$k_B T_c \chi(T_c) = L^{\gamma/\nu} \, \tilde{\chi}(0) \, (1 + \chi^{corr} L^{-x_{corr}} + \ldots) \quad , \tag{114}$$

χ^{corr} being another amplitude factor and x_{corr} the leading correction exponent. Such a correction shows up as a mild curvature on the log-log plot, and is hence easily missed. In order to take this correction into account, it is advisable to consider pairs of sizes (L,bL) for scale factors b > 1, and study the ratio (Binder 1981a)

$$\frac{\ell n\left[\chi(bL,T_c)/\chi(L,T_c)\right]}{\ell nb} = \frac{\gamma}{\nu} - \frac{\chi^{corr}L^{-x_{corr}}}{\ell nb}\left(1-b^{-x_{corr}}\right) + \ldots \qquad (115)$$

Thus the recipe is to plot the left hand side of Eq. (115) vs. $(\ell nb)^{-1}$: for each choice of L one should obtain a curve which all extrapolate linearly to the same value (γ/ν) as $(\ell nb)^{-1} \to 0$. This method was tried with some success also for non-trivial cases such as two-dimensional Ising antiferromagnets with competing next nearest neighbor interactions (Landau and Binder 1985), which belong to the universality class of the XY-model with cubic anisotropy and have non-universal exponents (Krinsky and Mukamel 1977).

Comparing Eqs. (109),(110) and using the fact that $\left\langle m^2\right\rangle_{T_c} \propto L^{-2\beta/\nu}$ we immediately see that the fluctuation relation $k_BT\chi = L^d\langle m^2\rangle$ yields the hyperscaling relation (Fisher 1974), $\gamma/\nu = d - 2\beta/\nu$: finite size scaling as written in Eqs. (109)-(112) implies hyperscaling (Binder 1981a, Brézin 1982). However, there occur indeed situations where hyperscaling does not hold, and then a generalization of finite size scaling is necessary. A well-known example are systems at dimensionalities d above the marginal dimension d* above which mean field theory of critical behavior starts to become valid (Fisher 1974). For Ising systems (as well as for the n-vector model) $d^* = 4$, and clearly the meanfield exponents ($\gamma_{MF} = 1$, $\nu_{MF} = 1/2$, $\beta_{MF} = 1/2$) do not satisfy hyperscaling for $d > 4$. In the general case {including anisotropic system shapes (Binder and Wang 1989), free surfaces, etc.} several characteristic lengths come into play, and the behavior can be very complicated (Brézin and Zinn-Justin 1985). However, for systems with a L^d geometry and fully periodic boundary conditions a simple modified form of finite size scaling holds (Binder et al. 1985), the correlation length ξ being replaced by a "thermodynamic length" ℓ_T (Binder 1985) defined by

$$\ell_T^d = k_BT\chi' m^{-2} \propto (1 - T/T_c)^{-(\gamma+2\beta)} = (1 - T/T_c)^{-2} \qquad (116)$$

where in the last step mean field exponents were used. Eq. (116) can be motivated by noting that for $T < T_c$ and large L the order parameter distribution $p_L(m)$ can be approximated as a sum of two gaussians centered at the spontaneous magnetization (cf. Fig. 6), for H = 0,

$$p_L(m) \propto \exp\left[\frac{-\left(m - m_{spont}\right)^2 L^d}{2k_BT\chi'}\right] + \exp\left[\frac{-\left(m + m_{spont}\right)^2 L^d}{2k_BT\chi'}\right] \qquad (117a)$$

and the arguments of the exponentials can be scaled as follows

$$\frac{\left(m \pm m_{spont}\right)^2 L^d}{2k_BT\chi'} = \frac{\left(m/m_{spont} \pm 1\right)^2}{2}\frac{L^d}{k_BT\chi' m_{spont}^2} = \frac{\left(m/m_{spont} \pm 1\right)^2}{2}\left(\frac{L}{\ell_T}\right)^d \qquad (117b)$$

While some consequences of this mean field finite size scaling initially seemed to be in disagreement with simulations on five-dimensional Ising models (Binder 1985, Rickwardt et al. 1994), recently the source of the difficulty has been traced down as corrections to scaling (Mon 1996, Luijten 1996, Parisi and Ruiz-Lorenzo 1996).

Another violation of hyperscaling is believed to occur in random field Ising models {RFIM} (for reviews, see e.g. Imry 1984, Nattermann and Villain 1988, Rieger 1995) and random field Potts models {RFPM} (Eichhorn and Binder 1995, 1996). If these systems have a second order transition from the ferromagnetic to the paramagnetic state at all, the exponents are believed to satisfy a modified hyperscaling law (e.g. Schwartz 1991)

$$\gamma + 2\beta = (d - \theta)\,\nu\,, \quad \theta = 2 - \eta \tag{118}$$

In spite of Eq. (118) the standard finite size scaling relations Eqs. (109)-(111) still hold, notwithstanding the fact that then $L^d \left\langle m^2 \right\rangle_{T_c} \propto L^{d-2\beta/\nu}$: in this case $\langle m \rangle^2$ is non-zero, due to the excess of random field of one particular sign in any finite sample, and one must distinguish between the "connected" susceptibility $\{k_B T \chi = L^d([\langle m^2 \rangle - \langle m \rangle^2])_{av} \underset{T=T_c}{\propto} L^{\gamma/\nu}\}$ and the "disconnected susceptibility" $\chi_{dis} \equiv L^d [\langle m \rangle^2]_{av}$, $[...]_{av}$ meaning a "quenched average" (Binder and Young 1986) over the random field configurations. While χ_{dis} $(T = T_c) \propto L^{\bar{\gamma}/\nu}$ and $\bar{\gamma}$ satisfies hyperscaling ($\bar{\gamma} + 2\beta = d\nu$), in the connected susceptibility a smaller exponent ($\gamma = \bar{\gamma}/2$) results, because the two leading terms cancel each other, and only a subleading correction remains. This is only possible because in the scaling limit of the distribution $P_L(m)$ the position of the peaks scale with a less negative exponent ($-\beta/\nu$) than the width ($(\gamma/\nu - d)/2$). Since for $L \to \infty$ at T_c $P_L(m)$ becomes a sum of delta functions, the cumulant intersection method is less useful: U_L {Eq. (108)} tends to 2/3 at T_c as in the low temperature phase, and there is no well defined intersection point (Eichhorn and Binder 1996). In contrast, for other random systems such as spin glasses (Binder and Young 1986) or Potts glasses (Binder and Reger 1992) the cumulant intersection method has been the most useful method to check for the existence of static phase transitions in thermal equilibrium (Young 1996), since the lack of cumulant intersections can be taken as evidence that the system is at or below its lower critical dimension for a spin glass transition.

Non-trivial extensions of finite size scaling are necessary to deal with tricritical phenomena (Wilding and Nielaba 1996) and anisotropic critical phenomena, where the correlation length diverges with a (larger) exponent $\nu_\parallel$ in a distinct direction $\left\{\xi_\parallel \propto |1 - T/T_c|^{-\nu_\parallel}\right\}$ than in the perpendicular direction (s) $\left\{\xi_\perp \propto |1 - T/T_c|^{-\nu_\perp}, \nu_\perp \leq \nu_\parallel\right\}$. The latter case occurs at uni-axial Lifshitz points as they occur for the anisotropic next nearest neighbor Ising (ANNNI) model (Selke 1988), for critical wetting transitions (Dietrich 1988), and - last but not least - for driven systems far from equilibrium, such as the charged lattice gas under the action of an electrical field (Schmittmann and Zia 1995).

Denoting the linear dimensions of the system in the parallel and perpendicular directions as $L_\parallel$ or $L_\perp$, respectively, an extension of finite size scaling to this case (Binder and Wang 1989) showed that in addition to the variable $\varepsilon L_\parallel^{1/\nu_\parallel}$ {cf. Eqs. (109)-(112)} one needs a second variable, a generalized aspect ratio $L_\parallel^{\nu_\perp/\nu_\parallel} / L_\perp$ {this factor reduces to the standard aspect ratio $L_\parallel / L_\perp$ for isotropic critical phenomena, of course, needed to describe shape effects near criticality, see Binder and Wang (1989) and Albano et al. (1989a)}. After a long controversy about the critical behavior of the two-dimensional driven lattice gas a finite size scaling study along these lines (Wang 1996) finally obtained consistency with the field-theoretic predictions. We return now to "simple" critical phenomena such as the liquid-gas transition but consider systems that lack the particular particle-hole symmetry of the Ising lattice gas model, e.g. off-lattice fluids. Not only has then the critical point to be searched for in a two-dimensional

parameter space (temperature T and the chemical potential μ, for instance), but also there are rather strong corrections to scaling induced by a coupling between order parameter density and energy density fluctuations (Wilding and Bruce 1992, Wilding 1993, 1995, Wilding and Müller 1995). The critical part of the energy density scales with L as $L^{-(1-\alpha)/\nu}$ where α is the specific heat exponent (e.g. Milchev et al. 1986), and this needs to be disentangled from the order parameter that scales as $L^{-\beta/\nu}$. Wilding and Bruce (1992) and Wilding (1993, 1995) solved this problem by a linear transformation from the density ρ and energy density u to the appropriate "scaling fields". Using this technique in the context of grand-canonical simulations of simple fluids, a satisfactory analysis of their critical region became feasible (Wilding 1995, 1996). Also a successful extension of this concept to asymmetrical polymer mixtures (Müller and Wilding 1995) was given. For critical properties, these techniques are superior to both the "Gibbs ensemble" method (Panagiotopoulos 1987, 1992, 1994, Smit 1993, Allen 1996) and standard finite size scaling applied to subboxes (Rovere et al. 1990, 1993).

Thus, finite size scaling techniques have become a very powerful tool for analyzing critical phenomena by computer simulations. Nevertheless, there are still problems applying this approach, in particular when one considers crossover from one universality class to another (Binder and Deutsch 1992, Deutsch and Binder 1993a, Mon and Binder 1993, Luijten et al. 1996, Binder et al. 1996). Then the scaling functions $\tilde{M}, \tilde{\chi}, \tilde{\chi}'$ and $\tilde{U}$ in Eqs. (109)-(112) not only depend on the variable L/ξ (which vanishes at T_c) but on a second variable L/ξ_{cross}, ξ_{cross} being the correlation length in the center of the crossover region. Asymptotic criticality is reached only for $L >> \xi_{cross}$, and the cumulant intersection for locating T_c works only in this limit, since at T_c $\tilde{U}$ is not a constant but still a function of L/ξ_{cross}, see Fig. 12 for an example. Another particularly intriguing problem is the crossover between d - dimensional critical behavior and (d - 1) dimensional critical behavior in thin films (Binder 1974, Freirie et al. 1994, Rouault et al. 1995), where it is unclear to what extent such systems can be characterized by an effective dimensionality d_{eff} in between these dimensions. Particular difficulties occur also for the crossover from "pure" to "impure" behavior in systems with random impurities (Wang et al. 1990, D'Onorio de Meo et al. 1995) or random fields (Rieger 1995, Pereyra et al. 1993, 1995, Eichhorn and Binder 1996). For such problems, finite size techniques are successful only if a huge computational effort is invested in the quenched average $[...]_{av}$ over the random samples (Rieger 1995), and often the lack of very efficient algorithms is a severe limitation.

4.3 First order versus second order transitions; phase coexistence and phase diagrams

In an infinite system, a first order transition is characterized (Binder 1987) by a jump in first derivatives of the thermodynamical potential and by delta-function singularitites in second derivatives (Fig. 13). In finite systems, these singularities again are rounded and shifted (Imry 1980, Fisher and Berker 1982, Blöte and Nightingale 1982, Cardy and Nightingale 1983, Privman and Fisher 1983, Binder and Landau 1984, Fisher and Privman 1985, Challa et al. 1986, Privman and Rudnick 1990, Borgs and Kotecky 1990, Borgs et al. 1991, Lee and Kosterlitz 1991, Herrmann et al. 1992, Vollmayr et al. 1993, Tsypin 1994).

Let us first consider the simplest case, the field-driven transition in the Ising system for $T < T_c$, where the symmetry of the problem implies that the transition is only rounded by finite size but not shifted. The behavior is understood most simply be generalizing Eq. (117a), including the dependence on magnetic field (Binder and Landau 1984). The weights of the two peaks are no longer equal, but rather given by Boltzmann factors involving the Zeeman energy, $\pm H m_{spont} L^d$. This yields, for $L \to \infty$ and m near one of the two branches of Fig. 13,

$$P_L(m) \propto \exp(Hm_{spont} L^d/k_BT) \exp\{ -(m - m_{spont} - \chi' H)^2 L^d/k_BT\} + \exp(-Hm_{spont} L^d/k_BT) \exp\{ -(m + m_{spont} - \chi' H)^2 L^d/k_BT\} \quad (119)$$

Here we have taken into account that for $H \neq 0$ the gaussian peaks occur no longer for $m = \pm m_{spont}$ but rather for $m = \pm m_{spont} + \chi' H$. This approach yields for the magnetization

$$\langle m \rangle = \chi' H + m_{spont} \tanh (Hm_{spont} L^d/k_BT) \quad (120)$$

and thus the rounding of the singularity of the susceptibility is described by

$$\chi(H,T,L) = \chi' + m_{spont}^2 (L^d/k_BT)/\cosh^2 (Hm_{spont} L^d/k_BT) \; . \quad (121)$$

Thus the delta function is smeared out into a peak of height proportional to L^d and of width ΔH proportional to L^{-d}. Fig. 14 shows that in the $d = 2$ Ising ferromagnet this simplified description {Eq. (119) ignores contributions with inhomogeneous order parameter distributions containing interfaces in the finite system, see Sec. 4.4} works rather well even for very small systems.

The symmetry $\chi(H,T,L) = \chi(-H,T,L)$ of the Ising model can be broken, for example, by multispin interactions (Binder and Landau 1989, Borgs and Kappler 1992), by boundary fields (in systems with free surfaces, see e.g. Fisher and Nakanishi 1981, Albano et al. 1989b, Binder and Landau 1992), etc. In this case the "transition" (monitored by the peak position of χ) in the finite system no longer occurs at $H = 0$ but rather at a shifted field H_0, $H_0 \propto L^{-\lambda}$.

The first case (asymmetric bulk transition) leads to a shift exponent $\lambda = d$ (Binder and Landau 1984), i.e. the shift is of the same order as the rounding. In the second case, symmetry breaking boundary fields (note that for the gas-liquid transition of fluids this case is called "capillary condensation"), the shift is much larger than the rounding, $\lambda = 1$, because it is controlled by a competition of surface and bulk terms.

While the symmetry of the ordinary Ising model (without multispin interactions, boundary fields, etc.) implies that at the transition (for $H = 0$) the two peaks of $P_L(m)$ {Fig. 6, Eqs. (117a) and (119)} have both equal height and equal weight, some confusion has arosen (Challa et al. 1986) which of these two properties carries over to the transition at $H_c \neq 0$ in the asymmetric case. It now has been rigorously proven (Borgs and Kotecky 1990, Borgs et al. 1991) and nicely confirmed by simulations (Borgs and Kappler 1992) that the "equal weight rule" (Binder and Landau 1984) is correct, and one has now a better understanding (Tsypin 1994) why the "equal height rule" (Challa et al. 1986) is incorrect.

This "equal weight rule" has become a convenient tool for establishing phase boundaries of off-lattice fluids (Wilding 1995, 1996) and asymmetric mixtures (Deutsch and Binder 1993b, Deutsch 1993, Müller and Binder 1995, Müller and Wilding 1995). While in the Ising magnet (or the isomorphic lattice gas model) phase coexistence occurs at $H = 0$ and hence only temperature needs to be varied to locate T_c, no simple symmetry relates the two coexisting phases in the general case. Then it is non-trivial to locate the chemical potential $\mu_c(T)$ {or chemical potential difference $\Delta\mu_c(T)$, in the case of the mixture} where phase coexistence occurs. Near the critical point it is convenient to use histogram reweighting (Ferrenberg and Swendsen 1988) to sample $P_L(m)$ over a sufficient range of values in the (T,μ) {or $(T,\Delta\mu)$} plane. Defining m^* in the region where $P_L(m)$ has a double-peak structure as the value where

$\langle m^2\rangle - \langle m\rangle^2$ is maximal, the weights of the two peaks are equal. For the case of an asymmetric (polymer) AB-mixture with pairwise interactions $\varepsilon_{AA} = \lambda\,\varepsilon_{BB}$ with $\lambda \neq 1$ the order parameter for chain lengths $N_A = N_B = N$ can still be chosen as $m = (n_A - n_B)/(n_A + n_B)$, where n_A, n_B are the numbers of A,B-chains in the system, as in Fig. 11. However, while in the fully symmetric case $m^* = 0$, m^* is different from zero in the general case. The weights of the A-rich and A-poor phases then are defined as (Deutsch and Binder 1993b)

$$P_{poor} = \int_{-1}^{m^*} P_L(m)dm\,, \qquad P_{rich} = \int_{m^*}^{1} P_L(m)dm \tag{122}$$

For implementing the equal-area rule it is convenient to use the ratio R of these weights defined as

$$R \equiv \min\{P_{poor}/P_{rich}\,,\, P_{rich}/P_{poor}\} \xrightarrow[L\to\infty]{} \begin{cases} 1 \text{ for } \Delta\mu = \Delta\mu_c(T) \\ 0 \quad \text{else} \end{cases} \tag{123}$$

or the connected part of the cumulant $U_L^{conn}(T) = 1 - \langle m^4\rangle_{conn}/3\langle m^2\rangle^2$. Both R and U_L^{conn} have very sharp peaks at $\Delta\mu = \Delta\mu_c(T)$ (Deutsch 1993, Deutsch and Binder 1993b). Varying T along the line $\Delta\mu = \Delta\mu_c(T)$ in the $(T,\Delta\mu)$ plane one now can study U_L^{conn} or ratios such as $\langle m^2\rangle/\langle|m|\rangle^2$, cf. Fig. 11, and obtain both T_c and the coexistence curve from a finite size scaling analysis with high precision.

We now turn to thermally driven first-order transitions, using the Potts model, Eq. (99), as an explicit example. At the transition point $T = T_c$ the energy jumps from E_- to E_+ (Fig. 13), i.e.

the free energy branches $F_-(T)$ and $F_+(T)$ intersect at a finite angle, $F_\pm = E_\pm - T\,S_\pm$, with $F_-(T_c) = F_+(T_c)$. Thus $\Delta F \equiv F_+ - F_-$ vanishes at T_c, and near T_c we can expand linearly in $\Delta T = T - T_c$, to express weight factors a_+, a_- of these phases as

$$a_\pm \equiv \exp\{\mp \Delta F L^d/(2k_BT)\} \approx \exp\{\pm (E_+ - E_-)\,\Delta T L^d/(2k_B T_c^2)\} \tag{124}$$

Of course, we must take into account that in the q-state Potts model there is a single disordered state but q distinct ordered phases.

The order parameter $\vec{m}$ of the Potts model involves a $n = q - 1$-dimensional space, and the distribution $P_L(\vec{m})$ is anisotropic in this space {e.g., for q = 3 sharp peaks occur near $(m_1, m_2) = (1,0)$, $(-1/2, \sqrt{3}/2)$ and $(-1/2, -\sqrt{3}/2)$, respectively, see Vollmayr et al. (1993) and Stephanow and Tsypin (1991)}. It is then convenient to study either the distribution of the energy $P_L(E)$ (Challa et al. 1986) or the distribution of the absolute value of the order parameter $P_L(m)$ (Vollmayr et al. 1993). Approximating each peak by a (multivariate) Gaussian for $P_L(\vec{m})$, one finds

$$P_L(m) \propto \frac{L^{nd/2}}{\chi_+^{n/2}} \frac{a_+ m^{n-1}}{a_+ + q a_-} \exp\left\{-\frac{m^2 L^d}{2k_B T \chi_+}\right\} + \frac{q a_-}{a_+ + q a_-} \frac{L^{d/2}}{\chi_-^{1/2}} \exp\left\{-\frac{(m - m_{spont})^2 L^d}{2k_B T \chi_-}\right\} \tag{125}$$

where χ_+, χ_- characterize the order parameter fluctuations in the disordered and ordered phases, respectively, and m_{spont} is the order parameter as $T \to T_c^-$. Similarly, the energy distribution becomes (Challa et al. 1986, Borgs and Kotecky 1990, Borgs et al. 1991)

$$P_L(E) \propto \frac{a_+}{C_+^{1/2}} \exp\{(E - E_+ - C_+ \Delta T)^2 L^d/(2k_B T^2 C_+)\} +$$

$$+ \frac{qa_-}{C_-^{1/2}} \exp\{(E - E_- - C_- \Delta T)^2 L^d/(2k_B T^2 C_-)\} , \qquad (126)$$

C_+ , C_- being the specific heats of the coexisting disordered and ordered phases, respectively.

Eqs. (125),(126) form the basis of the phenomenological theory of finite size effects at first order transitions. Again it is convenient to introduce suitable fourth-order cumulants,

$$g_L(T) \equiv \{[\langle m^4\rangle/\langle m^2\rangle^2]_{T\to\infty,L\to\infty} - [\langle m^4\rangle/\langle m^2\rangle^2]_{T,L}\}$$
$$/\{[\langle m^4\rangle/\langle m^2\rangle^2]_{T\to\infty,L\to\infty} - [\langle m^4\rangle/\langle m^2\rangle^2]_{T=0,L\to\infty}\} \qquad (127)$$

and

$$V_L \equiv 1 - \langle E^4\rangle/(3\langle E^2\rangle^2) \quad . \qquad (128)$$

One then can show (Vollmayr et al. 1993) that $g_L(T)$ develops a minimum at T_{min}, that tends to $-\infty$ as L^d and an (approximate) crossing point at $g(T_{cross}) \approx 1 - n/(2q)$. The positions T_{min}, T_{cross} scale as

$$T_{min} - T_c \propto L^{-d} \ , \ T_{cross} - T_c \propto L^{-2d} \quad . \qquad (129)$$

This behavior is illustrated in Fig. 15.

In addition, the energy cumulant develops a minimum that carries information on the latent heat,

$$V_L^{min} = \frac{2}{3} - \frac{1}{3}\left\{\frac{(E_+ - E_-)(E_+ + E_-)}{2E_+E_-}\right\}^2 + 0\left(L^{-d}\right) \quad , \qquad (130)$$

the position of this minimum being at

$$T_V(L)/T_c - 1 = \{k_B T_c/L^d(E_+ - E_-)\}\ \ell n\,(q E_-^2 / E_+^2), \qquad (131)$$

and also the position of the specific heat maximum contains a similar shift proportional to the inverse volume,

$$T_c(L)/T_c - 1 = \{k_B T_c/L^d(E_+ - E_-)\}\ \ell n\, q \quad , \qquad (132)$$

The height being again linked to the latent heat,

$$C_L^{max} = (C_+ + C_-)/2 + (E_+ - E_-)^2 L^d/(4 k_B T_c^2) \qquad (133)$$

Since the temperature region δT over which the rounding of the delta function peak occurs is just given by taking the argument of the exponential functions in Eq. (124) of order unity,

$$\delta T = 2 k_B T_c^2 / [(E_+ - E_-) L^d] \quad , \qquad (134)$$

we conclude that rounding and shifting of the specific heat peak are of the same order of magnitude, and the shift in the position of the minima of $g_L(T)$ and V_L is of the same order of magnitude ($\propto L^{-d}$) as well. However, on this scale the shift of the crossing points of $g_L(T)$ is

negligibly small (Fig. 15), namely proportional to L^{-2d}. Therefore, the cumulant intersection method is useful to locate any phase transition, irrespective of its order. For first order transitions, in principle the best method (Borgs et al. 1991) for locating T_c is to look for intersection temperatures T_i of energies $E(T,L) \equiv \langle E \rangle$ and $E(T, 2L)$,

$$E(T_i,L) = E(T_i,2L) \quad , \tag{135}$$

since T_i should differ from T_c only by exponentially small corrections.

However, it must be stressed that the description presented in Eqs. (124)-(134) is greatly simplified and phenomenological, it holds only for $L >> \xi_+, \xi_-$, the correlation lengths in the two coexisting phases at T_c . High precision studies of the Potts model in d = 2 with q = 8,10 and 20 (note that E_+, E_-, T_c are known exactly for all q, see Wu (1982)) have shown that one easily makes systematic errors in the estimation of E_+ and E_- if the limit $L >> \xi_+, \xi_-$ is not reached (Billoire et al. 1992, 1993). In contrast, Gross et al. (1996) suggest that a much faster convergence occurs in the microcanonical ensemble. At this point, we note also that the computationally most efficient way to locate a first order transition often is not the finite size scaling method {both the multicanonical sampling (Berg and Neuhaus 1992) and the microcanonical one (Gross et al. 1996) involve then a study of states with energies E in the interval $E_- < E < E_+$, which are controlled by configurations with slowly relaxing interfaces}, but the simple thermodynamic integration method, where one studies pure phases throughout. An example for this statement is provided by the Ising model on the face-centered cubic (fcc) lattice with nearest neighbor antiferromagnetic interactions in a magnetic field H: there occurs for small enough fields an ordered phase with two sublattices with positive magnetization and two sublattices with negative magnetization (↑↑↓↓), while for larger fields another ordered phase with three sublattices with positive magnetization (↑↑↑↓) is stable. This problem is isomorphic to the problem of order-disorder phenomena for binary (AB) alloys on the fcc lattice (example: CuAu-alloys, see Binder 1986 for a review), and although the phase diagram of this model is studied since nearly 60 years (Shockley 1938), it is still incompletely understood (Kämmerer et al. 1996)! The problem is the location of the triple point T_t between the disordered phase, the "AB phase" (↑↑↓↓ in spin representation) and the "A_3B phase" (↑↑↑↓). While in the molecular field approximation (Shockley 1938) such a triple point does not even occur (the A_3B phase and AB_3 phase enclose the AB phase, and a direct transition from the AB to the disordered phase occurs only in one point in the phase diagram, in which the A_3B and AB_3 phase boundaries meet), more sophisticated treatments yield triple points, but the precise location has been rather controversial {estimates for T_t range from $T_t = 0$ to $T_t \approx 1.5\ J/k_B$, see Binder 1986). Studies of this problem with finite size scaling are very difficult, due to the high ground state degenerancy of the model and the fact that one deals with more-component order parameters (Kämmerer et al. 1996). However, using large lattices (L = 64, i.e. $N = 4.64^3 = 1{,}048576$ lattice sites) one can obtain the phase diagram rather precisely (Fig. 16). However, even a million of lattice sites is not enough to resolve the width of the two-phase coexistence regions near the triple point - which could also be a new type of multicritical point. Substantially larger lattices would be needed to clarify this problem!

Unfortunately, this example is not atypical, but distinction of weak first order transitions from second-order ones often is not unambigously possible, or at least very difficult! A longstanding and experimentally relevant problem is the transition of N_2 adsorbed as a two-dimensional monolayer on graphite from the "herringbone structure" at low temperature to the orientationally disordered plastic crystal phase at high temperatures (Marx et al. 1994). Since thermodynamic integration is less convenient for continuous degrees of freedom, in this case

the (weakly) first order character was established from a study of orientational correlations at both sides of the transition. And a particularly hard problem is the melting of hard disks (Weber et al. 1995): although the Monte Carlo method in statistical physics started with the consideration of the equation of state of this system (Metropolis et al. 1953), it turns out that still the width of the two-phase coexistence region is unknown {early estimates, e.g. Alder and Wainwright (1962), overestimated the density jump substantially}.

4.4 Different boundary conditions; surface and interface properties

Choosing periodic boundary conditions (or screw periodic boundary conditions, which are used for lattice models storing lattice sites in a one-dimensional array going through the lattice in a typewriter fashion) are useful to focus on bulk properties of the model, undisturbed by surface effects. However, sometimes one is interested in surface or interface properties, and then a different choice of boundary conditions may be useful. E.g., for studying the properties of small magnetic particles one may simply simulate an Ising or Heisenberg model on a lattice with linear dimensions L_x, L_y, L_z in the three lattice directions and use "free surface" boundary conditions (i.e., neighbors adjacent to the surface are just missing). Of course, one can generalize this boundary condition to small particles of arbitrary shape, e.g. approximately spherical particles (Binder et al. 1970, Wildpaner 1974), and it may be of physical interest to consider surface effects more complicated than simply "missing neighbors", such as exchange interactions that differ in the surface from their value in the bulk (Binder and Hohenberg 1974), surface anisotropies or surface fields, etc. The same choices also apply to the simulation of thin films, where one usually chooses a LxLxD geometry with two free LxL surfaces but periodic boundary conditions in the x,y-directions parallel to these surfaces (Binder 1974). We shall not give any details here but rather refer to recent reviews (Binder et al. 1995, Landau 1996).

Somewhat more involved is the study of surface properties of "semi-infinite" solids. If the disturbance created by the surface in the interior of the solid decays sufficiently fast with the distance from the surface, the straightforward solution is to use again the above LxLxD geometry but make D so large that in the middle of the system bulk behavior is indeed recovered. This simple recipe works well for the study of surface critical phenomena in Ising magnets (Landau and Binder 1990), wetting phenomena (Binder et al. 1989), surface-induced ordering and disordering in lattice models for metallic alloys (Schweika et al. 1996), etc. However, this approach does become cumbersome when large characteristic lengths appear in the system, e.g. at a temperature distance a few percent below the critical temperature of an Ising model a thickness D = 160 lattice spacings may be barely sufficient (Binder et al. 1989). The situation becomes particularly cumbersome when the perturbation due to the surface decays with a power law of the distance z from the free surface. This happens, e.g., for Heisenberg ferromagnets (Binder and Hohenberg 1974) where $m(z \to \infty) - m(z) \propto z^{-1}$. In this case it was tried to work with one free surface only and use the "self-consistent effective field" boundary condition (SCFBC) at the opposite wall to simulate "bulk" behavior there (Binder and Hohenberg 1974). SCFBC were proposed (Müller-Krumbhaar and Binder 1972) as an alternative to the periodic boundary condition for studying phase transitions in the bulk, the advantage being that the effective field provides a symmetry breaking and when $L \approx \xi$ one does not have a rounding off of the transition but a crossover to a mean-field type transition. A popular variation of this technique, where one analyses the change of these mean-field singularities when the linear dimension L is varied, is called the "Monte Carlo coherent anomaly method (MCCAM)" (Katori and Suzuki 1987, Ito and Suzuki 1991).

The study of free surfaces is by no means restricted to the case of lattice models, of course. Simulations of off-lattice models of solids with free surfaces can address problems such as

surface melting or faceting transitions (DiTolla et al. 1996), surface reconstruction, etc. We shall not discuss these issues here, since actually often Molecular Dynamics methods are applied to these problems and anyway most of these studies are still in rather early stages. In contrast, a problem that has been studied for a long time are the physical properties of fluid droplets, where the surface area and shape of the droplet may fluctuate (e.g. Lee et al. 1973). This problem is of fundamental interest for a better understanding of nucleation theory (Zettlemoyer 1969, 1977, Abraham 1974, Binder and Stauffer 1976). Of course, in this case one usually confines the droplet in a box with repulsive walls, in order to prevent that atoms evaporate from the droplet and escape far away from the cluster. While such techniques seem to work well at low temperatures close to the triple point, where the vapor pressure of the fluid is rather small, the technique becomes problematic at higher temperatures, in particular near the critical point (Binder and Kalos 1980, Furukawa and Binder 1982). One then can analyze this situation in terms of the equilibrium between the fluid droplet and the surrounding gas that is also confined in the box, and analyze the properties of the two subsystems (droplet, gas) separately {see also Binder and Stauffer (1972) for an early study of lattice gas droplets}. These concepts exemplify once more that one can study arbitrarily defined subsystems in simulations which then exhibit in a sense "fluctuating boundary conditions": e.g., using a division of a fluid in the NVT ensemble into n subsystems of volumes v = V/n, particles can be exchanged freely through the virtual "walls" of the subsystem, and so density fluctuations are easily sampled while in the total system the density $\rho = N/V$ is held fixed. Such techniques are useful for both the study of liquid-gas transitions (Rovere et al. 1988, 1990, 1993) and fluid-solid transitions (Weber et al. 1995). While these subsystems are defined such that their particle number fluctuates but their volume and shape is fixed, in the study of fluid droplets one does not fix size and shape of their volume but rather their number or their chemical potential, respectively.

Often one is also interested in studying the properties of flat interfaces between coexisting phases. Typically one is interested in the "intrinsic" profile $\rho_{int}(x)$ of the order parameter distinguishing the phases, and the interfacial free energy f_{int}. We now discuss the boundary conditions that one is using in this context, using again the Ising ferromagnet as an example. The boundary condition used in first principle work is a "fixed-spin" boundary condition, half of the boundary of a system of size $L^{d-1} M$ having spins fixed at +1 as neighbors, the other half has spins fixed at -1, as indicated in Fig. 17 (a). With this boundary condition, the average position of the interface is precisely fixed, and so the profile $\rho(x)$ and the mean-square width $w_d(L) = \left\langle \left[\frac{1}{L^{d-1}} \int d^{d-1}y x_{int}(\vec{y}) \right]^2 \right\rangle^{1/2}$ are well-defined. However, in this way one does not always obtain the "intrinsic" profile (which in fact is difficult to define in an unambigous way), because {above the interfacial roughening transition temperature T_R (Abraham 1986, van Beijeren and Nolden 1987)} the interfacial profile is unstable against long wavelength capillary wave excitations. Over a length scale L these capillary waves give rise to an interfacial width of the order

$$w^2_{d=3}(L) \propto \frac{1}{\kappa} \ell n(L/\xi) \qquad \text{or} \qquad w^2_{d=2}(L) \propto L/\kappa \quad , \tag{136}$$

where κ is the "interfacial stiffness". For d = 2, $T_R = 0$ while in the three-dimensional nearest neighbor Ising model $T_R \approx 2.4535\ J/k_B$ (Hasenbusch and Pinn 1996). Note that for the liquid-gas interface or interfaces between different fluid phases we always have $T_R = 0$ also in d = 3 dimensions and for such isotropic systems $\kappa = f_{int}/k_BT$, while κ exceeds f_{int}/k_BT in lattice systems where the interfacial tension in general depends on the orientation of the interface (Van Beijeren and Nolden 1987, Mon et al. 1989, Hasenbusch and Pinn 1993).

The boundary condition of Fig. 17 (a) is inconvenient for simulations and thus one rather uses "fixed spins" only in the boundaries parallel to the interface and periodic boundary conditions in the other direction(s), Fig. 17 b (Mon and Jasnow 1984). One sometimes obtains the interfacial free energy by carrying out a simulation also with boundary conditions (++) on both surfaces (Fig. 17 (c)), to sample the energy difference $\Delta E = E_{+-} - E_{++}$, which then is attributed to the interface contribution. The interfacial free energy can then be obtained from $\Delta E(T)$ via thermodynamic integration. By related methods the interface free energy of the Ising model has been found rather accurately (Mon 1988). One must not forget, however, that interfacial profiles obtained from a geometry as in Fig. 17b (see e.g. Leamy et al. 1973) are not meaningful without a detailed discussion of how properties do depend on the linear dimensions L,M of the system. Even in the limit where L gets very large one finds a strong dependence of the interfacial profile on the other linear dimension in the direction perpendicular to the interface, see Fig. 18 (Kerle et al. 1996). Similar size effects on interfacial profiles are also expected for off-lattice models, of course. Often there one chooses a geometry LxLxD with D >> L and periodic boundary conditions (pbc) throughout, starting from an initial configuration where a "slab" of phase with order parameter $\langle \rho_+ \rangle$ coexists with phases with order parameter $\langle \rho_- \rangle$ both to the right and to the left of the slab, so one records two interfacial profiles (e.g. Alejandre 1995 a,b). In view of these size effects, methods are somewhat problematic where one computes f_{int} from the profile $\rho(x)$ using suitable generalizations of van der Waals theory (Abraham 1974,. Rao and Levesque 1976). An alternative method uses the profile of the pressure tensor, Eq. (72), $\Pi_N(x) = \Pi_{zz}$, $\Pi_T(x) = (\Pi_{xx} + \Pi_{yy})/2$, to compute the interfacial tension from the formula (e.g. Rao and Berne 1978, Smit 1988)

$$f_{int} = \int dx \{\Pi_N(x) - \Pi_T(x)\} \quad , \tag{137}$$

the integration again being extended over the region of the interfacial profile (in the homogeneous phases the pressure is isotropic, of course, and hence $\Pi_N(x) = \Pi_T(x)$). Related formulas can also be used to obtain the surface free energy associated with walls (e.g. Pandey et al. 1996). We are not aware of any systematic investigation that size effects have on Eq. (137), however.

For lattice systems such as Ising ferromagnets or antiferromagnets (Schmid and Binder 1992 a,b) it often is convenient to use instead of the boundary condition of Fig. 17 (b) an antiperiodic boundary condition (apbc). E.g., for an Ising ferromagnet in DxLxL geometry this means $S(x \pm D,y,z) = - S(x,y,z)$, with (x,y,z) being the coordinate of the lattice site i. Then any perturbation by walls or boundary fields is strictly avoided, but a disadvantage is that this situation still has full translational invariance: the interface can be anywhere in the system, and actually in the course of a Monte Carlo run will undergo a diffusive motion. If one wants to estimate the interfacial energy only, this delocalization of the interface does not matter, one simply has to obtain the free energy difference between this system and a corresponding simulation with pbc, $f_{int} = D[F_{apbc} - F_{pbc}]$ {recalling that F denotes a free energy per spin}. For a study of interfacial profiles, one has to create a second coordinate system, whose origin is fixed to the center of the diffusing interface, and record profiles in this frame (Schmid and Binder 1992 a,b).

If one is interested in the interfacial free energy f_{int} only, a convenient method consists in the sampling of how the minimum of the order parameter distribution $P_L(\rho)$ in between $\langle \rho_+ \rangle$, $\langle \rho_- \rangle$ decreases with increasing linear dimension {Fig. 17(d)}. This technique (Binder 1982) is particularly convenient, since it yields f_{int} as a byproduct of a simulation of bulk properties of the model system in a L^d geometry. This method relies on the fact that for $L >> \xi$ the state of

the system near the minimum is dominated by a configuration with two (on the average flat) domain walls running parallel to each other and to a lattice plane through the system: Therefore, one expects

$$P_L(\rho = \rho_{min}) \propto \exp(- 2L^{d-1} f_{int}/k_BT) \quad , \qquad (138)$$

because the excess free energy cost of the configuration sketched in Fig. 17 (d) is given by two interfaces of area L^{d-1} each. The validity of Eq. (138) is checked by recording $P_L(\rho)$ for a wide range of L, noting that the probability should for $L >> \xi$ be nearly constant for a whole range of ρ around ρ_{min} , since changing ρ changes then only the volume fraction of the two coexisting phases, but not their interfacial contributions. However, since $P_L(\rho)$ from $<\rho_->,<\rho_+>$ to ρ_{min} varies over many orders of magnitude, one needs to apply "multicanonical" sampling in order to reach sufficient accuracy (Berg and Neuhaus 1992, Berg et al. 1993): after proper reweighting, an order parameter distribution which in between $<\rho_->$ and $<\rho_+>$ is nearly flat is simulated. For the Ising magnet this so-called "multimagnetic" (Hansmann et al. 1992) sampling has yielded very precise interfacial free energies (Berg et al. 1993) and the critical vanishing of f_{int} near T_c could be investigated. Even rather complex systems such as models for polymer mixtures have been successfully studied with this technique (Mueller et al. 1995).

5. Miscellaneous Topics

5.1 Applications to dynamic phenomena

In Sec. 3.4 we have already seen that Monte Carlo (MC) sampling can be interpreted as a "time averaging" along a stochastic trajectory through phasespace, and this notion can be made precise in terms of a markovian master equation for the probability $P(\bar{X},t)$ that the system is in state $\bar{X}$ at time t {Eq. (47)}. Of course, the dynamical properties of a system described by such a stochastic trajectory differs in general from dynamic properties derived from a deterministic trajectory: remember that the Molecular Dynamics [MD] method amounts to solve Newton's equation of motion numerically (Ciccotti and Hoover 1986, Sprik 1996). In fact, for obtaining the dynamical properties of systems such as simple Lennard-Jones fluids MD is the only reasonable approach, and while MC is a perfectly valid approach for obtaining static properties of simple fluids in thermal equilibrium, the relaxation of density fluctuations seen in a Monte Carlo run has nothing to do with the actual way that density fluctuations in fluids decay.

But MC is a reasonable and useful method for describing dynamic properties of systems where the considered degrees of freedom are a slow subset of all degrees of freedom. This slowness results from a weak coupling of these degrees of freedom to the fast ones, which then act like a heat bath. A good example is the diffusion process in solid alloys (Fig. 1), where the phonons of the crystal act like a heat bath. Suppose we would simulate such a mixed crystal at low temperatures by MD - most of the computer effort would be spent for simulating the lattice vibrations (which typically have a time constant of 10^{-13} sec), while the time constant on which jumps of A-atoms or B-atoms to vacant sites occur is orders of magnitude larger. It is easily possible then that in a MD run none (or only a few) such random jump events induced by the phonons are observed. While special MD techniques exist to simulate the detailed properties of such rare events (Ciccotti and Ferrario 1996), and such techniques are clearly useful for estimating the jump rates Γ_A, Γ_B for specific materials, MD clearly is impractical to study the collective dynamic properties on time scales large in comparison with the time scale of an isolated jump. If Γ_A, Γ_B can be assumed as given parameters, MC can straightforwardly

simulate directly the random hopping processes (Kehr et al. 1989, Kehr and Binder 1984). The MC technique is unique also for simulating slow non-equilibrium processes, which happen on macroscopic time scales, such as growth of ordered domains in adsorbed monolayers at surfaces (e.g. Sadiq and Binder 1984, Mouritsen 1990, Bray 1994), diffusion-limited growth of aggregates (Herrmann 1986, Meakin 1988), simulations of the growth of thin solid films via molecular beam expitaxy and related techniques (e.g. Family and Vicsek 1991, Landau and Pal 1996) etc. While these examples all refer to cases where one wishes to understand real systems in terms of crudely simplified coarse-grained models, there exist also models such as the Glauber Kinetic Ising model (Glauber 1963, Kawasaki 1972) where a master equation description is postulated not with the primary intention to describe any experimentally accessible systems but rather to elucidate general questions of statistical mechanics. In this context we recall that Ising magnets do not have any dynamics of their own - spin flips are thought to result as a consequence of a weak spin lattice coupling. These kinetic Ising models are of great interest to understand critical dynamics (Hohenberg and Halperin 1977) and MC methods have been used extensively for their study (e.g. Stoll et al. 1973, Landau et al. 1989). Of course, one can also identify problems where both MC and MD can be applied, e.g. the slow Brownian motion of polymer chains in dense polymer melts (Binder 1995, Kremer and Grest 1990, 1995, Paul et al. 1991). MC has then the advantage that unphysical "moves" (crossing of chains, "slithering snake"-motion, semigrand-canonical AB interchanges in mixtures, etc.) are permissible to equilibrate the system: one may then set a clock to zero, at which point these unphysical moves are turned off, in order to study the further time evolution of the system applying an algorithm that is physically reasonable (e.g. the random hopping algorithm of the bond fluctuation model, see Binder and Paul (1997) for a review). Of course, the MC dynamics does lack any hydrodynamic mechanisms which in principle are present in MD work. In addition, MC can model only diffusive motions and relaxation, but does not account for oscillatory motions that are present in shorter time scale. Such limitations must be kept in mind in the applications of MC methods to study the dynamics of polymers (Binder 1995) or other slow processes: relaxation of the magnetization in spin glasses (Binder and Young 1986), relaxation of molecular orientation in quadrupolar glasses (Müser and Nielaba 1995), etc.

After this general overview we briefly treat one example in more detail, to illustrate the great potential of the approach, and the type of questions that one can address: interdiffusion in binary solid mixtures (Fig. 1). The considered degrees of freedom are occupation variables c_i^A, c_i^B of lattice sites i which are unity if the site i is taken by an A-atom or a B-atom, respectively, and zero else. The phonons of the crystal induce then random hops with jump rates Γ_A, Γ_B to vacant lattice sites.

We now recall the description of this problem in the framework of phenomenological non-equilibrium thermodynamics: one postulates "constitutive equations" for the current densities $\vec{J}_A, \vec{J}_B$ of A,B atoms, namely linear relations between them and the driving forces, the gradients of chemical potential differences between A(B) atoms and vacancies V ($\mu_A - \mu_V$, $\mu_B - \mu_V$),

$$\vec{J}_A = - (\Lambda_{AA}/k_BT) \nabla (\mu_A - \mu_V) - (\Lambda_{AB}/k_BT) \nabla (\mu_B - \mu_V) \quad , \tag{139}$$

$$\vec{J}_B = - (\Lambda_{BA}/k_BT) \nabla (\mu_A - \mu_V) - (\Lambda_{BB}/k_BT) \nabla (\mu_B - \mu_V) \, . \tag{140}$$

Here Λ_{AA} , $\Lambda_{AB} = \Lambda_{BA}$, Λ_{BB} are the "Onsager coefficients". Eqs. (139),(140) are at best approximately valid, of course: non-linearities and fluctuations are neglected. Taken together

with the continuity equations that express the conservation laws for the local concentrations $c_A(\vec{r},t)$, $c_B(\vec{r},t)$

$$\partial c_A(\vec{r},t)/\partial t + \nabla . \vec{J}_A = 0 \quad , \quad \partial c_B(\vec{r},t)/\partial t + \nabla . \vec{J}_B = 0 \tag{141}$$

it is a matter of simple algebra (Kehr et al. 1989) to obtain a complete description of the interdiffusion process for a random alloy. E.g., the interdiffusion constant D_i, which describes how a weak deviation of the concentration difference between A and B from its average value spreads out, is given by

$$D_i = \frac{\Lambda_{AA}\Lambda_{BB} - \Lambda_{AB}^2}{\Lambda_{AA} + 2\Lambda_{AB} + \Lambda_{BB}} \left(\frac{1}{c_A} + \frac{1}{c_B} \right) , \qquad c_V \to 0 \ . \tag{142}$$

However, there are many questions about such a treatment: how are the Onsager coefficients related to the atomistic rates Γ_A, Γ_B (Fig. 1)? Is the "mean field" character of Eqs. (139),(140) an accurate description? Etc. In particular, it is common to neglect the off-diagonal coefficient Λ_{AB} (Brochard et al. 1983, Kramer et al. 1984), since nothing is known about it - but it is questionable whether Λ_{AB} is really small in comparison with Λ_{AA} and Λ_{BB} .

All these questions can be answered by "taylored" computer experiments: by imposing chemical potential gradients either on the A-atoms or on the B-atoms one can create steady-state currents in the system (particles leaving the box at one boundary reenter at the opposite one, because of the periodic boundary conditons!). Thus the Onsager coefficients can simply be measured from their definitions, Eqs. (139), (140). Fig. 19 shows that for $\Gamma_A/\Gamma_B \ll 1$ it is

wrong to neglect Λ_{AB} in comparison with Λ_{AA}. However, using the so determined Onsager coefficients in Eq. (142) provides an accurate description of interdiffusion, as Fig. 20 shows.

Fig. 20 also illustrates again that basic concepts of statistical physics can be implemented very directly in simulations, such as linear response: one applies a wavevector-dependent chemical potential difference $\Delta\mu(\vec{k})$ $\{k = 2\pi/\lambda\}$ to the system, to prepare an initial state of the model where a concentration wave with wavelength λ is present. In the example shown, the amplitude is chosen such that δc_A (t = 0) = δc_B (t = 0) = 0.02. At time t = 0, this perturbation $\Delta\mu(\vec{k})$ is suddenly switched off, and then one simply watches the decay of the concentration wave with time. Different wavelengths are used (Fig. 20) to check that one is actually in the long wavelength limit. And while the full mean field treatment {Eq. (142)} based on the actual Onsager coefficients works well, approximations (Brochard et al. 1983, Kramer et al. 1984) where the Onsager coefficients are somehow related to self-diffusion coefficients are not accurate in this case. Note that self-diffusion coefficients are straightforwardly obtained from meansquare displacements of tagged particles.

This is just one example out of many to show that MC simulations do have their place to study dynamic phenomena. For more details, as well as a discussion of alternative approaches such as MD and Brownian Dynamics (Ermak and McCammon 1978, van Gunsteren et al. 1981, Doll and Dion 1976, Ciccotti and Ryckaert 1980, Giró et al. 1985, Lemak and Balabaev 1995) where one numerically solves Langevin equations, we have to refer to the literature (Binder 1992b, Binder and Ciccotti 1995).

5.2 A brief introduction to path integral Monte Carlo (PIMC) methods

So far the discussions of this article have been confined to the framework of classical statistical mechanics throughout. However, this is an approximation - the basic laws of nature are quantum-mechanical, and thus it is very important to be able to take quantum effects into account in simulation techniques as well. Thus the development of MC techniques to study ground state as well as finite-temperature properties of interacting quantum many-body systems is an active area of research (for reviews see Ceperley and Kalos, 1979, Schmidt and Kalos 1984, Kalos 1984, De Raedt and Lagendijk 1985, Berne and Thirumalai 1986, Suzuki 1986, 1992, Schmidt and Ceperley 1992, De Raedt and von der Linden 1992, Hammond et al. 1994, De Raedt 1996, Ceperley 1996, Kreer and Nielaba 1996, Kawashima and Gubernatis 1996). These methods are of interest for a widespread variety of problems, including elementary particles (e.g. De Grand 1992), the structure of atomic nuclei (e.g. Carlsson 1988), superfluidity of Helium (e.g. Schmidt and Ceperley 1992), high T_c superconductors (e.g. Frick et al. 1990), hydrogen in metals (Gillan and Christodolous 1993), magnetism (e.g. Reger and Young 1988), surface physics (e.g. Marx et al. 1993, Kreer and Nielaba 1996) isotope effects in lattice dynamics (Müser et al. 1995, etc.). Here we cannot attempt to review all these applications, nor can we describe all the different techniques: variational Monte Carlo (VMC), Green's function Monte Carlo (GFMC), projector Monte Carlo (PMC), path-integral Monte Carlo (PIMC), grand-canonical quantum Monte Carlo (GCMC), world-line quantum Monte Carlo (WLQMC), etc. We note that some of these techniques are still under development, and there are sometimes serious problems hampering large-scale applications (such as the famous "minus sign problem" hampering the applications to multi-fermion systems, see e.g. De Raedt and von der Linden 1992). Here we shall not address any methods for ground-state properties (like VMC, GFMC), but are concerned with the PIMC method only that addresses properties at non-zero temperatures.

Unlike Eq. (3) we now consider an average $\langle \hat{A} \rangle$ where the Hamiltonian $\hat{\mathcal{H}}$ is treated as a quantum-mechanical operator, and we do not assume that the eigenvalues and eigenstates of $\hat{\mathcal{H}}$ are known explicitly,

$$\langle \hat{A} \rangle = (1/Z)\mathrm{Tr}\, \exp(-\hat{\mathcal{H}}/k_BT)\,\hat{A}\,, \quad Z = \mathrm{Tr}\, \exp(-\hat{\mathcal{H}}/k_BT)\,. \tag{143}$$

Here $\hat{A}$ is the operator associated with the classical observable $A(\bar{X})$ in Eq. (3). For simplicity, we consider first a single particle in one dimension exposed to a potential V(x), for which $\hat{\mathcal{H}} = -(\hbar^2/2m)d^2/dx^2 + V(x)$. In position representation ($|x\rangle$ is an eigenvector of the position operator) the partition function becomes

$$Z = \int dx \langle x|\exp(-\hat{\mathcal{H}}/k_BT)|x\rangle\,. \tag{144}$$

Eq. (144) is not straightforward to evaluate since the operators of kinetic energy $\{-(\hbar^2/2m)d^2/dx^2\}$ and potential energy $\{V(x)\}$ do not commute. Writing $\exp(-\hat{\mathcal{H}}/k_BT)$ formally as $[\exp(-\mathcal{H}/k_BTP)]^P$, where P is a positive integer, we can insert a complete set of states between the factors:

$$Z = \int dx_1 \ldots \int dx_P \langle x_1|\exp(-\hat{\mathcal{H}}/k_BTP)|x_2\rangle|\ldots|x_P\rangle \langle x_P|\exp(-\hat{\mathcal{H}}/k_BTP)|x_1\rangle \tag{145}$$

For large P, it is a good approximation to ignore the fact that kinetic and potential energy do not commute. Hence one gets

$$\left\langle x\left|\exp\left(-\hat{\mathcal{H}}/k_B TP\right)\right|x'\right\rangle \approx \left(\frac{k_B TmP}{2\pi\hbar^2}\right)^{1/2} \exp\left\{\frac{-k_B TmP}{2\pi\hbar^2}(x-x')^2\right\} \exp\left\{-\frac{1}{2k_B TP}\left[V(x)+V(x')\right]\right\} \tag{146}$$

and thus

$$Z = \left(\frac{k_B TmP}{2\pi\hbar^2}\right)^{P/2} \int dx_1 \ldots \int dx_P \exp\left\{-\frac{1}{k_B T}\left[\frac{1}{2}\sum_{S=1}^{P}\kappa\left(x_S - x_{S+1}\right)^2 + P^{-1}\sum_{S=1}^{P} V\left(x_S\right)\right]\right\} , \tag{147}$$

where $\kappa = k_B TmP/\hbar^2$. In the limit $P \to \infty$, Eq. (147) becomes exact. Apart from the prefactor, Eq. (147) is precisely the configurational partition function of a classical system, namely a ring polymer consisting of P beads coupled by harmonic springs with spring constant κ, each bead being under the action of a potential V(x)/P.

This approach is straightforwardly generalized to a system of N interacting quantum particles - one ends up with a system of N classical cyclic "polymer chains". However, an important distinction to physical melts of ring polymers is that in the present case beads of different chains interact with each other only if they are in the same "time slice" (i.e., have the same "Trotter index" s).

As a result of this isomorphism, classical MC methods can be readily applied to sample such quantum-mechanical problems. At high temperatures, κ gets very large, and then the system always behaves classically, since then the cyclic chains contract essentially to point particles again. At low temperatures, however, they are spread out over distances comparable to the thermal de Broglie wavelength, and in this way also zero-point motions are accounted for. However, PIMC becomes increasingly difficult at low temperatures, since P has to be the larger the lower T: If σ is a characteristic distance over which the potential V(x) changes, one

must have $\hbar^2/m\sigma^2 << k_B TP$ in order that two neighbors along the "polymer chain" are at a distance much smaller than σ. The appropriate value of this "Trotter dimension" P is determined empirically in most cases (typically one carries out runs for several choices of P and checks where thermal properties no longer change).

The step leading to Eq. (146) can be viewed as a special case of the Suzuki-Trotter-formula (e.g. Suzuki 1986)

$$\exp\left(\hat{A}+\hat{B}\right) = \lim_{P\to\infty}\left[\exp\left(\hat{A}/P\right)\exp\left(\hat{B}/P\right)\right]^P . \tag{148}$$

Eq. (148) is used for mapping d-dimensional quantum problems on lattices to equivalent classical problems in (d+1) dimensions: e.g., the Ising chain in a transverse magnetic field gets mapped onto a special two-dimensional Ising lattice, with a linear dimension P in the additional "Trotter direction" (which corresponds to the imaginary time direction of the path integral).

For rigid molecules the operator of angular momentum appears in $\hat{\mathcal{H}}$ in Eq. (144) and this requires another extension of the formalism. The fact that a rotation with an angle of 2π leaves the physical situation invariant creates subtle problems. For two-dimensional rotators (confined to rotate in a plane) the rotation angle φ plays a similar rôle as the coordinate x in Eq. (147), but in addition one has a summation over "winding numbers" expressing the fact how many multiples of 2π the angle passes along the ring polymer (Marx and Nielaba 1992, Marx et al. 1993b). Then in addition to "local" Monte Carlo moves $\varphi_s \to \varphi_s'$, which conserve the winding number, "global" moves are also needed to change the winding number. And for rotators with

two angular degrees of freedom one runs again into "minus sign" problems (Marx 1994, Müser 1996)!

As an example for the type of questions that one can address, Fig. 21 shows the order parameter and energy of N_2 adsorbed on graphite (Marx et al. 1993a). It is seen that quantum fluctuations depress the temperature of the order-disorder transition (which is rounded due to finite size effects, of course) by about 10%, and the order parameter saturates at 90% of its classical value due to zero-point vibrations. While the latter behavior is accounted for by quasi-harmonic theory, and the former effect could be accounted for by the Feynman-Hibbs approximation, there is in fact no approximate treatment accurate at temperatures in the ordered phase just below the transition. Note that such simulations are still rather difficult, since Trotter dimensions up to P = 500 needed to be used.

5.3 Some Recent Algorithmic Developments

The availability of vector processors and of massively parallel supercomputers has made necessary to develop Monte Carlo codes that take advantage of this specialized hardware and are optimized in order to perform on such machines as fast as possible (Landau 1992, Heermann and Burkitt 1992, Heermann 1996). On these problems, we shall not give any details here. We only mention that one always heavily exploits the freedom that one has in MC calculations (of static averages) in defining the precise order in which one carries out updating operations in the configurations of the system. E.g., for simulating Ising-type lattice models on vector processors it is preferable not to go through the lattice sites in the standard typewriter type fashion, but rather to decompose the lattice in sublattices such that the degrees of freedom on one sublattice do not interact with each other {for a nearest neighbor Ising square lattice,

this is already achieved by the well-known "checkerboard decomposition" into a "white" and a "black" sublattice, introduced by Oed (1982) for the Floating Point System AP-190L and used for a study of the Ising model interfacial tension (Binder 1982)}. In combination with multispin coding {multiple spins of one system are packed in a single word, as first suggested by Zorn et al. (1981)} or multilattice simulations {spins from 64 different lattices are packed into 64 bit words, see Bhanot et al. (1986)} very efficient algorithms result, as described in detail by Landau (1992). The principle of this checkerboard algorithm, that degrees of freedom which lack a direct interaction can be updated independently, is the basis of many related applications {e.g. spin-exchange kinetic Ising models (Zhang 1989, Amar et al. 1988), random Ising models (Heuer 1990) or Potts models (Eichhorn and Binder 1995, 1996), lattice models for alloys (Dünweg and Binder 1987) and polymer melts (Wittmann and Kremer 1990, 1992) etc.}.

At the time of writing vector processors are losing ground in comparison to parallel supercomputers. The concepts for efficient use of parallel processors are rather similar to those used in "vectorization" of programs - one has to identify tasks that can be carried out independently and concurrently. A straightforward idea is "domain decomposition", i.e. the system is geometrically decomposed into subsystems. For systems with short range interactions, interactions between degrees of freedom belonging to different subsystems occurs only in a rather narrow boundary region of each subsystem. If these subsystems are themselves sufficiently large, the overhead for communication between processors can be made sufficiently small in practice (Heermann and Burkitt 1992, Heermann 1996). Useful applications result when the physics of the problem requires large total system sizes, e.g. interfaces in polymer mixtures were simulated on lattices containing about 16 million sites (Müller et al. 1995), and simple Ising square lattices up to size of $10^6 \times 10^6$ could be studied (Linke et al. 1995, 1996). Of course, other strategies of parallelization may be preferable for different applications: doing MC with longrange interactions, one may simply split the ensemble of N particles into p

portions of N/p particles, each processor then calculates the energy change of one of these portions in a MC update. And even simpler is a method that is sometimes called "poor man's parallelization" (Heermann 1996): the system is simply replicated p times, each processor carries out the same program but with different random numbers (and perhaps also with a different starting configuration), and so the only communication among processors that is needed is the averaging of the results form individual processors in order to obtain the final results. This approach is very natural for systems containing randomly quenched disorder (Eichhorn and Binder 1995): one has to carry out anyway the average $[...]_{av}$ over the quenched disorder by averaging over a large number of equivalent replicas of the system, each containing a different realisation of the variables characterizing the quenched disorder (random bonds, random fields, randomly diluted sites, etc.): thus this disorder average is done in parallel, each processor is working on its own replica of the system.

Another very important line of research on Monte Carlo algorithms considers the construction of clever moves for the MC updates in order to sample the phase space most efficiently, i.e. to decorrelate successive configurations as fast as possible. E.g., for the Ising model at the critical temperature T_c the standard single spin flip algorithm suffers from the problem of "critical slowing down" (Hohenberg and Halperin 1977), which means in a finite size scaling context that the relaxation time τ scales with the linear dimension like $\tau \propto L^z$, z being the "dynamic exponent" of the model ($z \approx 2$). Many ideas have been followed to ease this problem: Fourier acceleration (e.g. Batrouni et al. 1985, Dagotto and Kogut 1987), multigrid MC (Goodman and Sokal 1986, 1989, Kandel et al. 1989, Hasenbusch et al. 1991, Janke and Sauer 1994, 1995), over-relaxation (Creutz 1987) etc. The most successful approach seems to be the cluster algorithms (Swendsen and Wang 1987, Wolff 1988a,b, Wolff 1989a,b,c, Edwards and Sokal 1988, 1989, Ben-Av et al. 1990, Wang et al. 1990, Kandel and Domany 1991, Swendsen et al. 1992, Machta et al. 1995, Liverpool and Glotzer 1996) based on the mapping (Fortuin and Kasteleyn 1972) between Potts models and percolation (see Sec. 4.2). For ferromagnetic Ising, Potts, and vectorspin models these algorithms reduce the dynamic exponent z to a very small value (in favorable cases $z = 0$, e.g. for the single cluster algorithm (Wolff 1989a) in $d \geq 4$ dimensions, see Tamayo et al. 1990). While extensions exists to antiferromagnetic Potts models (Wang et al. 1990), interfaces in solid-on-solid models and Ising models (Hasenbusch and Meyer 1991, Hasenbusch and Pinn 1996), and quantum MC problems (Gubernatis and Kawashima 1996), so far this approach could not be generalized to off-lattice problems, and also many lattice problems involving frustration (spinglasses, lattice gauge problems, etc.) still await the formulation of a useful cluster algorithm.

A very promising approach also is the combination of cluster algorithms with other advanced methods, e.g. with multigrid MC (Kandel et al. 1988) or with multicanonical sampling (the so-called "multibondic algorithm" (Janke and Kappler 1995)).

A recently developed method that works both for lattice and off-lattice problems and has interesting parallels to cluster algorithms (Frenkel 1993) is the so-called "Configurational Bias Monte Carlo" (CBMC) method (Siepmann 1990, Siepmann and Frenkel 1992, de Pablo et al. 1992). This method was originally invented for macromolecules but is presumably useful for many other problems {see Frenkel (1993) and Frenkel and Smit (1996) for more details}.

While in the techniques mentioned above the dynamics of the Monte Carlo "cluster moves" clearly is unphysical, and there is no connection in an Ising simulation using a cluster algorithm with the dynamics of a single spin-flip algorithm, techniques have also been developed (e.g. use of absorbing Markov chains (Novotny 1995) or rescaling techniques inspired by the renormalization group ideas, see Barkema and Marko 1993). For studying nucleation kinetics

in Ising models at low temperatures or the dynamics of coarsening in the simulation of quenching experiments one can observe dynamic processes over 25 decades in time - a task that would be impossible for straightforward dynamic MC.

Finally we mention the reweighting techniques {see Dünweg (1996) and Frenkel and Smit (1996) for recent reviews}. The "single histogram method" starts from the observation that the energy distribution at temperature T can be obtained from the distribution $P(E,T_0)$ at a neighboring temperature T_0 by

$$P(E,T) = P(E,T_0)\exp[-(1/T-1/T_0)E/k_B]/\sum_E P(E,T_0)\exp[-(1/T-1/T_0)E/k_B] \qquad (149)$$

This idea is not at all new (Salsburg et al. 1959) but only recently it is very widely used - first of all one now can generate "histograms" $P(E,T_0)$ with the necessary statistical accuracy, which was not possible in the early days of Monte Carlo, and secondly it was recognized by Ferrenberg and Swendsen (1988) that at a critical point the width of the distribution due to critical fluctuations is sufficiently broadened to allow a reweighting over the temperature interval $|T - T_c|$ of order $L^{-1/\nu}$, i.e. the region of interest for a finite size scaling analysis, irrespective of the linear dimension L. In particular the combined use of several histograms at suitably chosen neighboring temperatures (or other control parameters), the so-called "multiple histogram extrapolation" (Ferrenberg and Swendsen 1989, Swendsen et al. 1992) has become a standard tool in the study of critical phenomena. We emphasize that one can do a reweighting in several parameters simultaneously (e.g. temperature and chemical potential, in a study of criticality in fluids, see Wilding (1996)). Reweighting densities also is possible and is called "density scaling" (Valleau 1993).

Particularly useful are also reweighting schemes built into the simulation procedure {"umbrella sampling" (Valleau and Torrie 1977), "multicanonical MC" (Berg and Neuhaus 1992), "entropic sampling" (Lee 1993), "broad histogram method" (de Oliveira et al. 1996) etc.}. Basically, one is sampling the states not with the Boltzmann probability $\{\propto \exp(-\mathcal{H}/k_BT)\}$ but with a modified probability, $\propto \exp(-\mathcal{H}_{eff}/k_BT)$. This will produce an energy distribution

$$P(E) = \exp[S(E) - \mathcal{H}_{eff}/k_BT]/\sum_E \exp[S(E) - \mathcal{H}_{eff}/k_BT]. \qquad (150)$$

The optimal choice would be if P(E) were flat, i.e. if $\mathcal{H}_{eff}/k_BT$ is just the entropy (apart from an additive constant). Thus one could proceed in an iterative way, choosing first $\mathcal{H}_{eff}^{(0)} = E/k_BT_0$ for some reasonable T_0, estimate P(E) via a histogram, and then use $\mathcal{H}_{eff}^{(1)} = \mathcal{H}_{eff}^{(0)} + \ell n\,(P(E)R)$, R being the total number of energy entries, etc. Of course, one must be very careful that the runs are long enough so that P(E) is reliably estimated. In the end, thermal averages of observables A are then obtained as

$$\langle A\rangle_T = \langle A\exp[(\mathcal{H}_{eff} - \mathcal{H})k_BT]\rangle \,/\, \langle\exp[(\mathcal{H}_{eff} - \mathcal{H})/k_BT]\rangle \quad . \qquad (151)$$

Such techniques are particularly useful to study first order transitions, and to obtain interfacial tensions between coexisting phases, as discussed in Sec. 4.4.

A related approach {"simulated tempering" (Marinari and Parisi 1992), "expanded ensemble" (Lyubartsev et al. 1992)} considers the temperature just as an additional degree of freedom, specifying properly transition rules for jumping from one temperature to another one.

Clearly, all we could give here was a sketchy guide to the original literature in a rapidly developing and very promising field! But it is clear that algorithmic developments are as important as improvements in the computer performance for the growing impact of Monte Carlo simulation in statistical physics.

6. A few concluding remarks

In this article, we have attempted to provide an introductory and tutorial overview of Monte Carlo simulation, primarily addressed to the non-specialist. Thus we have given the basic aspects of the technique in some detail, and we have also described in some depth the finite size effects, which on the one hand seriously hamper all simulation work, but on the other hand also can be used as a tool for extracting quantitatively reliable predictions on bulk and interfacial properties, via the appropriate finite size scaling considerations.

In presenting these points, we have chosen to illustrate them with material exclusively taken from the research group of the author. It must be stressed that this choice of examples was purely a matter of convenience only, and it should be clear from the extensive list of references that many groups have contributed very significantly to the development of techniques that were described here. Thus the bias in the choice of examples should not at all be mistaken as a statement on the validity and/or importance of other results.

In this article, we have also chosen to emphasize classical MC work on equilibrium properties of lattice models, and have dealt only very briefly with topics such as the statistical mechanics of off-lattice models, non-equilibrium phenomena such as simulations of irreversible growth, and quantum problems in statistical thermodynamics. Thus we have only tried to give the reader a flavor of what can be done and what new problems arise when one applies MC methods in these fields. The same disclaimer holds with respect to the many clever algorithms that have been devised to carry out simulations in a more efficient way - we only intended to "wet the readers appetite" to the rich literature on all these interesting problems and approaches.

Nevertheless, we hope that this article can give a clear hint to the usefulness of these computer simulation methods, and the challenge they pose in applying them properly and using them as a powerful tool of research. Also with respect to the technical aspects of this "tool", it is clear that this article could only describe "work in progress", there is still much room for good ideas for the further refinement of the technique and for developing applications to new problems, and thus one can understand the fascination that the computer simulation approach has, leading to a truly explosive growth of the literature in this area.

Acknowledgements: The author's knowledge of the subject has slowly grown in a longstanding and very stimulating interaction with numerous coworkers and colleagues. At this point, I can thank only a few of them, to whom I am particularly indebted since I could use material from joint research for this article, in particular D.P. Landau, D.W. Heermann and K. Kremer, and also H.-P. Deutsch, B. Dünweg, E. Eisenriegler, R. Evans, A.M. Ferrenberg, J.D. Gunton, S. Kämmerer, K. Kaski, K.W. Kehr, D. Marx, M.d'Onorio de Meo, H. Müller-Krumbhaar, P. Nielaba, O. Opitz, J.D. Reger, S. Reulein, M. Scheucher, D. Stauffer and K. Vollmayr.

Figure Captions

Fig. 1: Schematic description of interdiffusion in the ABV model of a random binary alloy (AB) with a small volume fraction ϕ_v of vacant lattice sites, and interdiffusion proceeds via the vacancy mechanism; A-atoms may jump to vacant sites with a jump rate Γ_A, and B-atoms with a jump rate Γ_B. (For simplicity, it is assumed that all pairwise interaction energies are zero, and hence these jump rates do not depend on the occupation of neighboring lattice sites).

Fig. 2: Plot of $g(N) \equiv \ell n\,[(Z_{SAW}(N)/(z-1)^N/(Z_{SAW}(N+2)/(z-1)^{N+2}]$ versus $2/N$ (upper part) and corresponding plot for the non-reversal random walk (NRRW) (lower part). Cases (i),(ii),(iv),(v) correspond to infinite temperature, while cases (iii) and (vi) correspond to $T = T_a$, the temperature of the adsorption transition. Cases (i) and (iv) refer to chains with both ends anchored at the wall, while all other cases refer to "mushrooms" (chains with one end anchored at the wall). Straight lines show the exponents quoted in the figure. From Eisenriegler et al. (1982).

Fig. 3: Probability distribution $P_L(s)$ of the magnetization s per spin of LxLxL subsystems of a simple cubic Ising ferromagnet with $N = 24^3$ spins and periodic boundary conditions, for zero magnetic field and temperature $k_BT/J = 4.0$ (note that the critical temperature occurs at about $k_BT_c/J \approx 4.5114$ (Ferrenberg and Landau 1991). Actually the distribution is symmetric around $s = 0$ and thus another peak occurs around $s = -m_{sp}$ that is not shown here. Note that the linear dimension L here and in the following discussion of lattice models always is measured in units of the lattice spacing. From Binder (1981a).

Fig. 4: Various examples for "dynamic Monte Carlo" algorithms for self-avoiding walks (SAWs): sites taken by beads are shown by dots, and bonds connecting the bead are shown by lines. Bonds that are moved are shown as wavy line (before the move) or broken line (after the move), while bonds that are not moved are shown as full lines. a) Generalized Verdier-Stockmayer (1962) algorithm on the simple cubic lattice showing three types of motions: end-bond motion, kink-jump motion, 90° crankshaft rotation; b) "slithering snake" algorithm; c) "pivot" algorithm. From Kremer and Binder (1988).

Fig. 5: Examples of moves $\vec{X}_t \rightarrow \vec{X}_t'$ commonly used in Monte Carlo simulations for some standard models of statistical mechanics. (a) Single spin-flip Ising model (interpreted dynamically, this is the Glauber kinetic Ising model). (b) Nearest-neighbor exchange Ising model (interpreted dynamically, this is the Kawasaki kinetic Ising model). (c) Two variants of algorithms for the XY model, using a random number η equally distributed between zero and one: left, the angle φ_i' characterizing the new direction of the spin is chosen completely at random; right, φ_i' is drawn from the interval $[\varphi_i - \Delta\varphi, \varphi_i + \Delta\varphi]$ around the previous direction φ_i. (d) Moves of the coordinates of an atom in a two-dimensional fluid from its old position(x_i, y_i) to a new position equally distributed in the square of size $(2\Delta x)(2\Delta y)$ surrounding the old position. (e) Moves of a particle in a given single-site potential $V(\phi)$ from an old position ϕ_i to a new position ϕ_i'. From Binder and Heermann (1988).

Fig. 6: Schematic evolution of the order parameter distribution $P_L(s)$ from $T > T_c$ to $T < T_c$ (from above to below, left part) for an Ising ferromagnet, where s is the magnetization

per site, in a box of volume $V = L^d$ (= L^3 in d = 3 dimensions). The right part shows the corresponding temperature dependence of the mean order parameter $\langle|s|\rangle$, the susceptibility $k_BT\chi' = L^d (\langle s^2\rangle - \langle|s|\rangle^2)$, and the reduced fourth-order cumulant $U_L = 1 - \langle s^4\rangle/[3\langle s^2\rangle^2]$. Dash-dotted curves indicate the singular variation that results in the thermodynamic limit, $L \to \infty$.

Fig. 7 Estimates of the spontaneous magnetization of the three-dimensional Ising model with nearest-neighbor interaction J on the simple cubic lattice at a temperature k_BT/J = 4.425 below criticality ($k_BT_c/J = 4.5114$, see Ferrenberg and Landau (1991)). These estimates are obtained from extrapolating the size dependence of the position (s_{max}) of the maximum of the probability distribution $P_L(s)$ of LxLxL subsystems of a total system of size 24^3, and of moments $\langle|s|\rangle_L$ and $\langle s^2\rangle^{1/2}$. The direct estimate for the magnetization of the total system (M_N) is also included. From Kaski et al. (1984).

Fig. 8: a) Magnetization (full curves) and percolation probability (broken curves) for the d = 2 nearest neighbor Ising ferromagnet plotted vs. reduced temperature for three system sizes as indicated. Periodic boundary conditions were used throughout, and all data were generated with the algorithm of Swendsen and Wang (1987). From D'Onorio de Meo et al. (1990).

b) Normalized fluctuation of the largest cluster, $N\left(\left\langle P_\infty^2\right\rangle - \langle P_\infty\rangle^2\right)$, full curves, and second moment of the cluster size distribution, $\sum{}' \ell^2 n_\ell$, broken curves, plotted vs. T/T_c, for the same model as in a). From D'Onorio De Meo et al. (1990).

Fig. 9: Schematic temperature variation of the normalized susceptibilities $k_BT\chi\,(L,T) = L^d (\langle m^2\rangle - \langle m\rangle^2) = L^d \langle m^2\rangle$ and $k_BT\chi'\,(L,T) = = L^d (\langle m^2\rangle - \langle|m|\rangle^2)$. The dash-dotted curve illustrates the observed behavior for $L^d (\langle m^2\rangle - \langle m\rangle^2)$ in simulations with the single spin flip algorithm: for observation times t_{obs} of the order of the equilibration time τ_e {note $\ell n\tau_e \propto L^{d-1} f_{int}\,(T)$, where $f_{int}\,(T)$ is the interfacial tension} one finds an interpolation between $k_BT\chi$ (at high temperatures where $t_{obs} >> \tau_e$) and $k_BT\chi'$ (at low temperatures where $t_{obs} << \tau_e$). For small L and large t_{obs} this "transition" may be rather far below T_c and should not be confused with the phase transition. For $L \to \infty$, of course, this temperature region between the temperature where $t_{obs} = \tau_e$ and $T = T_c$ shrinks and ultimately vanishes: symmetry breaking at T_c simply appears via "ergodicity breaking". From Binder and Heermann (1988).

Fig.10: Finite size scaling plot of $k_BT\chi'\,L^{-\gamma/\nu}$ versus $|\varepsilon|L^{1/\nu}$, where $\varepsilon = T/T_c - 1$, for the two-dimensional Ising model with nearest neighbor ferromagnetic interaction at the square lattice. The exactly known value of T_c (Onsager 1944) and of the critical exponents {$\nu = 1$, $\gamma = 7/4$, see e.g. Fisher (1974)} are used. Three different lattice sizes are included, as indicated in the figure. Upper branch of the scaling function refers to $T < T_c$, lower branch to $T > T_c$. From D'Onorio De Meo et al. (1990).

Fig.11: Plot of $\langle m^2\rangle/\langle|m|\rangle^2$ versus reduced temperature, for a lattice model of a symmetrical polymer mixture {using the bond fluctuation model with chain lengths $N_A = N_B = N$ = 128 at volume fraction $\phi = 0.5$ of occupied sites, and a square well interaction $\varepsilon(= \varepsilon_{AB} = -\varepsilon_{AA}/2 = -\varepsilon_{BB}/2)$ of range $\sqrt{6}$ }. Three lattice sizes are shown as indicated, and a semi-grand canonical ensemble is used (allowing attempted moves while chains change

their identity, A $\Leftrightarrow$ B, at fixed configuration, in addition to local hopping moves that relax the chain configurations). Smooth curves are based on multihistogram extrapolations (Ferrenberg and Swendsen 1989). From Deutsch and Binder (1992).

Fig.12: Plot of the cumulant $U_L(T_c)$ for the two-dimensional Ising transition in thin films of thickness D with competing surface fields $H_1 = - H_D = 0.55J$ versus the crossover scaling variable ξ_{cross}/L. Here $\xi_{cross} = \exp(\kappa_c D/2)$ where $\kappa_c^{-1} = \xi_b (1 + \omega/2)$, ξ_b being the true correlation length in the bulk, and ω (≈ 0.86) is the universal amplitude associated with interfacial stiffness. Arrow on the ordinate shows the universal value of the d = 2 Ising universality class, $U^* = 0.615$. From Binder et al. (1996).

Fig.13: Schematic variation of the specific heat and internal energy with temperature near a temperature-driven first order transition at T_c (left part). The energy jumps from E. (for $T \to T_c^-$) to E_+ (for $T \to T_c^+$), $E_+ - E_.$ being the latent heat (this jump gives the delta function in the specific heat). Full curve in the lower part shows the equilibrium behavior in a finite system (observed for $t_{obs} >> \tau_e$), while broken curves indicates the hysteresis (metastable states) that one may observe for $t_{obs} << \tau_e$. In the right part, the variation of the susceptibility and magnetization at the field-driven transition of the Ising model at H = 0 is shown schematically. Now the delta function singularity of χ represents the magnetization jump from $-m_{sp}$ to $+m_{sp}$. Again for M(H) the full curve shows the equilibrium behavior ($t_{obs} >> \tau_e$), while broken curves indicate metastable states (for $t_{obs} << \tau_e$). From Binder and Heermann (1988).

Fig.14 a) Susceptibility $\chi(H,T,L)$ of nearest neighbor Ising square lattices at $k_BT/J = 2.1$ plotted versus magnetic field for various L's. Curves are guides to the eye only. b) Same data replotted in scaled form, $\chi(H,T,L)/L^2$ plotted versus scaled field HL^2/J. Arrow indicates the asymptotic value $m^2_{spont}\ J/\ k_BT$ calculated from the exact solution (Yang 1952). Note that $k_BT_c/J \cong 2.269$ for the Ising model (Onsager 1944). Broken curve is the scaling function $\cosh^{-2}(...)$ from Eq. (121), omitting the additive constant χ'. From Binder and Landau (1984).

Fig.15: a) Plot of $g_L(T)$ {Eq. (127)} vs. the normalized temperature distance $-A(T - T_c)$, where A is the scaled latent heat, $A = (E_. - E_+)\ \chi_./(m^2_{spont}\ T_c)$, for a susceptibility ratio $\chi^2 \equiv \chi_+/\chi_. = 4$. Parameter of the curves {calculated from Eq. (125)} is the rescaled linear dimension $\ell \equiv L\ (m^2_{spont}/2\ k_BT_c\ \chi_.)^{1/d}$.
b) Plot of $g_L(T)$ as obtained from Monte Carlo simulations for the 3-state Potts model in d = 3. From Vollmayr et al. (1993).

Fig.16: a) The phase diagram of the nearest neighbor Ising antiferromagnet on the fcc lattice in the field-temperature plane near the $AB(\uparrow\uparrow\downarrow\downarrow)$ - $A_3B(\uparrow\uparrow\uparrow\downarrow)$ transition line. The transition points were obtained by thermodynamic integration (full symbols) or by direct inspection of the order parameter hysteresis loops (open symbols). All transition lines are of first order (note that the lines connecting the points are guides to the eye only). Errors are not shown, since error bars are always smaller than the symbol size.
b) Same as a) but in the magnetization-temperature plane. The first order lines of part a) correspond to two-phase regions, which become extremely narrow as the temperature approaches the triple (or multicritical) point. From Kämmerer et al. (1996)

Fig.17: Boundary conditions for a two-dimensional Ising system which lead to the formation of an interface below the critical point. (a) Spins are fixed at ± 1 at the boundaries, as indicated. Thick solid line denotes the position $x_{int}(y)$ of the (coarse-grained) interface between the phases with negative and positive spontaneous magnetization. The limit L $\rightarrow \infty$, M $\rightarrow \infty$ is considered. (b) Standard boundary conditions for the computer simulation of a system containing an interface. Instead of fixed spins at the two free surfaces one may apply boundary fields of opposite sign that stabilize the two phases. Note that the linear dimension M must satisfy M >> 2ξ, where ξ is the bulk correlation length of order parameter fluctuations. (c) Boundary conditions of a reference system without an interface. (d) Finite system with periodic boundary conditions in all directions and its order parameter distribution $P_L(\rho)$ (schematic). Then near an order parameter $\rho = \rho_{min}$ a minimum of $P_L(\rho)$ develops, which corresponds to a situation with two interfaces running parallel to a lattice direction through the system (left part). These interfaces separate the pure phases with order parameters $<\rho_->$ and $<\rho_+>$ corresponding to the maxima of the distribution. From Binder (1982).

Fig.18: Order parameter profile of the layer magnetization m_n vs. layer number n of a nearest neighbor Ising ferromagnet on the simple cubic lattice at $T/T_{cb} = 0.9554$, using a LxLxD geometry with boundary fields $H_1/J = -0.55$ at the LxL plane situated at n = 0, $H_1/J = +0.55$ at n = D + 1, and L = 128. Arrows show the values of the positive and negative spontaneous magnetization, $\pm m_b$. The table shows the values estimated for the width w of the interface for the various thin film thicknesses D (all lengths being measured in units of the lattice spacing). From Kerle et al. (1996).

Fig.19: Onsager coefficients Λ_{AB} (upper part) and Λ_{AA} (lower part) for a two-dimensional non-interacting random alloy model (ABV model, cf. Fig. 1) plotted vs. Γ_A/Γ_B (left part) or concentration c_A (right part), with c_A as parameter (a) or Γ_A/Γ_B as parameter (b). All data were obtained from LxL square lattices with L = 80 and $c_V = 0.004$. Curves are guides to the eye only. From Kehr et al. (1989).

Fig.20: Amplitudes of concentration waves with wavelengths λ as a function of time t (in units of Monte Carlo steps (MCS) per particle), after a chemical potential variation with the same wavelength has been shut off at t = 0. Open circles represent A-atoms, full dots B-atoms, for a lattice of L^3 sites, with L = 80, $c_A = c_B = 0.48$, $c_V = 0.04$, $\Gamma_A/\Gamma_B = 0.1$. Three different wavelengths λ are shown (the arrow indicates the initial concentration amplitude for $\lambda = 40$). Note that one must choose $\lambda\nu = L$ with ν integer, to comply with the periodic boundary conditions. The curves represent theoretical predictions, based on the use of actual Onsager coefficients (cf. Fig. 19) in a mean field theory based on Eqs. (139)-(141) {for $c_V \rightarrow 0$ this theory predicts a single exponential decay proportional to $\exp[-D_i(2\pi/\lambda)^2 t]$ with D_i given by Eq. (142), while for nonzero c_V $c_A(t)$, $c_B(t)$ decay with superpositions of two exponentials). From Kehr et al. (1989).

Fig.21: Herringbone structure order parameter for N_2 adsorbed on graphite plotted vs. temperature. Center of gravity of the 900 N_2 molecules are fixed in the plane where the graphite potential {as parametrized by Steele (1978)} has its minimum on the regular sites of a triangular lattice, allowing only for one rotational degree of freedom (φ) per molecule. Apart from the corrugation potential nitrogen atoms interact with Lennard-Jones forces and quadrupole-quadrupole interactions. Full line: quantum simulation; dotted line: classical simulation; dashed line: quasiharmonic theory; triangles: Feynman-

Hibbs expansion around classical path. Insert shows corresponding data for the energy.

From Marx et al. (1993a).

Abraham DB 1986 Phase Transitions and Critical Phenomena Vol. 10 ed. Domb C and Lebowitz JL (London: Academic)

Abraham FF 1974 Homogeneous Nucleation Theory (New York: Academic)

Abraham FF, Schreiber DE and Barker J 1974 J. Chem. Phys. 60 1976

Albano EV, Binder K, Heermann DW and Paul W 1989a Z. Physik B77 445

Albano EV, Binder K, Heermann DW and Paul W 1989b J. Chem. Phys. 91 3700

Alder BJ and Wainwright TE 1962 Phys. Rev. 127 359

Alejandre J, Tildesley DF and Chapela GA 1995a Mol. Phys. 85 651

Alejandre J, Tildesley DF and Chapela GA 1995b J. Chem. Phys. 102 4574

Alexandrowicz Z 1975 J. Stat. Phys. 13 231

Alexandrowicz Z 1976 J. Stat. Phys. 14 1

Allen MP 1996 Monte Carlo and Molecular Dynamics of Condensed Matter Systems eds Binder K and Ciccotti G (Bologna: Italian Physical Society) p. 255

Allen MP and Tildesley DJ 1987 Computer Simulation of Liquids (Oxford: Clarendon)

Allen MP and Tildesley DJ 1993 eds Computer Simulation in Chemical Physics (Dordrecht: Kluwer)

Amar JG, Sullivan FE and Mountain RD 1988 Phys. Rev. B37 196

Baker GA Jr and Kawashima N 1995 Phys. Rev. Lett. 75 994

Baker GA Jr and Kawashima N 1996 J. Phys. A: Math. Gen.

Barber MN 1983 Phase Transitions and Critical Phenomena, Vol. 8 eds. C Domb and JL Lebowitz (New York: Academic) p. 145

Barkema GT and Marko JF 1993 Phys. Rev. Lett. 71 2030

Batoulis I and Kremer K 1988 J. Phys. A21 127

Batrouni GG, Katz GR, Kronfeld AS, Lepage GP, Svetitsky B and Wilson KG 1985 Phys. Rev. D32 2376

Baumgärtner A 1985 J. Polym. Sci. C Symp. 73 181

Ben-Av R, Kandel D, Katznelson E, Lauwers PG and Solomon S 1990 J. Stat. Phys. 58 125

Berg BA 1992 Dynamics of First Order Phase Transitions eds. Herrmann HJ, Janke W and Karsch F (Singapore: World Scientific)

Berg BA and Neuhaus T 1992 Phys. Rev. Lett. 68 9

Berg BA, Hansmann U and Neuhaus T 1993 Z. Physik B90 229

Berne BJ and Thirumalai D 1986 Annu. Rev. Phys. Chem. 37 401

Bhanot G, Creutz M and Neuberger H 1984 Nucl. Phys. B235 417

Bhanot G, Duke D and Salvador R 1986 J. Stat. Phys. 44 985

Billoire A, Lacaze R and Morel A 1992 Nucl. Phys. B370 773

Billoire A, Neuhaus T and Berg BA 1993 Nucl. Phys. B396 779

Binder K 1972 Physica 62 508

Binder K 1974 Thin Solid Films 20 367

Binder K 1976 Ann. Phys. 98 390

Binder K 1981a Z. Phys. B43 119

Binder K 1981b Z. Phys. B45 61

Binder K 1982 Phys. Rev. A25 1699

Binder K 1983 J. Chem. Phys. 79 6387

Binder K 1985 Z. Phys. B61 13

Binder K 1986 Advances in Solid State Physics, Vol. 26 ed. Grosse P (Braunschweig: Vieweg) p. 133

Binder K 1987a Ferroelectrics 73 43

Binder K 1987b Rep. Progr. Phys. 50 783

Binder K 1992a Computational Methods in Field Theory eds Gausterer H and Lang CB (Berlin: Springer) p. 59

Binder K (ed) 1992b The Monte Carlo Method in Condensed Matter Physics (Berlin: Springer)

Binder K (ed) 1995 Monte Carlo and Molecular Dynamics Simulations in Polymer Science (New York: Oxford University Press)

Binder K and Deutsch HP 1992 Europhys. Lett. 18 667

Binder K and Heermann DW 1988 Monte Carlo Simulation in Statistical Physics. An Introduction (Berlin: Springer)

Binder K and Hohenberg PC 1974 Phys. Rev. B9 2194

Binder K and Kalos MH 1979 Monte Carlo Methods in Statistical Physics ed Binder K (Berlin: Springer) Chapter 6

Binder K and Kalos MH 1980 J. Stat. Phys. 22 363

Binder K and Landau DP 1980 Phys. Rev. B21 1941

Binder K and Landau DP 1984 Phys. Rev. B30 1477

Binder K and Landau DP 1989 Molecule-Surface Interaction ed Lawley KP (New York: Wiley) p. 91

Binder K and Landau DP 1992 J. Chem. Phys. 96 1444

Binder K and Paul W 1997 J. Polym. Sci., Part B: Polymer Phys

Binder K and Reger JD 1992 Adv. Phys. 41 547

Binder K and Sillescu H 1989 in Encyclopedia of Polymer Science and Engineering, Suppl. Vol. ed Mark H (New York: Wiley) p. 297

Binder K and Stauffer D 1972 J. Stat. Phys. 6 49

Binder K and Stauffer D 1976 Advanc. Phys. 25 343

Binder K and Wang JS 1989 J. Stat. Phys. 55 87

Binder K and Young AP 1986 Rev. Mod. Phys. 58 801

Binder K, Bowker M, Inglesfield JE, and Rous PJ 1995 Cohesion and Structure of Surfaces (Amsterdam: Elsevier)

Binder K, Evans R, Landau DP and Ferrenberg AM 1996 Phys. Rev. E53 5023

Binder K, Landau DP and Wansleben S 1989 Phys. Rev. B40 6971

Binder K, Nauenberg M, Privman V and Young AP 1985 Phys. Rev. B31 1498

Binder K, Rauch H, and Wildpaner V 1970 J. Phys. Chem. Solids 31 391

Blöte HWJ and Nightingale MP 1982 Physica A112 405

Blöte HWJ and Nightingale MP 1989 J. Stat. Phys. 33 285

Borgs C and Kappler S 1992 Phys. Lett. A171 37

Borgs C and Kotecky K 1990 J. Stat. Phys. 61 79

Borgs C, Kotecky R and Miracle-Sole S 1991 J. Stat. Phys. 62 529

Bortz AB, Kalos MH, and Lebowitz JL 1975 J. Comput. Phys. 17 10

Bray AJ 1994 Adv. Phys. 43 357

Brézin E 1982 J. Phys. (France) 43 15

Brézin E and Zinn-Justin J 1985 Nucl. Phys. B257 [FS14] 867

Brochard F, Jouffray J and Levinson P 1983 Macromolecules 16 2638

Brown RG and Ciftan M 1996 Phys. Rev. Lett. 76 1352

Bruce AD 1996 preprint

Cardy JL and Nightingale MP 1983 Phys. Rev. B27 4256

Carlsson J 1988 Phys. Rev. C38 1879

Carmesin I and Kremer K 1988 Macromolecules 21 2819

Ceperley DM 1996 Monte Carlo and Molecular Dynamics of Condensed Matter Systems eds Binder K and Ciccotti G (Bologna: Italian Physical Society) p. 443

Ceperley DM and Kalos MH 1979 Monte Carlo Methods in Statistical Physics ed Binder K (Berlin: Springer) p. 145

Challa MSS and Hetherington JH 1988 Phys. Rev. A38 6324

Challa MSS, Landau DP, and Binder K 1986 Phys. Rev. B34 1841

Ciccotti G and Ferrario M 1996 Monte Carlo and Molecular Dynamics of Condensed Matter Systems eds Binder K and Ciccotti G (Bologna: Italian Physical Society) p. 107

Ciccotti G and Hoover WG 1986 eds. Molecular Dynamics of Condensed Matter Systems (Amsterdam: North-Holland)

Ciccotti G and Ryckaert J-P 1980 Molec. Phys. 40 141

Compagner A 1991 Amer. J. Phys. 59 700

Compagner A 1995 Phys. Rev. E52 5634

Compagner A and Hoogland A 1987 J. Comput. Phys. 71 391

Coniglio A and Klein W 1980 J. Phys. A13 2775

Creutz M 1983 Phys. Rev. Lett. 50 1411

Creutz M 1987 Phys. Rev. D36 515

Dagotto E and Kogut J 1987 Phys. Rev. Lett. 58 299

Desai RC, Heermann DW and Binder K 1988 J. Stat. Phys. 53 795

Deutsch H-P 1993 J. Chem. Phys. 99 4825

Deutsch H-P and Binder K 1992 Macromolecules 25 6214

Deutsch H-P and Binder K 1993a J. Phys. II (France) 3 1049

Deutsch H-P and Binder K 1993b Macromol. Symp. 65 59

Doll JD and Dion DR 1976 J. Chem. Phys. 65 3762

Domb C and Green MS 1976 eds Phase Transitions and Critical Phenomena, Vol. 6 (London: Academic)

Dietrich S 1988 Phase Transitions and Critical Phenomena, Vol. XII eds Domb C and Lebowitz JL (London: Academic) p. 1

Dünweg B 1996 Monte Carlo and Molecular Dynamics of Condensed Matter Systems eds Binder K and Ciccotti G (Bologna: Italian Physical Society) p. 215

Dünweg B and Binder K 1987 Phys. Rev. B36 6935

Edwards RG and Sokal AD 1988 Phys. Rev. D38 2009

Edwards RG and Sokal AD 1989 Phys. Rev. D40 1374

Eichhorn K and Binder K 1995 Europhys. Lett. 30 331

Eichhorn K and Binder K 1996 J. Phys.: Condensed Matter 8 5209

Eisenriegler E, Kremer K and Binder K 1982 J. Chem. Phys. 77 6296

Ermak DL and Mc Cammon JA 1978 J. Chem. Phys. 69 1352

Escobedo FA and de Pablo JJ 1995 J. Chem. Phys. 103 2703

Family F and Vicsek T 1991 Dynamics of Fractal Surfaces (Singapore: World Scientific)

Feder J 1988 Fractals (New York: Plenum)

Ferrenberg AM and Landau DP 1991 Phys. Rev. B44 5081

Ferrenberg AM and Swendsen RH 1988 Phys. Rev. Lett. 61 2635

Ferrenberg AM and Swendsen RJ 1989 Phys. Rev. Lett. 63 1195

Ferrenberg AM, Landau DP and Wong YJ 1992 Phys. Rev. Lett. 69 3382

Fisher ME 1967 Physics 3 267

Fisher ME 1971 Critical Phenomena ed MS Green (New York: Academic) p. 1

Fisher ME 1974 Rev. Mod. Phys. 46 587

Fisher ME and Berker NA 1982 Phys. Rev. B26 2507

Fisher ME and Nakanishi H 1981 J. Chem. Phys. 75 5857

Fisher ME and Privman V 1985 Phys. Rev. B32 447

Fortuin CM and Kasteleyn PW 1972 Physica 57 536

Freirie F, O'Connor D and Stephens CR 1994 J. Stat. Phys. 74 219

Frenkel D 1993 Computer Simulation in Chemical Physics eds. Allen MP and Tildesley DJ (Dordrecht: Kluwer) p. 93

Frenkel D and Smit B 1996 Understanding Molecular Simulation: From Algorithms to Applications (New York: Academic)

Frick M, Pattnaik PC, Morgenstern I, Newns DM and von der Linden 1990 Phys. Rev. B42 2665

Furukawa H and Binder K 1982 Phys. Rev. A26 556

de Gennes PG 1979 Scaling Concepts in Polymer Physics (Ithaca, N.Y.: Cornell Univ. Press)

Gerling RW and Hüller A 1993 Z. Physik B90 207

Gillan MJ and Christodolous F 1993 Int. J. Mod. Phys. C4 287

Glauber RJ 1963 J. Math. Phys. 4 293

Goodman J and Sokal AD 1986 Phys. Rev. Lett. 56 1015

Goodman J and Sokal AD 1989 Phys. Rev. D40 2035

de Grand T 1992 Computational Methods in Field Theory eds. Gausterer H and Lang CB (Berlin: Springer) p. 159

Gross DHE, Ecker A, and Zhang XZ 1996 Ann. Physik 5 446

Gubernatis JE and Kawashima N 1996 Monte Carlo and Molecular Dynamics of Condensed Matter Systems eds Binder K and Ciccotti G (Bologna: Italian Physical Society) p. 519

van Gunsteren WF, Berendsen HJC and Rullmann JAC 1981 Molec. Phys. 44 69

Gunton JD, San Miguel M and Sahni PS 1983 Phase Transitions and Critical Phenomena, Vol. 8 eds Domb C and Lebowitz JL (New York: Academic) p. 267

Guttmann AJ 1989 Phase Transitions and Critical Phenomena, Vol. 13 eds Domb C and Lebowitz JL (London: Academic)

Hammersley JM and Handscomb DC 1964 Monte Carlo Methods (London: Chapman and Hall)

Hammond BL, Lester WA Jr and Reynolds PJ 1994 Monte Carlo Methods in ab initio Quantum Chemistry (Singapore: World Scientific)

Hammrich O 1993 Z. Phys. B92 501

Hansmann U, Berg BA and Neuhaus T 1992 Int. J. Mod. Phys. C3 1155

Harris R 1985 Phys. Lett. 111A 299

Hasenbusch M and Meyer S 1991 Phys. Rev. Lett. 66 530

Hasenbusch M and Pinn K 1993 Physica A 192 342

Hasenbusch M and Pinn K 1996 preprint HUB-EP-96/12

Hasenbusch M, Meyer S and Mack G 1991 Nucl. Phys. B (Proc. Suppl) 20 110

Heermann DW 1996 Monte Carlo and Molecular Dynamics of Condensed Matter Systems eds Binder K and Ciccotti G (Bologna: Italian Physical Society) p. 887

Heermann DW and Burkitt AN 1990 Physica A162 210

Heermann DW and Burkitt AN 1992 The Monte Carlo Method in Condensed Matter Physics (Berlin: Springer) p. 53

Heermann DW and Stauffer D 1980 Z. Phys. B40 133

Herrmann HJ 1986 Phys. Rep. 136 143

Herrmann HJ, Janke W and Karsch F 1992 eds Dynamics of First Order Phase Transitions (Singapore: World Scientific)

Heuer H-O 1990 Computer Phys. Commun. 59 387

Hill TL 1956 Statistical Mechanics (New York: McGraw Hill)

Hill TL 1963 Thermodynamics of Small Systems (New York: Benjamin)

Hohenberg PC and Halperin BI 1977 Rev. Mod. Phys. 49 435

Holm C and Janke W 1996 Phys. Rev. Lett.

Hu CK 1984 Phys. Rev. B29 5103

Hu CK and Mak SK 1989 Phys. Rev. B40 5007

Hüller A 1992 Z. Phys. B88 79

Hüller A 1994 Z. Phys. B95 63

Imry Y 1980 Phys. Rev. B21 2042

Imry Y 1984 J. Stat. Phys. 34 849

Ito N and Suzuki M 1991 Phys. Rev. B43 3483

James F 1990 Computer Phys. Commun. 60 329

Jannink G and des Cloizeaux J 1990 Polymers in Solution: Their Modeling and Their Structure (Oxford: Oxford University Press)

Janke W 1994 Computer Simulation Studies in Condensed Matter Physics VII eds. Landau DP, Mon KK and Schüttler H-B (Berlin: Springer) p. 29

Janke W and Kappler S 1995 Phys. Rev. Lett. 74 212

Janke W and Sauer T 1994 Nucl. Phys. B (Proc. Suppl.) 34 771

Janke W and Sauer T 1995 J. Stat. Phys. 78 75

Kalos MH 1984 Monte Carlo Methods in Quantum Problems (Dordrecht: Reidel)

Kalos MH and Whitlock P 1986 Monte Carlo Methods I: Basics

Kämmerer S, Dünweg B, Binder K, and D'Onorio de Meo M 1996 Phys. Rev. B53 2345

Kandel D and Domany E 1991 Phys. Rev. B43 8539

Kandel D, Ben-Av R and Domany E 1990 Phys. Rev. Lett. 65 941

Kandel D, Domany E and Brandt A 1989 Phys. Rev. B40 330

Kaski KK, Binder K and Gunton JD 1984 Phys. Rev. B29 3996

Katori M and Suzuki M 1987 J. Phys. Soc. Jpn 56 3113

Kawasaki K 1972 Phase Transitions and Critical Phenomena, Vol. 2 eds Domb C and Green MS (New York: Academic) p. 443

Kehr KW and Binder K 1984 Applications of the Monte Carlo Method in Statistical Physics ed Binder K (Berlin: Springer) Chapter 6

Kehr KW, Binder K and Reulein SM 1989 Phys. Rev. B39 4891

Kerle T, Klein J and Binder K 1996 Phys. Rev. Lett. 77 1318

Kikuchi M and Ito N 1993 J. Phys. Soc. Jpn 62 3052

Kim JK 1993 Phys. Rev. Lett. 70 1735

Kirkpatrick S 1979 Ill-Condensed Matter eds Balian R, Maynard R and Toulouse G (Amsterdam: North-Holland) p. 321

Kirkpatrick S and Stoll EP 1981 J. Comput. Phys. 40 517

Knuth D 1969 The Art of Computer Programming, Vol 2 (Reading, MA: Addison-Wesley)

Kramer EJ, Green P, and Palmstrom CJ 1984 Polymer 25 437

Kreer M and Nielaba P 1996 Monte Carlo and Molecular Dynamics of Condensed Matter Systems eds Binder K and Ciccotti G (Bologna: Italian Physical Society) p. 501

Kremer K and Binder K 1988 Computer Phys. Rep. 7 259

Kremer K and Grest GS 1990 J. Chem. Phys. 92 5057

Kremer K and Grest GS 1995 Monte Carlo and Molecular Dynamics Simulations in Polymer Science ed Binder K (New York: Oxford Univ. Press) p. 194

Kremer K, Baumgärtner A and Binder K 1982 J. Phys. A15 2879

Krinsky S and Mukamel D 1977 Phys. Rev. B16 2313

Kumar SK 1994 Computer Simulation of Polymers ed Colbourn EA (Harlow: Longman) p. 228

Landau DP 1992 The Monte Carlo Method in Condensed Matter Physics ed Binder K (Berlin: Springer) p. 23

Landau DP 1996 Monte Carlo and Molecular Dynamics of Condensed Matter Systems eds Binder K and Ciccotti G (Bologna: Italian Physical Society) p. 309

Landau DP 1976a Phys. Rev. B13 2997

Landau DP 1976b Phys. Rev. B14 255

Landau DP and Binder K 1985 Phys. Rev. B31 5946

Landau DP and Binder K 1990 Phys. Rev. B41 4633, 4786

Landau DP and Pal S 1996 Thin Solid Films 272 184

Landau DP, Tang SY and Wansleben S 1989 J. Phys. (Paris) 49, Colloq. 8, 1525

Landau LD and Lifshitz EM 1958 Statistical Physics (Oxford: Pergamon)

Leamy HJ, Gilmer GH, Jackson KA and Bennema P 1973 Phys. Rev. Lett. 30 601

Lee J 1993 Phys. Rev. Lett. 71 211

Lee J and Kosterlitz JM 1991 Phys. Rev. B43 3265

Lee JK, Barker JA and Abraham FF 1973 J. Chem. Phys. 58 3116

Lee KC 1995 J. Phys. A: Math. Gen. 28 4835

Lehmer DH 1951 Proceedings of the 2nd Symposium on Large-Scale Digital Computing Machinery (Cambridge, MA: Harvard Univ. Press) p. 142

Lemak AS and Balabaev NK 1995 Molecular Simulation 15 223

Levesque D, Weis JJ, and Hansen JP 1984 Applications of the Monte Carlo Method in Statistical Physics ed Binder K (Berlin: Springer) p. 37

Li XJ and Sokal AD 1989 Phys. Rev. Lett. 63 827

Li XJ and Sokal AD 1991 Phys. Rev. Lett. 67 1482

Linke A, Heermann DW and Altevogt P 1995 Computer Phys. Commun. 90 66

Linke A, Heermann DW, Altevogt P and Siegert M 1996 Physica A 222 205

Litz P, Langenbach S and Hüller A 1991 J. Stat. Phys. 66 1659

Liverpool TB and Glotzer SC 1996 Phys. Rev. E53, R4255

Luijten 1996 preprint

Luijten E and Blöte HWJ 1996 Phys. Rev. Lett. 76 1557

Luijten E, Blöte HWJ, and Binder K 1996 Phys. Rev. E54

Lyubartsev AP, Martsinovski AA, Shevkunov SV and Vorontsov-Velyaminov PN 1992 J. Chem. Phys. 96 1776

Machta J, Choi YS, Lucke A, Schweizer T and Chayes LV 1995 Phys. Rev. Lett 75 2792

Madras N and Sokal AD 1988 J. Stat. Phys. 50 109

Mandelbrot BB 1982 The Fractal Geometry of Nature (San Francisco: Freeman)

Margolina A and Herrmann HJ 1984 Phys. Lett. 104A 295

Marinari E and Parisi G 1992 Europhys. Lett. 19 457

Marsaglia GA 1968 Proc. Natl. Acad. Sci. (USA) 61 25

Marsaglia GA 1985 Computer Science and Statistics: The Interface ed L Billard (Amsterdam: Elsevier) p. 1

Marsaglia GA, Narasumhan B and Zaman A 1990 Computer Phys. Commun. 60 345

Marx D 1994 Molecular Simulation 12 33

Marx D and Nielaba P 1992 Phys. Rev. A45 8968

Marx D, Opitz O, Nielaba P and Binder K 1993a Phys. Rev. Lett. 70 2908

Marx D, Sengupta S and Nielaba P 1993b J. Chem. Phys. 99 6031

Marx D, Sengupta S, Opitz O, Nielaba P and Binder K 1994 Molecular Phys. 83 31

Meakin P 1988 Phase Transitions and Critical Phenomena, Vol. 12 eds Domb C and Lebowitz JL (New York: Academic) p. 336

Meirovitch H and Alexandrowicz Z 1977 Molecular Phys. 34 1027

Metropolis N, Rosenbluth AW, Rosenbluth MN, Teller AH and Teller E 1953 J. Chem. Phys. 21 1087

Milchev A, Binder K and Heermann DW 1986 Z. Phys. B63 521

Mon KK 1988 Phys. Rev. Lett. 60 2749

Mon KK 1996 Europhys. Lett. 34 399

Mon KK and Binder K 1992 J. Chem. Phys. 96 6989

Mon KK and Binder K 1993 Phys. Rev. E48 2498

Mon KK and Jasnow D 1984 Phys. Rev. A30 670

Mon KK, Wansleben S, Landau DP and Binder K 1989 Phys. Rev. B39 7089

Mouritsen OG 1990 Kinetics of Ordering and Growth at Surfaces ed Lagally MG (New York: Plenum) p 1

Müller M and Binder K 1995 Macromolecules 28 1825

Müller M and Paul W 1994 J. Chem. Phys. 100 719

Müller M and Wilding NB 1995 Phys. Rev. E51 2079

Müller M, Binder K and Oed W 1995 J. Chem. Soc., Faraday Trans. 91 2369

Müller-Krumbhaar H and Binder K 1972 Z. Physik 254 269

Müller-Krumbhaar H and Binder K 1973 J. Stat. Physik 8 1

Müser MH 1996 Molecular Simulation 17 131

Müser MH and Nielaba P 1995 Phys. Rev. B52 7201

Müser MH, Nielaba P and Binder K 1995 Phys. Rev. B51 2723

Najafabadi M and Yip S 1983 Scr. Metall. 17 7199

Nattermann T and Villain J 1988 Phase Transitions 11 5

Nienhuis B 1984 J. Stat. Phys. 34 731

Novotny MA 1993 Phys. Rev. Lett. 70 109

Novotny MA 1995 Phys. Rev. Lett. 74 1

Oed W 1982 Angew. Informatik 7 358

Ohno K and Binder K 1991 J. Stat. Phys. 77 6296

de Oliveira PMC, Penna TJP and Herrmann HJ 1996 Brazilian J. Phys. 26 677

d'Onorio de Meo M, Heermann DW and Binder K 1990 J. Stat. Phys. 60 585

d'Onorio de Meo M, Reger JD and Binder K 1995 Physica A220 628

Onsager L 1944 Phys. Rev. 65 117

de Pablo JJ, Laso M and Suter UW 1992 J. Chem. Phys. 96 2394

Palmer RG 1982 Adv. Phys. 31 669

Panagiotopoulos AZ 1987 Molec. Phys. 61 813

Panagiotopoulos AZ 1992 Molecular Simulation 9 1

Panagiotopoulos AZ 1994 Supercritical Fluids-Fundamentals for Application eds Kiran E and Levelt-Sengers JMH (Dordrecht: Kluwer)

Pandey RB, Milchev A and Binder K 1996 preprint

Parisi G and Ruiz-Lorenzo JJ 1996 Phys. Rev. B54 3698

Parrinello M and Rahman A 1980 Phys. Rev. Lett. 45 1196

Patrascioiu, A and Seiler E 1994 Phys. Rev. Lett. 73 3325

Paul W, Binder K, Heermann DW and Kremer K 1991 J. Phys. (Paris) II 1 37

Pereyra V, Nielaba P and Binder K 1993 J. Phys.: Condens. Matter 5 6631

Pereyra V, Nielaba P and Binder K 1995 Z. Phys. B97 179

Potts RB 1952 Proc. Cambr. Philos. Soc. 48 106

Privman V (ed) 1990 Finite Size Scaling and the Numerical Simulation of Statistical Systems (Singapore: World Scientific)

Privman V and Fisher ME 1983 J. Stat. Phys. 33 285

Privman V and Rudnick J 1990 J. Stat. Phys. 60 551

Promberger M and Hüller A 1995 Z. Phys. B97 341

de Raedt H 1996 Monte Carlo and Molecular Dynamics of Condensed Matter Systems ed Binder K and Ciccotti G (Bologna: Società Italiana di Fisica) p. 401

de Raedt and Lagendijk 1985 Phys. Rep. 127 233

de Raedt H and von der Linden 1992 The Monte Carlo Method in Condensed Matter Physics ed. Binder K (Berlin: Springer) p. 249

Rao M and Berne BJ 1978 Mol. Phys. 37 455

Rao M and Levesque D 1976 J. Chem. Phys. 65 3233

Ray JR 1991 Phys. Rev. A44 4061

Ray JR 1993 J. Chem. Phys. 98 2263

Recht JR and Panagiotopoulos 1993 Mol. Phys. 80 843

Reger JD and Young AP 198 Phys. Rev. B37 5987

Rickwardt Ch, Nielaba P, and Binder K 1994 Ann. Phys. (Leipzig) 3 483

Rieger H 1995 Phys. Rev. B52 6659

Rouault Y, Baschnagel J and Binder K 1995 J. Stat. Phys. 80 1009

Rovere M, Heermann DW and Binder K 1988 Europhys. Lett. 6 585

Rovere M, Heermann DW and Binder K 1990 J. Phys.: Condens. Matter 2 7009

Rovere M, Nielaba P and Binder K 1993 Z. Physik B90 215

Rosenbluth MN and Rosenbluth AW 1955 J. Chem. Phys. 23 356

Sadiq A 1984 J. Comput. Phys. 55 387

Sadiq A and Binder K 1983 Surf. Sci. 128 350

Sadiq A and Binder K 1984 J. Stat. Phys. 35 517

Salsburg ZW, Jacobson D, Fickett W and Wood WW 1959 J. Chem. Phys. 30 65

Sariban A and Binder K 1987 J. Chem. Phys. 86 5859

Sariban A and Binder K 1988 Macromolecules 21 711

Schmid F and Binder K 1992a Phys. Rev. B46 13553

Schmid F and Binder K 1992b Phys. Rev. B46 13565

Schmidt KE and Ceperley DM 1992 The Monte Carlo Method in Condensed Matter Physics ed Binder K (Berlin: Springer) p. 203

Schmidt KE and Kalos MH 1984 Applications of the Monte Carlo Method in Statistical Physics ed Binder K (Berlin: Springer) p. 125

Schmittmann B and Zia RKP 1995 The Phase Transitions and Critical Phenomena Vol 17 eds Domb C and Lebowitz JL (London: Academic)

Schwartz M 1991 Europhysics Lett. 15 777

Schweika W, Landau DP and Binder K 1996 Phys. Rev. B53 8937

Selke W 1988 Phys. Rep. 170 213

Shockley W 1938 J. Chem. Phys. 6 130

Siepmann JI 1989 Molec. Phys. 70 1145

Siepmann JI and Frenkel D 1992 Molec. Phys. 75 59

Smit B 1988 Phys. Rev. A37 3481

Smit B 1993 Computer Simulation in Chemical Physics eds Allen MP and Tildesley DJ (Dordrecht: Kluwer) p. 173

Sokal AD 1995 Monte Carlo and Molecular Dynamics Simulations in Polymer Science ed Binder K (New York: Oxford Univ. Press) Ch. 2

Sprik M 1996 Monte Carlo and Molecular Dynamics of Condensed Matter Systems eds Binder K and Ciccotti G (Bologna: Società Italiana di Fisica) p. 43

Stauffer D 1979 Phys. Rep. 54 1

Stauffer D 1985 An Introduction to Percolation Theory (London: Taylor and Francis)

Stauffer D and Aharony A 1992 Introduction to Percolation Theory (Basingstoke Hauts: Taylor and Francis)

Steele WA 1978 J. Phys. Chem. 82 817

Stoll E, Binder K and Schneider T 1973 Phys. Rev. B8 3266

Stephanow MA and Tsypin MM 1991 Nucl. Phys. B366 420

Swendsen RH and Wang JS 1987 Phys. Rev. Lett. 58 86

Swendsen RH, Wang JS and Ferrenberg AM 1992 The Monte Carlo Method in Condensed Matter Physics ed Binder K (Berlin: Springer) p. 75

Suzuki M 1986 ed Quantum Monte Carlo Methods (Berlin: Springer)

Suzuki M 1992 ed Quantum Monte Carlo Method in Condensed Matter Physics (Singapore: World Scientific)

Tamayo P, Brower RC and Klein W 1990 J. Stat. Phys. 58 1083

Tausworthe RC 1965 Math. Comput. 19 201

di Tolla FD, Tosatti E and Ercolesi F 1996 Monte Carlo and Molecular Dynamics of Condensed Matter Systems eds Binder K and Ciccotti G (Bologna: Società Italiana di Fisica) p. 345

Tsypin VA 1994 Phys. Rev. Lett. 73 2013

Valleau JP 1993 J. Chem. Phys. 99 4718

Valleau JP and Torrie GM 1977 Quantum Statistical Mechanics, Part A: Equilibrium Techniques ed. Berne BJ p. 169 (New York: Plenum)

Van Beijeren H and Nolden I 1987 Structure and Dynamics of Surfaces II eds Schommers W and Van Blanckenhagen P (Berlin: Springer)

Verdier PH and Stockmayer WH 1962 J. Chem. Phys. 36 227

Vollmayr K, Reger JD, Scheucher M and Binder K 1993 Z. Physik B91 113

Wall FT and Mandel F 1975 J. Chem. Phys. 63 4592

Wang JS 1991 Physica A164 240

Wang JS 1996 J. Stat. Phys. 82 1409

Wang JS, Swendsen RH and Kotecky R 1989 Phys. Rev. Lett. 63 109

Wang JS, Swendsen RH and Kotecky R 1990 Phys. Rev. B42 2465

Wang JS, Selke W, Dotsenko VS and Andreichenko VB 1990 Physica A164 221

Weber H, Marx D and Binder K 1995 Phys. Rev. B51 14636

Widom B 1963 J. Chem. Phys. 39 2808

Wilding NB 1993 Z. Physik B93 113

Wilding NB 1995 Phys. Rev. E52 602

Wilding NB 1996 Annual Reviews of Computational Physics IV ed Stauffer D (Singapore: World Scientific) p. 37

Wilding NB and Bruce AD 1992 J. Phys: Condens. Matter 4 3087

Wilding NB and Müller M 1994 J. Chem. Phys. 101 4234

Wilding NB and Müller M 1995 J. Chem. Phys. 102 2562

Wilding NB and Nielaba P 1996 Phys. Rev. E53 926

Wildpaner V 1974 Z. Physik 270 215

Wittmann H-P and Kremer K 1990 Computer Phys. Commun. 61 309

Wittmann H-P and Kremer K 1992 Computer Phys. Commun. 71 343

Wolff U 1988a Phys. Rev. Lett. 60 1461

Wolff U 1988b Nucl. Phys. B300 [FS22] 501

Wolff U 1989a Phys. Rev. Lett. 62 361

Wolff U 1989b Phys. Lett. B228 379

Wolff U 1989c Nucl. Phys. B322 759

Wolff U 1992 Computational Methods in Field Theory eds Gausterer Hand Lang CB (Berlin: Springer) p. 127

Wood WW 1968 Physics of Simple Liquids ed Temperley HNV, Rushbrooke GS, Rowlinson JS (Amsterdam: North-Holland)

Wu FY 1982 Rev. Mod. Phys. 54 235

Yang CN 1952 Phys. Rev. 85 808

Young AP 1996 Monte Carlo and Molecular Dynamics of Condensed Matter Systems eds Binder K and Ciccottic G (Bologna: Società Italiana di Fisica)

Zettlemoyer A 1969 ed Nucleation (New York: M. Dekker)

Zettlemoyer A 1977 ed Nucleation II (New York: M. Dekker)

Zhang MQ 1989 J. Stat. Phys. 56 939

Zorn R, Herrmann HJ and Rebbi C 1981 Computer Phys. Commun. 23 337

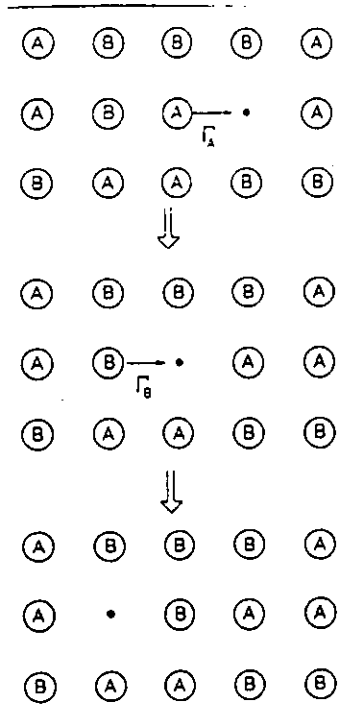

Fig. 1

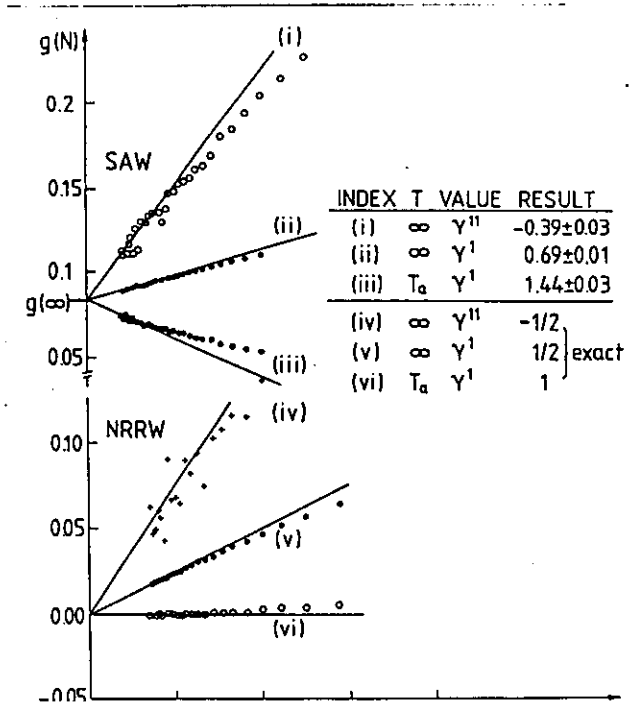

INDEX	T	VALUE	RESULT
(i)	∞	γ^{11}	−0.39±0.03
(ii)	∞	γ^{1}	0.69±0.01
(iii)	T_a	γ^{1}	1.44±0.03
(iv)	∞	γ^{11}	−1/2
(v)	∞	γ^{1}	1/2 exact
(vi)	T_a	γ^{1}	1

Fig. 2

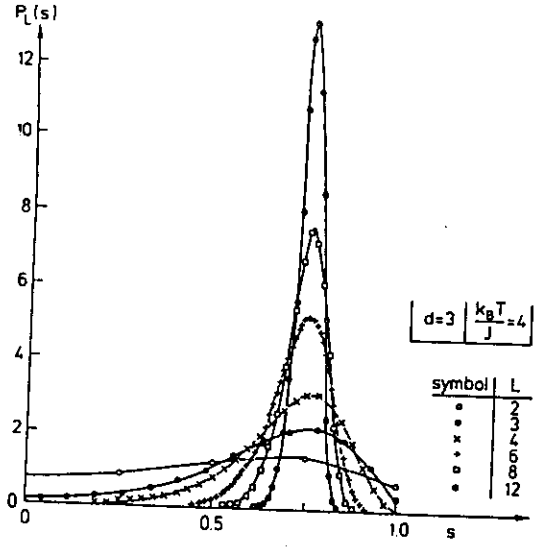

Fig.3

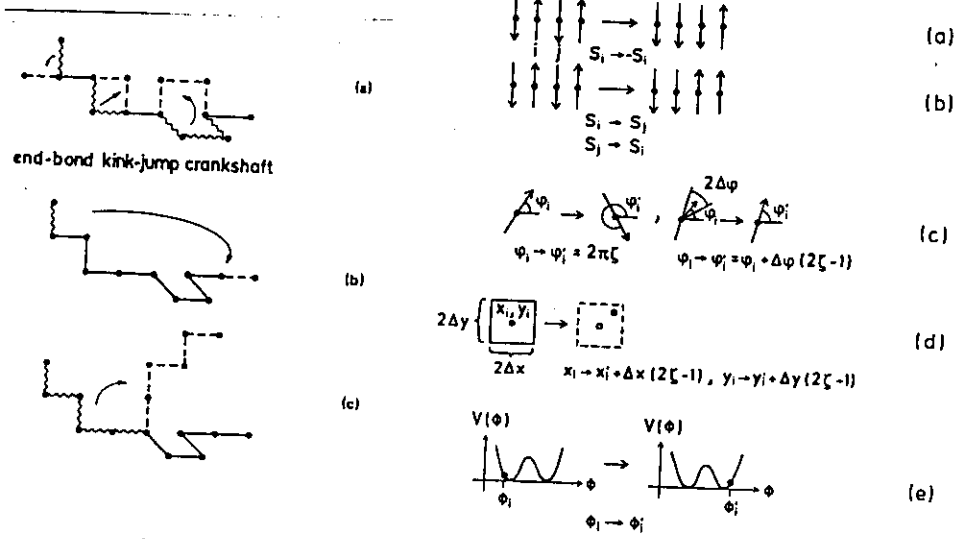

Fig.4

Fig.5

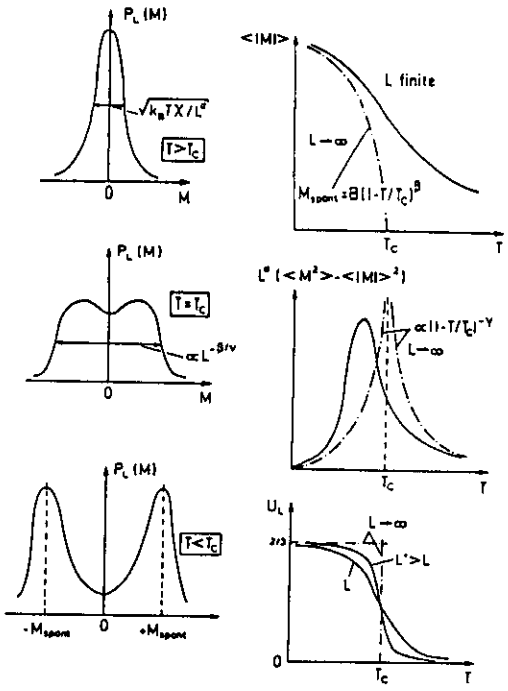

Fig.6

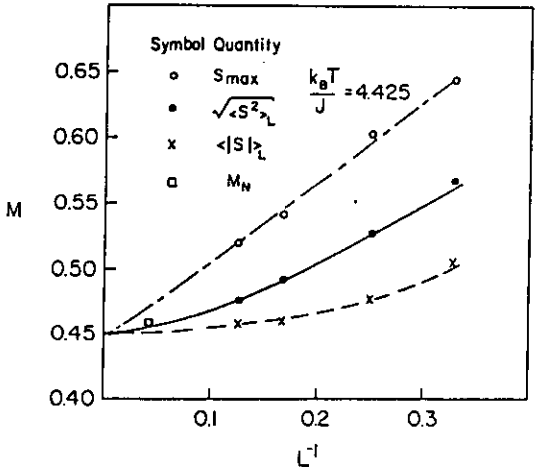

Fig.7

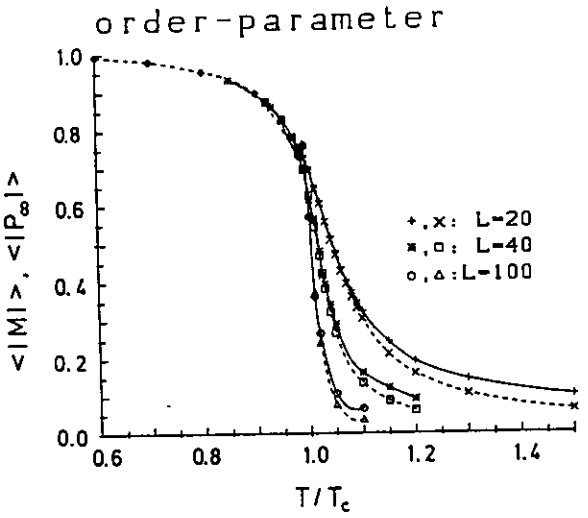

Fig. 8

a)

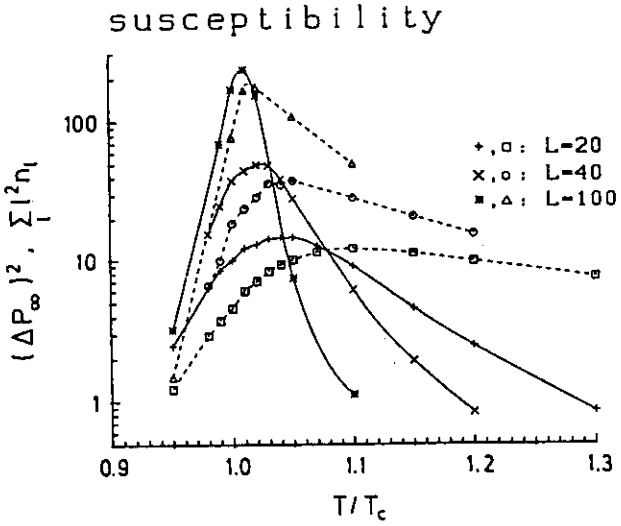

b)

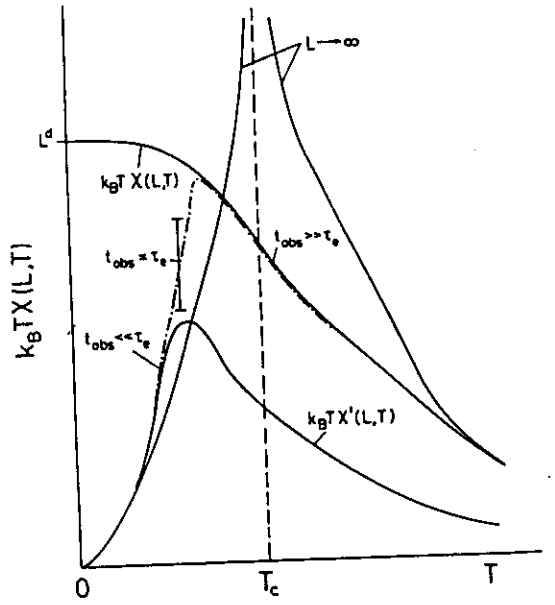

Fig. 9

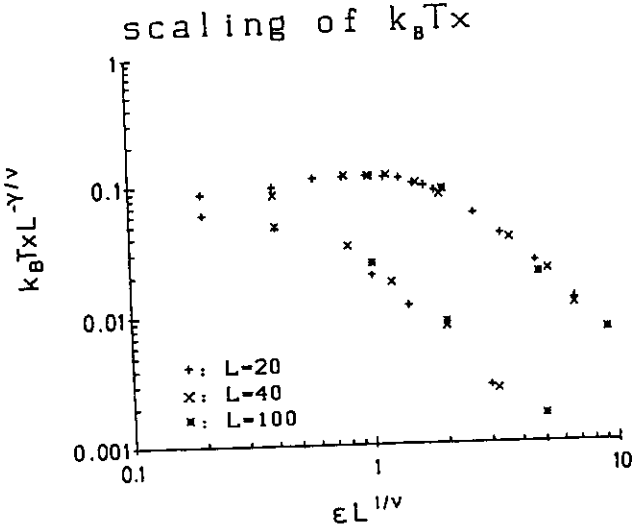

Fig. 10

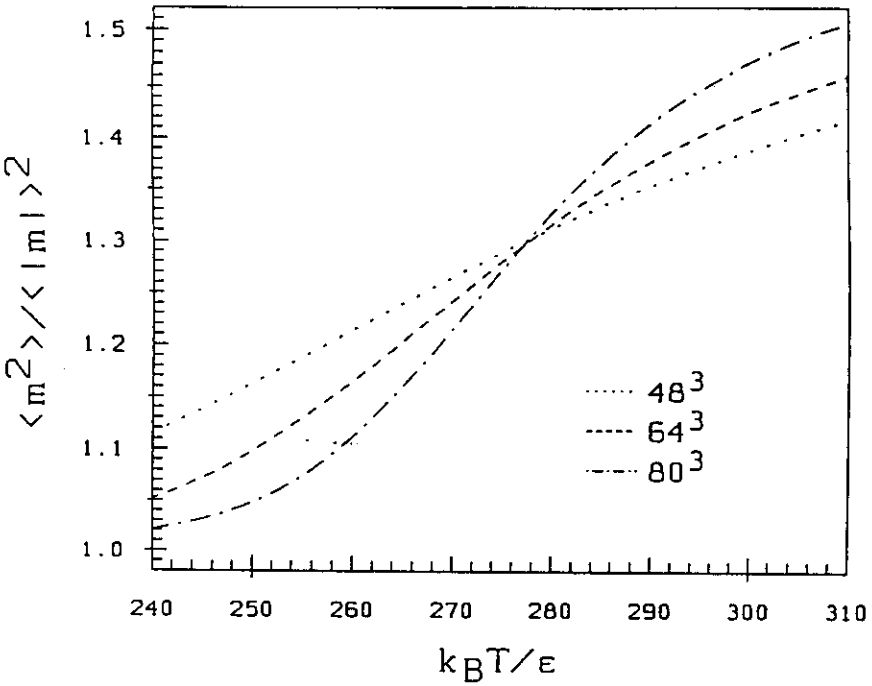

Fig. 11

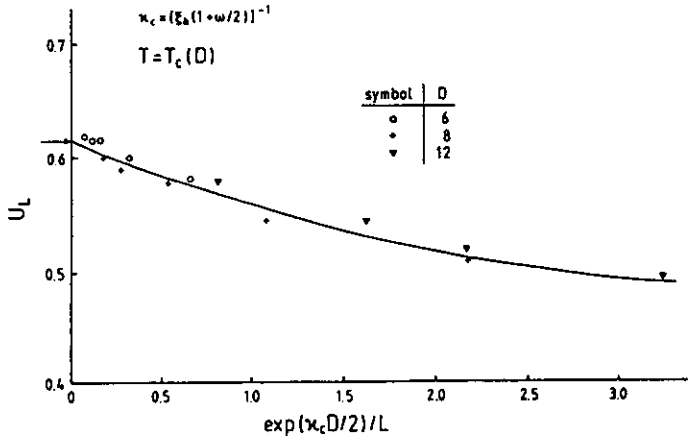

FIG. 12

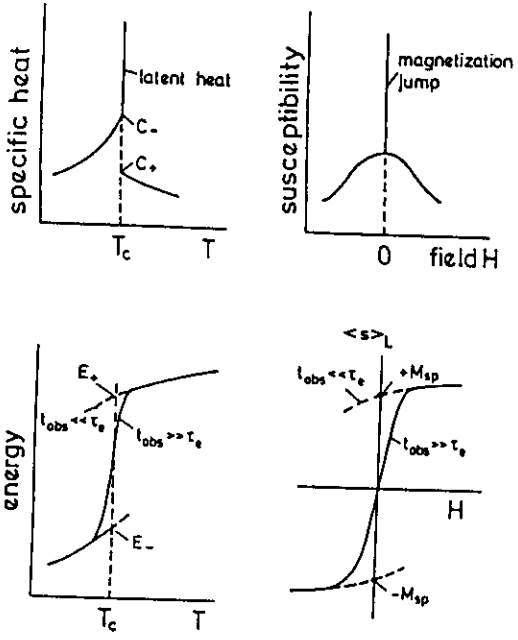

Fig. 13

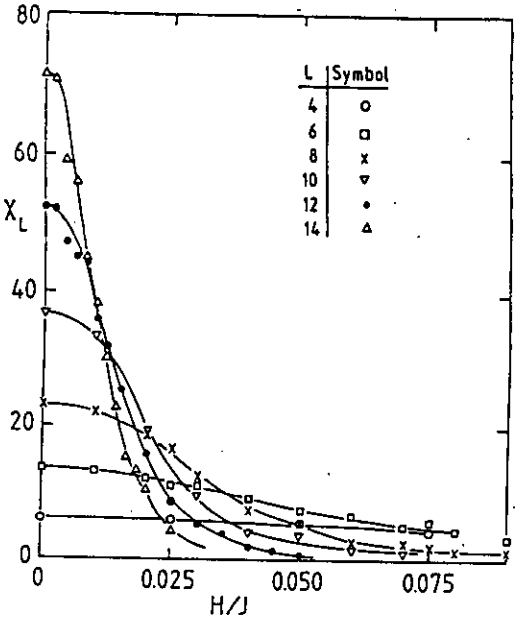

Fig. 14a)

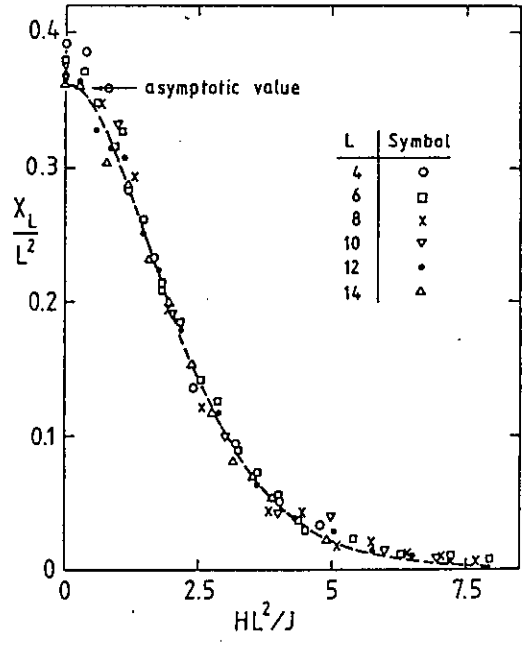

Fig. 14b)

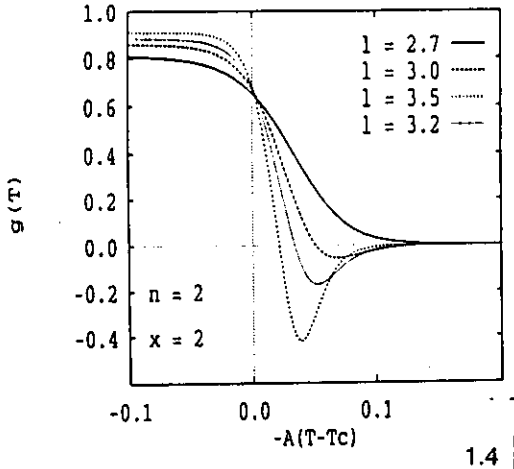

Fig_15 a)

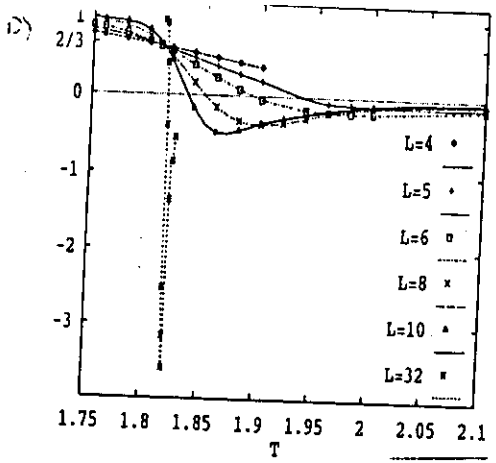

Fig_16 b)

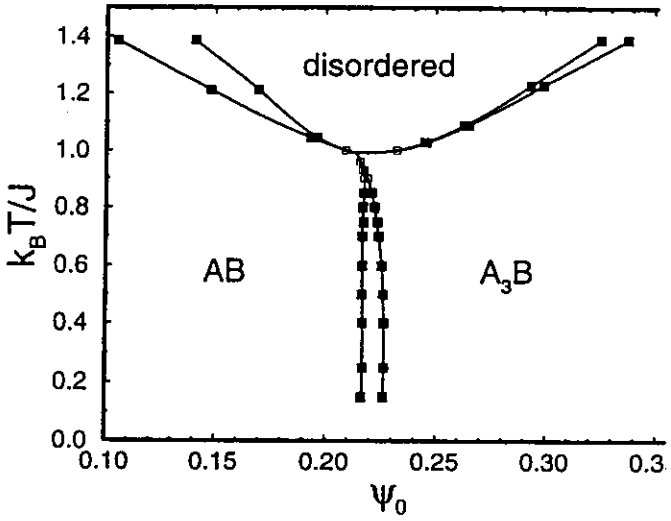

c)

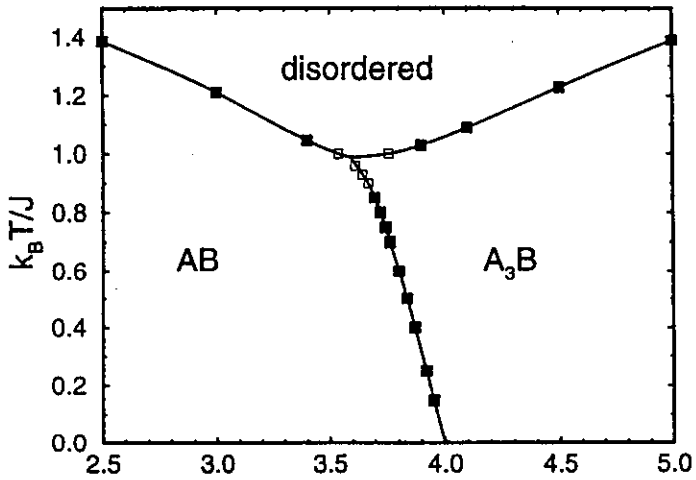

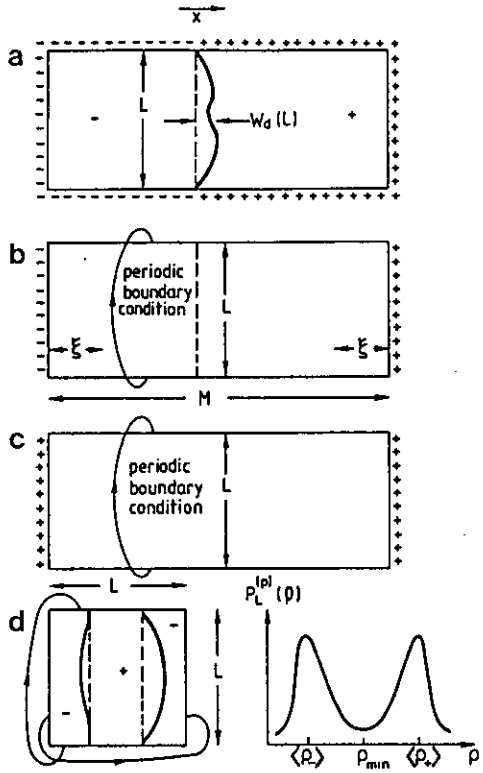

FIG.17

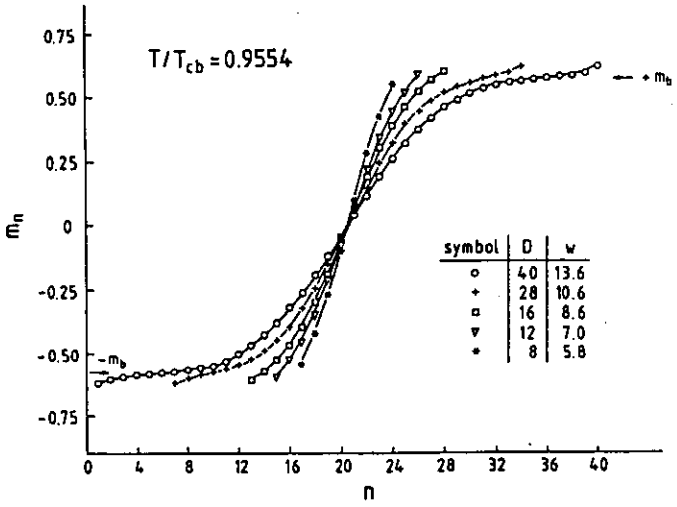

FIG.18

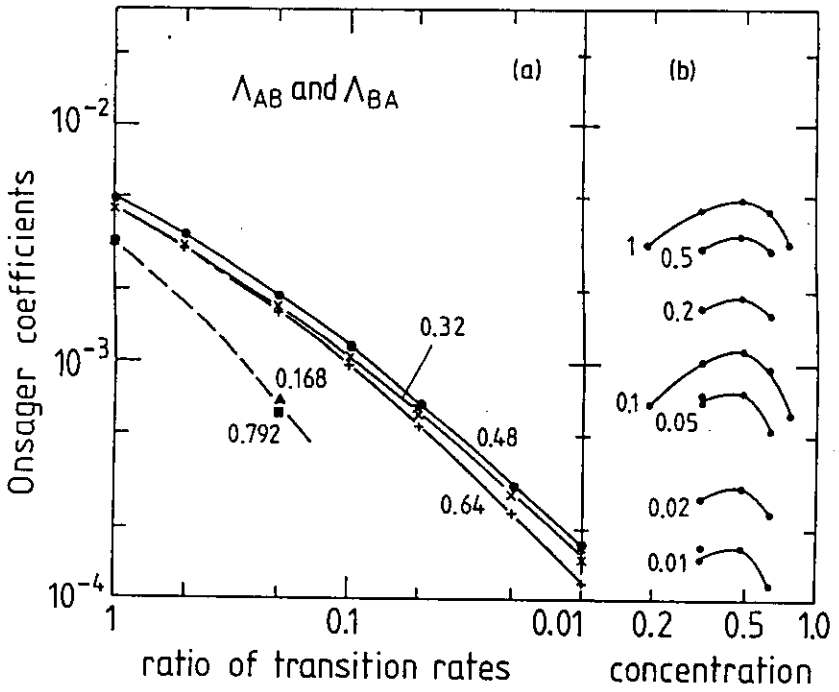

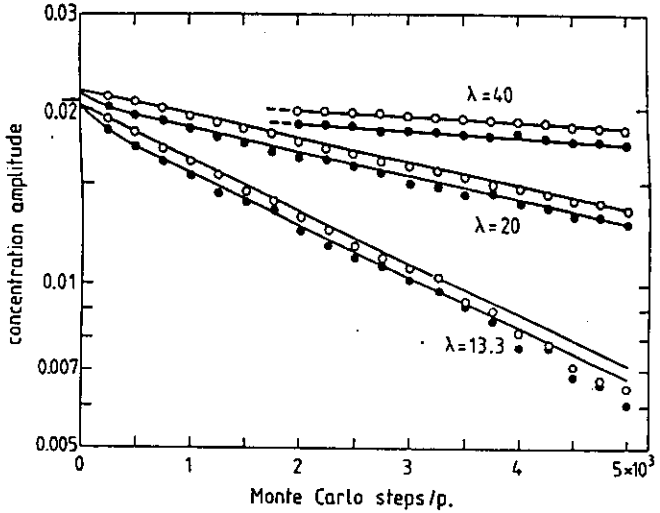

Fig-20

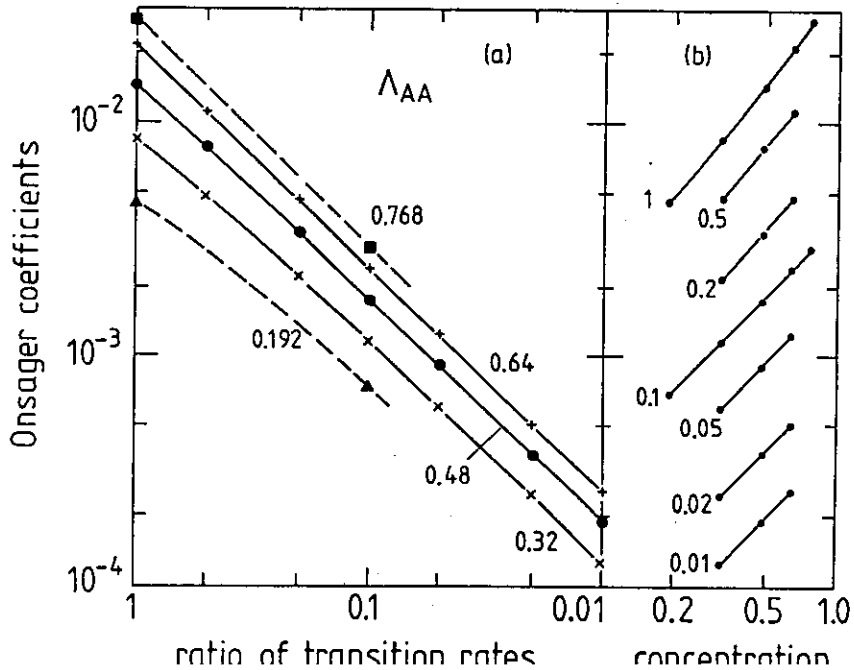

Fig 19

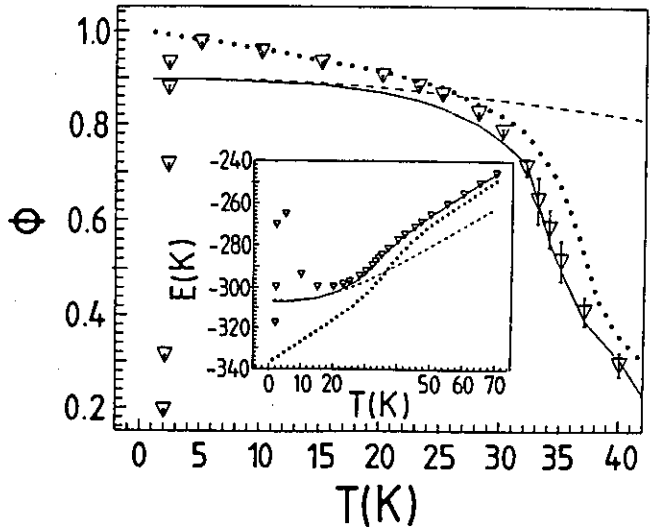

Fig.21